Development of Techniques for Analysis of the Human Retinal Ganglion Cell Transcriptome: Application to the Role of Calcium in RGC Death in Glaucoma

Ning Ma

A THESIS PRESENTED FOR THE DEGREE OF DOCTOR OF PHILOSOPHY AT THE UNIVERSITY OF EAST ANGLIA, NORWICH, UK

SCHOOL OF PHARMACY

October 2013

Acknowledgements

Abstract

Purpose: Irreversible retinal ganglion cell (RGC) death is the reason for visual loss in glaucoma. However, the mechanisms of RGC death remain unclear. The aim of this research was to develop methods to study mRNA expression profiles in human RGCs, then to use the data to investigate the role of calcium in RGC death.

Methods: A planar sectioning technique was developed to isolate mRNA from serial sections of the human retina. QRT-PCR of neuronal markers validated the technique. Global gene expression analysis, using Illumina arrays, compared expression in the retina ganglion cell layer (RGCL) and entire macula (Mac). Immunohistochemistry and QRT-PCR validated gene array data. RGC death was investigated using a simulated ischemia (oxygen glucose deprivation, OGD) model in human organotypic retinal cultures (HORCs). Cell survival was measured by LDH, and RGC loss by immunohistochemistry and QRT-PCR. Western blot assessed proteases.

Results: The sectioning technique developed enabled isolation of relatively large quantites of high quality mRNA from 20μm retinal sections from the macular region of the human retina. Marker genes for retinal neurons verified accurate profiling of gene expression across the retina. Gene arrays provided a list of genes that were most enriched in the RGCL. *AHNAK2* and *HSP41B* were the two most enriched genes in the RGCL. *CAPN1* (calpain 1), a calcium-dependent cysteine proteases, was in the gene list. Its expression was confirmed to be mainly in the inner retina. OGD caused calpain activation and induced RGC death. Two TRP channels, TRPM-2 and TRPC-3, which mediate Ca^{2+} influx, were found that predominantly expressed in the RGCL. Involvement in RGC death in the OGD model using the TRP inhibitor ACA could not be confirmed.

Conclusions: The technique developed has enabled determination of the human RGCL transcriptome and has allowed expression profiling of gene of interest across the retina. This could prove to be a powerful tool in the investigation of pathways involved in neurodegeneration in the retina.

Table of Contents

List of Figures

Chapter 6

List of tables

Abbreviations

AC	amacrine cells
ACA	anthranilic acid
ADP	Adenosine Diphosphate
ATP	Adenosine Triphosphate
BC	bipolar cells
BP_m	mean blood pressure
CICR	Ca^{2+}-induced Ca^{2+} release
DAG	Diacylglycerol
DAPI	4, 6-diamidino-2-phenylindole
DICR	depletion induced Ca^{2+} release
BCA	Bicinchoninic acid assay
BDNF	brain derived neurotrophic factor
DAG	diacylglycerol
DMSO	Dimethyl sulfoxide
DMEM	Dulbecco's modified Eagle medium
dNTP	deoxyribonucleoside triphosphate
DPBS	Dulbecco's Phosphate Buffered Saline
DTT	dithiothreitol
ECM	Extracellular matrix
EDTA	Ethlenediaminetet raacetic acid
EMEM	Eagle's minimum essential medium
ER	Endoplasmic reticulum
FC	fold change
FCS	foetal calf serum
FDR	false discovery rate
GAPDH	Glyceraldehyde-3-phosphate
GCL	ganglion cell layer
HC	horizontal cells
HE	Haemotoxylin and Eosin
HORCs	Human organotypic retinal cultures
IgG	Immunoglobulin gamma

INL	**inner nuclear layer**
IOP	**normal intraocular pressure**
IP$_3$	**Inositol (1, 4, 5) trisphosphate**
IP$_3$R	**inositol 1,4,5-trisphosphate receptors**
IPL	**inner plexiform layer**
LCM	**laser capture microdissection**
LD	**Lactate dehydrogenase**
M	**macular retina**
M-PE	**mammalian protein extraction reagent**
NCX	**Na$^+$ / Ca^{2+} exchanger**
NFL	**Nerve fiber layer**
NOPG	**normal intraocular pressure**
ODG	**glucose deprivation**
ONL	**outer nuclear layer**
ONH	**optic nerve head**
OPL	**outer plexiform layer**
OPP	**ocular perfusion pressure**
OS	**outer segment**
PACG	**primary angle closure glaucoma**
PBS	**Phosphate buffered saline**
RGC	**retinal ganglion cells**
PI3	**Phosphatidylinositol 3**
PIP2	**Phosphatidyl inositol 4, 5-bisphosphate**
PKA	**protein kinase A**
PKC	**protein kinase C**
PLC	**Phospholipase C**
PMCA	**plasma membrane Ca^{2+}-ATPase**
POAG	**Primary open angle**
PR	**photoreceptor cells**
PVDF	**polyvinylidene difluoride**
ROCs	**receptor-operated channels**
RPE	**retinal pigment epithelium**
RIN	**integrity number**

RT   **Room temperature**

RTK   **receptor tyrosine kinase**

RT-PCR **Reverse transcriptase-polymerase chain reaction**

RyR   **ryanodine receptors**

SERCA   **sarco(endo)plasmic reticulum Ca^{2+}-ATPase**

SEM   **Standard error mean**

SF   **Serum free**

SOCs   **second messenger operated channels**

VOCs   **voltage-operated channels**

TUNEL   **Terminal deoxynucleotidyl transferase UTP nick end labeling**

Chapter 1

Introduction

1 Anatomy of the eye

1.1 Gross anatomy

The eye is a highly complex organ (Figure 1.1) with the primary function of photoreception. This is a precise physiological process, where the co-ordinated function of the components of the eye allows light energy to be transformed into electrical signals which are transmitted through the optic nerve to the brain, where the signal can be interpreted and perceived as an image. A full review of eye anatomy and function is given in Forrester (2002).

The human eye is a spheroid approximately 2.5cm in diameter with a volume of approximately 6.5ml (Forrester, Dick et al. 2002). It is made of three layers (Figure 1.1). The outer layer is the fibrous coat, which consists of the cornea and sclera. These provide protection and structural support, as well as enabling light to enter the eye. The middle layer is the uvea, the vascular tract which is composed of the iris, the ciliary body and the choroid. The inner layer is the neural layer and includes the retina and retinal pigment epithelium (RPE). The interior of the eye contains the aqueous humour in the anterior, the vitreous humour in the posterior of the eye and the lens is situated between them. The following sections will describe the components of the eye in more detail, focussing primarily on the retina.
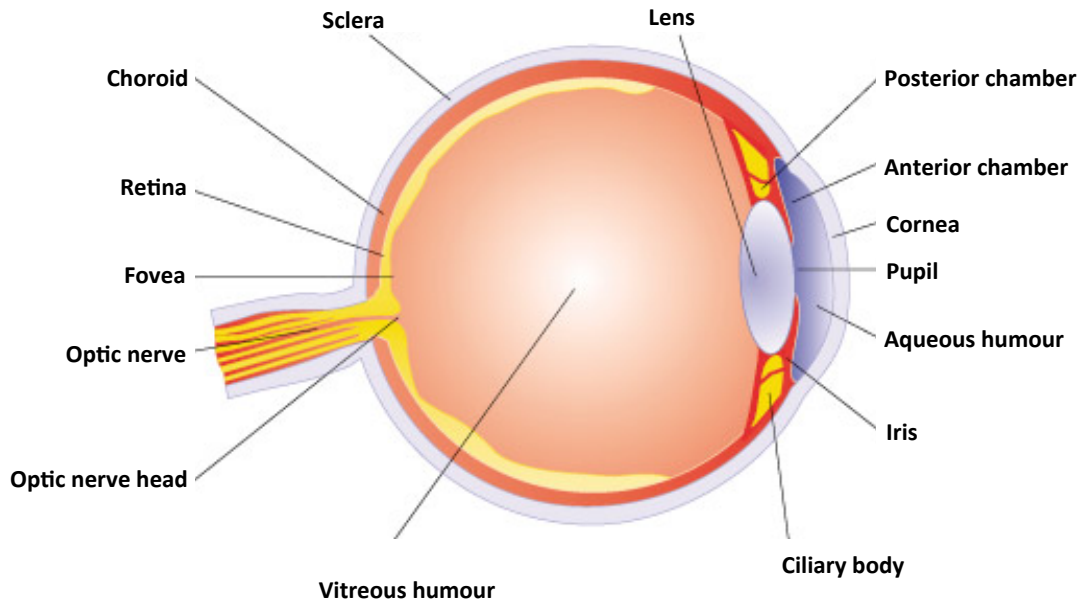
Figure 1.1 The human eye with a schematic enlargement of the retina. Image from http://www.best4glasses.co.uk/images/eyeball.jpg

1.2 The Cornea

The cornea is a transparent and avascular tissue. Its primary function is refraction of light into the eye, and the highest degree of refraction occurs at its surface. It has rich nerve supply via long ciliary nerves of the ophthalmic division of the trigeminal nerve. The cornea is also an important barrier helping prevent trauma and infection and also helps to maintain the shape of the eye.

1.3 The Sclera

The sclera is the white, opaque, viscoelastic outer fibrous coat of eye. It consists of connective tissue which gives it the properties required, most importantly its strength. This provides protection for the inner structures of the eye. The thickness of the sclera varies throughout the eye: the thinnest is where the extraocular muscles are attached and the thickest occurs at the lamina cribrosa where the optic nerve leaves the eye.

1.4 The Iris

The iris is a circular disc consisting mainly of smooth muscle. It is the coloured part of the eye. The iris separates the space in the front of the lens into the anterior and posterior chamber. The iris smooth muscle controls the diameter of the pupil to regulate the amount of the light entering the eye.

1.5 The Ciliary Body

The ciliary body lies at the base of the iris (Figure 1.2). It is divided into the ciliary epithelium, the ciliary body stroma and ciliary muscle. The ciliary body performs several functions, including aqueous humor production from the ciliary epithelium (see below) and accommodation which allows the focusing of light by the action of the ciliary muscle.
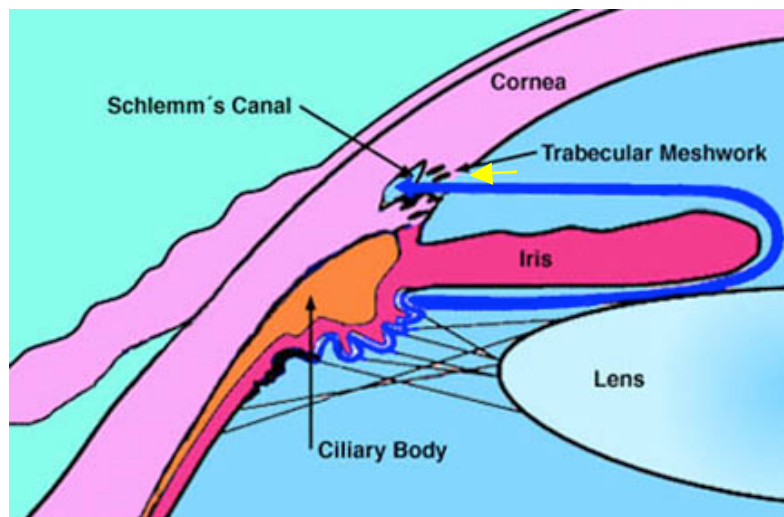
Figure 1.2 The anterior eye and the aqueous humour flow. The direction of the thick arrow is the pathway of aqueous humour flow, secreted from the ciliary body, passing through the posterior chamber to the anterior chamber and draining through the trabecular meshwork and Schlemm's canal. Image from http://www.littlerockeye.com/wp-content/uploads/2012/09/LI_1.jpg

1.6 The Choroid

The choroid is the posterior portion of the uvea. It lies between the retina and the sclera and adheres to the RPE by Bruch's membrane. The choroid has an abundance of blood vessels and pigmented cells. The human choroid consists of five layers: Bruch's membrane, the

17

choriocapillaris, two blood vessel layers and the suprachoroid. As it is enriched with blood vessels, the main responsibility of the choroid is to nourish the outer layer of retina.

1.7 The Anterior and posterior chambers/ aqueous humour

The anterior chamber is located between the iris and the cornea (Figure 1.2). Within the anterior chamber there are several important structures, including Schlemm's canal, the scleral spur, the iris root, the trabecular meshwork and the ciliary muscle. Schlemm's is the channel that the aqueous humour flows through to allow drainage from the eye. In this way, it helps maintain normal intraocular pressure (IOP) and also removes waste products from the anterior eye. The trabecular meshwork is divided into three parts: the uveal meshwork, the corneoscleral meshwork, and the cribriform meshwork. The latter provides the greatest resistance to aqueous outflow and is therefore of most significance in control of IOP. The trabecular meshwork is situated between the cornea and the iris (Figure 1.2). This area is referred to as the angle. The aqueous humour is watery liquid that fills the space of the anterior and posterior chambers. It is secreted by the ciliary epithelium of ciliary body into the posterior chamber (the space between the lens and the iris), passes around the lens and flows through the pupil into the anterior chamber and drains at the angle via the trabecular meshwork and Schlemm's Canal (Figure 1.2). The aqueous humour supplies the nourishment to the lens and the cornea. It also plays an important role in maintenance of the shape of the eye via the IOP. The IOP is normally in the range of approximately 10-21mmHg with a mean of approximately 16mmHg. A balance of secretion and drainage of aqueous humour maintains normal IOP.

1.8 The Lens

The lens is located behind the iris and is held in place by the suspensary ligaments which are connected and distance to the ciliary body (Figure 1.2). The lens is an important component in the refractive system of the eye and is responsible for the fine focussing of light on the retina. The shape of the lens is controlled by the ciliary muscle, which on contraction increases the curvature of the lens. By doing this, the refraction of light by the lens will be modulated, in order to focus light from near objects onto the retina. When the ciliary muscle is relaxed, the lens is pulled and flat and taut by the IOP, enabling focussing of light from distance objects.

1.9 The Vitreous Humour

The vitreous humour is a transparent viscoelastic gel and occupies approximately 80% of the cavity of the eye posterior to the lens. The vitreous humour consists of water (98-99%), proteins, and collagen. It is used to maintain the shape of the eye and help keep the retina attached to the RPE and choroid.

1.10 The Retina

The retina is located at the internal face of the choroid and it is also the innermost layer of the eye. It is made up of the neurosensory retina and the retinal pigment epithelium. The neurosensory retina contains millions of photoreceptors which convert light from the external environment into neural impulses. The retina is a multi-layered organ made up of multiple neuronal and non-neuronal cell types (Figure 1.3). The thickness of the retina varies: the thickest area is close to the optic nerve, which is over 0.23 mm. The optic disc is the area where ganglion cell axons exit the eye and it is also the entrance for the central retinal vessels. It is approximately 1.5mm-1.75mm in diameter and there are no photoreceptors located in this area. No visual transduction can therefore occur here which is known as the "blind spot". The central retina, also known as posterior pole, is a 5-6 mm diameter circular region called the macula lutea. The macula lutea appears yellow in colour, which is an important anatomic characterization, due to the abundance of xanthophyll carotenoid pigment in this region which helps protect the retina. The fovea centralis (also called the foveola) is a 0.35 mm diameter area in the centre of the macula lutea. It is the most sensitive part of the retina and is where the image focuses. In this area, the cone photoreceptors reach maximum density, at almost 15000 cells/ mm^2. Cone concentration decreases rapidly from the centre to the rim, where there are 4000-5000 cells/ mm^2.
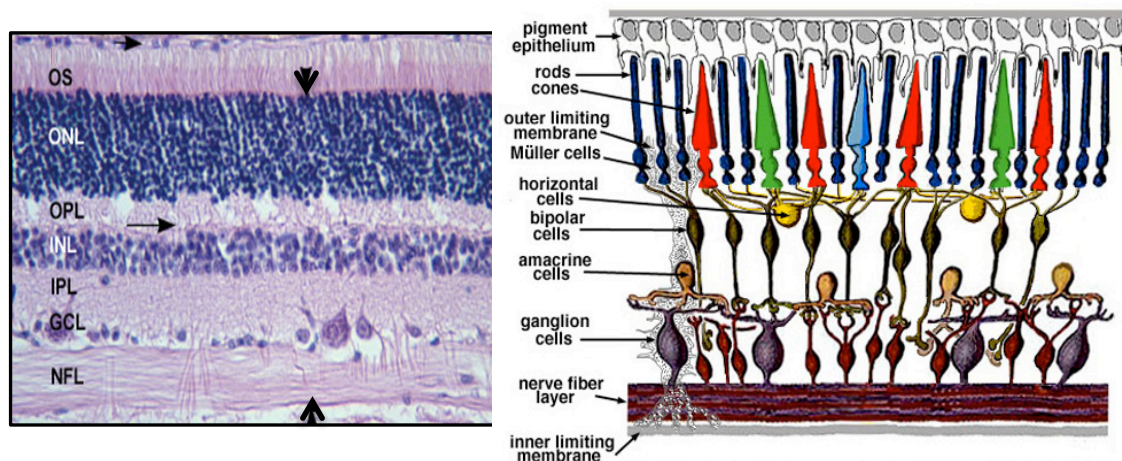
Figure 1.3 Histological image (transverse section) of the retina (left) and schematic diagram of cells types of retina (right). Nerve fiber layer (NFL), ganglion cell layer (GCL), inner plexiform layer (IPL), inner nuclear layer (INL), outer plexiform layer (OPL), outer nuclear layer (ONL), outersegment (OS). Arrow (short)- retina pigment epithelium (RPE), arrow (long)-middle limiting membrane, arrowhead (upper)-outer limiting membrane, arrow (lower)-inner limiting membrane. Images from "the eye" www.theness.com/images/blogimages/retina.jpeg and www.vetmed.ucdavis.edu/.../archive/s_4661_a.jpg

1.10.1 The Retina Pigment Epithelium

The retinal pigment epithelium (RPE) is a monolayer of hexagonal cells, which extends from the optic nerve head to the ora serrata. The thickness of the RPE is greatest in the macula and tends to be thinner at the periphery. It has numerous functions, including maintaining adhesion of the neurosensory retina; acting as a barrier between the choroid and neurosensory retina (the blood-retinal barrier); absorbing light and reducing light scatter in order to improve image resolution and transporting and storing metabolites and vitamins. It also plays a key role in phototransduction, recycling the visual pigment to the photoreceptors as well as in maintenance of the photoreceptors, including turnover of the outer segment.

1.10.2 The Neurosensory Retina

Within the retina, there are several neuronal cell types, specifically photoreceptor cells (PR), horizontal cells (HC), amacrine cells (AC), bipolar cells (BC) and retinal ganglion cells (RGC). Their cell bodies are organised in three nuclear layers with PR nuclei in the outer

nuclear layer (ONL), HC, AC and BC nuclei in the inner nuclei layer (INL) and RGCs in the innermost layer (Figure 1.3).

1.10.2.1 Photoreceptors

There are two kinds of photoreceptors (Figure 1.3), the rods and the cones. Cones have a maximum density in the fovea, while rods are mainly present in the more peripheral retina. They are responsible for phototransduction: the transduction of light to an electrical signal. Cone photoreceptors are responsible for colour vision and enable high spatial but low light sensitivity. In the human, there are 3 types of cones which are sensitive to blue, green or red light. Rod photoreceptors have relatively low spatial acuity and low sensitivity to colour. However, they have highly light sensitivity for vision in low light environments, and are important in detection of motion. The foveal region contains the highest density of cone photoreceptors and a low density of rod photoreceptors; the peripheral retina contains the lowest density of cone photoreceptors and highest of rod photoreceptors. Photoreceptors are located in the outer layer of the retina and their nuclei make up the outer nuclear layer.

1.10.2.2 Bipolar cells, Horizontal and Amacrine cells

Bipolar cells are located in the mid-layers of the retina with their cell bodies in the inner nuclear layer (Figure 1.3). The dendrites of bipolar cells receive input from either cones or rods, giving two main types of bipolar cell, the rod bipolar type and cone bipolar type. At their distal end, bipolar cells synapse with ganglion cells transmitting the signal between these two cells. The ratio of bipolar/photoreceptor cells is higher in the central compared to peripheral retina, which enables greater acuity in the foveal region. The bipolar cells also have input from horizontal cells.

Horizontal and amacrine cells are located in the outer and inner parts of the inner nuclear layer respectively. They can communicate laterally across the retina, modifying and integrating the information that comes from the photoreceptor and bipolar cells.

1.10.2.3 Ganglion cells

Ganglion cells are located in the inner region of the retina and are the last part of the neuronal pathway in the retina (Figure 1.3). There are approximately 1.2-1.5 million retinal ganglion cells in the human retina. In the macula, there are up to seven layers of RGCs. This is because in this region there is up to 1 photoreceptor cell vs 1 RGC to enable high visual acuity. The thickness of the retinal ganglion cell layer decreases from the fovea (60-80um) to the peripheral retina (10-20um). Their cell bodies exist in the ganglion cell layer and their axons form the nerve fibre layer. At the optic disc, the ganglion cell axons assemble passing through the lamina cribrosa in the optic nerve head, to form the optic nerve.

1.10.2.4 Retinal neuroglia

The retinal neuroglia supports retinal neurons, with critical roles in assisting several processes, such as metabolic support, neurotransmitter uptake and immune function. Müller cells are the major glial cells in the retina (Figure 1.3). The cells extend from the inner limiting membrane to the outer limiting membrane with their nuclei in the INL. They ensheath blood vessels and neuronal cells. Astrocytes are mainly located between the nerve fibre layer and inner nuclear layer. They display a perpendicular direction to the neuronal cell bodies and Müller cells. Microglia cells are located predominantly in two areas: the junction between the nerve fibre layer and the ganglion cell layer and the junction of the inner nuclear layer and the outer plexiform layer. They provide immune function in the retina.

1.11 The blood supply of the retina

The retina is an extremely active tissue, consuming more oxygen than any other human tissue and it therefore requires a large blood supply. In the human, a branch from the central retinal vessel supports the inner two-thirds of retina, while the choroidal circulation supports the outer one-third. The central retinal artery comes from the ophthalmic artery and enters the eye via the optic disc. There are four branches: the superior nasal and temporal arteries and the inferior nasal and temporal arteries. There are also capillary networks throughout the retina. The density of capillaries in the macula is higher than any other part of the retina and the density reduces towards to the peripheral retina. In the central fovea, there is a 0.5mm diameter area that is capillary-free. The retinal veins are located with the retinal arteries, and the central retinal vein leaves via the optic nerve head.

1.12 Glaucoma

1.12.1 What is glaucoma

Glaucoma is an optic neuropathy resulting in a progressive and irreversible deficit of visual field, which is defined with both defects of optic disc structure and visual functions (Foster, Buhrmann et al. 2002; Agarwal, Gupta et al. 2009; Quigley 2011). The functional and structural defects are due to the progressive death of retinal ganglion cells and loss of their axons in the optic nerve (Quigley 2011). Glaucoma is the second leading cause of blindness in the world (Coleman 2003).

1.12.2 Classification of glaucoma.

Glaucoma is divided into primary and secondary glaucoma, according to the cause of the disease. It is further subdivided into open-angle glaucoma and closed-angle glaucoma (Figure 1.4) according to the structural changes in the anterior chamber angle (Figure 1.4 & 1.5). Open angle glaucoma, the angle between the iris and the cornea remains open. In closed angle glaucoma, drainage through the trabecular meshwork is physically blocked by surround tissue. Primary open angle (POAG) and primary angle closure glaucoma (PACG) are further subdivided (Figure 1.4), depending on whether intraocular pressure is raised and natural history, respectively.
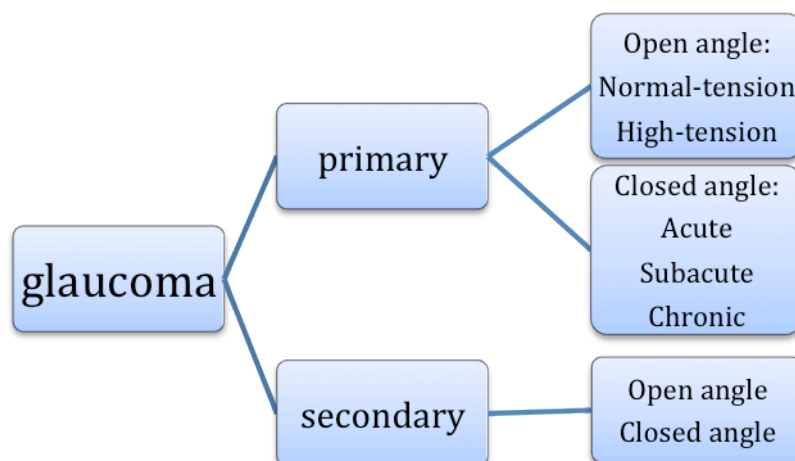
Figure 1.4 Classification of glaucoma. Chart modified from the book Glaucoma identification & co-management (Rudnicka and Owen 2007).
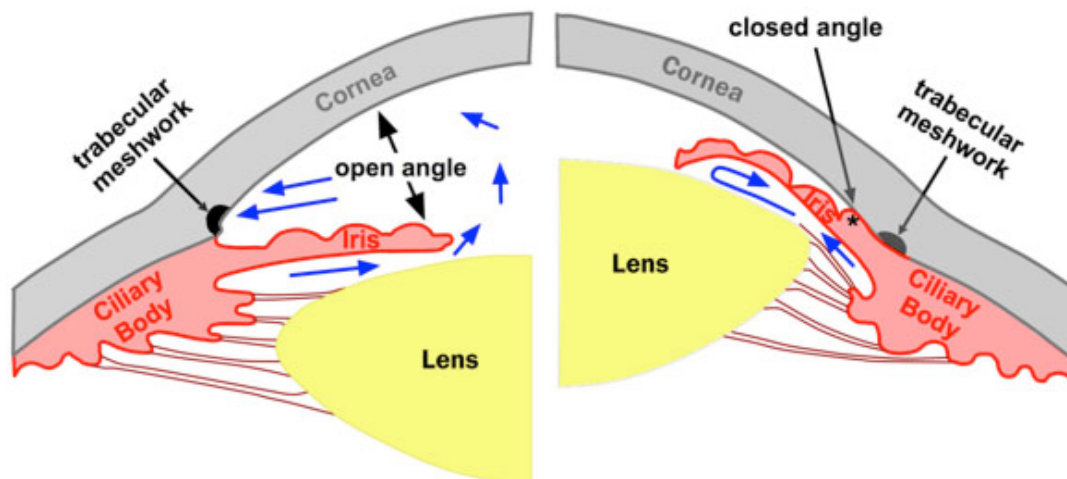
Figure 1.5 The comparison of primary open angle glaucoma (POAG) and primary angle closure glaucoma (PACG). In POAG there is a decrease in rate of drainage through the trabecular meshwork causing an increased IOP, but the angle remains open; in PACG the iris blocks the trabecular meshwork and the angle is closed.Image from "Med Rounds publications" http://webeye.ophth.uiowa.edu/dept/service/glaucoma/images/open-closed.jpg

1.12.3 Prevalence and risk factors

Population-based studies have shown that approximately 2.5% of people over 40 years have glaucoma worldwide (Quigley 2011). This causes significant levels of blindness, for example in China it has been shown that of 9.4 million people suffering from glaucoma, 55% of them are blind in one eye and 18.1% of them have fully lost vision of both eyes (Foster and Johnson 2001).

The POAG is responsible for the majority of cases of glaucoma in white and black people in the America, Europe and Africa (Racette, Wilson et al. 2003; Weinreb and Khaw 2004; Giangiacomo and Coleman 2009), although it has recently been established that the prevalence of PACG is increasing in these areas (Day, Baio et al. 2012). In Asian countries, angle closure glaucoma is the major form of glaucoma (Foster and Johnson 2001; Foster, Buhrmann et al. 2002) and 87% of people with ACG worldwide are of Asian origin (Giangiacomo and Coleman 2009).

Intraocular pressure (IOP) is the key risk factor for glaucoma development. In the healthy condition, mean IOP is 16mmHg and normally ranges from 10 to 21 mmHg. The Barbados Eye Studies demonstrated that prevalence of OAG was closely related to the IOP level. Specifically, the study found that with each 1mmHg increase in IOP was increased the chance of developing OAG by approximately 12% (Nemesure, Honkanen et al. 2007). Furthermore, the Advanced Glaucoma Intervention study of PACG patients indicated that patients with IOP $\geq$ 16mmHg 5 years after initial intervention, had a greater loss of visual field compared to those with an IOP < 16mmHg (Inatani, Iwao et al. 2008). However, reducing IOP does not absolutely prevent progression of glaucoma (Hitchings 2004).

In addition, elevated IOP is not an essential requirement for glaucoma development, and some glaucoma patients have normal intraocular pressure (NPG). Approximately 30-40% of POAG patients fail to show increased IOP but have visual defects (Hoyng and Kitazawa 2002). Treating NPG by lowering IOP can slow down the progression of glaucoma, but still does not prevent the occurrence of glaucomatous neuropathy (Heijl, Leske et al. 2002). Although the causes of NPG are not clear, vascular dysregulation has been proposed as an important risk factor for NPG (Hitchings 2004) and ocular perfusion pressure fluctuations have been shown to play a significant role in visual field progression in NPG (Sung, Lee et al. 2009).

The IOP has been shown to slightly increase with age (Bonomi, Marchini et al. 1998). The prevalence of both of POAG and PACG is closely related to age (Foster and Johnson 2001; Yoshida, Okada et al. 2001) and epidemiological studies have reported that people who are over 70 years of age have 3-4 times the risk for glaucoma compared to people who are between 40 and 50 years old (Rudnicka and Owen 2007). Prevalence of glaucoma also relates to race. In American, black people have a six times higher chance of getting POAG compared with white people of the same age. Progression of POAG is also more rapid in black people compared to white (Racette, Wilson et al. 2003). Also, people who have myopia have a higher risk of glaucoma. In the Blue Mountains Eye Study, based on 3654 Australians aged 49 to 97 years old, people with myopia were found to have a 2 to 3-fold higher risk of developing glaucoma compared to non-myopia people independent of other factors (Mitchell, Hourihan et al. 1999; Giangiacomo and Coleman 2009). Family history is another high risk factor for glaucoma (Tielsch, Katz et al. 1994; Kong, Chen et al. 2011). For example, in the study of a Chinese population, it has been found that the siblings of patients with PACG had

as high as a 50% chance of heritability of a narrow angle and therefore susceptibility to PACG (Amerasinghe, Zhang et al. 2011).

1.12.4 Diagnosis of glaucoma

To diagnose glaucoma, several tests are performed, including measurement of IOP, visual field tests and optic nerve assessment. Tonometry is the most common method to measure the IOP. However, as discussed earlier, IOP is not always raised in patients with glaucoma. In glaucoma, there is a loss if visual field, therefore perimetry checks are used to detect whether visual field is affected. In addition, optic nerve head examination is used to determine the presence of glaucoma. In the healthy retina, there are about 1.2 million ganglion cell axons exiting the eye at the optic nerve head. Since retinal ganglion cells die in the glaucoma, their axons are lost and this can be detected at the optic nerve head. The optic cup is enlarged in glaucoma patients (Figure 1.6) (Garway-Heath, Ruben et al. 1998; Williams 2007). Normally, the ratio of cup size/ disc size is smaller than 0.5 and increases in glaucoma. However, this number may be variable between patients, including effects of race (Garway-Heath, Ruben et al. 1998). Therefore, if a patient has one of the following conditions, it is proposed the optic disc has been damaged by glaucoma (Williams 2007):

1.   The ratio of cup size/disc size is above 0.5.

2.   The vertical cup/disc ratio is bigger than the horizontal cup/disc ratio.

3.   There is asymmetry between the cup/disc ratios of the two eyes of more than 0.2.
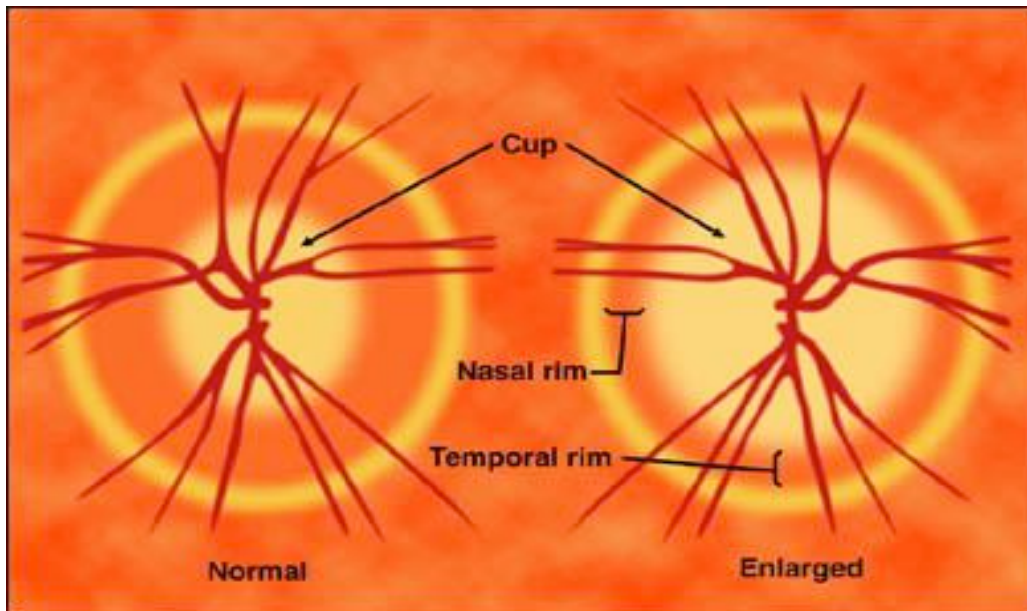
Figure 1.6 The optic nerve head and optic cup. The optic cup is located at the center of the optic nerve head. In the normal optic nerve head (left) the ratio of cup size to optic disc size is approximate 0.3; in the glaucoma one (right) the ratio is approximate 0.9. Image from http://www.e-sunbear.com/glauc_diag.html

1.13 Pathogenesis of glaucoma

There are two main hypotheses relating to the pathogenesis of glaucoma, the mechanical hypothesis and the vascular hypothesis. The mechanical hypothesis relates to damage as a result of elevated IOP. The vascular hypothesis relates to vascular dysregulation resulting in decreased blood flow to the retina leading to RGC cell death.

It is most likely that the pathological process involves both of these factors and that in most cases (where IOP is raised) they act together to lead ultimately to occurrence of neurodegeneration in the glaucoma. Each hypothesis is described in further detail below.

1.13.1 The mechanical theory of glaucoma

Intraocular pressure plays an important role in maintaining physiological function and structure of the eye. However, elevated IOP is the primary risk factor for glaucoma and leads to structural and functional defects (Quigley 2011). It has been shown that raised IOP leads to RGC death in many experimental models, including in mouse (Tsuruga, Murata et al. 2012),

rat (Biermann, Oterendorp et al. 2012), rabbit (Solomon, Kimron et al. 2003), monkey (Sasaoka, Nakamura et al. 2008) and pig (Ruiz-Ederra, Garcia et al. 2005).

Increased IOP has been shown to affect the stress-strain in the optic nerve head. The forces on the scleral shell, the lamina cribrosa and the scleral canal are proposed to ultimately lead to damage to the retinal ganglion cell axons causing death of the RGCs (Claude, Burgoyne et al. 2005) (Figure 1.7). The lamina cribrosa is considered as a weak spot biomechanically because of its discontinuity with the corneo-scleral shell (Downs, Roberts et al. 2011; Strouthidis and Girard 2013). The lamina cribrosa is where retinal ganglion cell axons exit the eye globe (Strouthidis and Girard 2013). Figure 1.7 shows a model to demonstrate the compressive strain in the lamina region with IOP at the normal level (15mmHg) and elevated level (25mmHg). Retinal optic nerve head (ONH) start to remodel when exposed chronically to elevated IOP and eventually changes its morphology becoming "cupped" (Downs, Roberts et al. 2011). Elevated IOP has been shown to change the specific extracellular matrix (ECM) in the retinal ganglion cell layer, and ECM remodeling is a proposed link with RGC death in glaucoma (Guo, Moss et al. 2005).
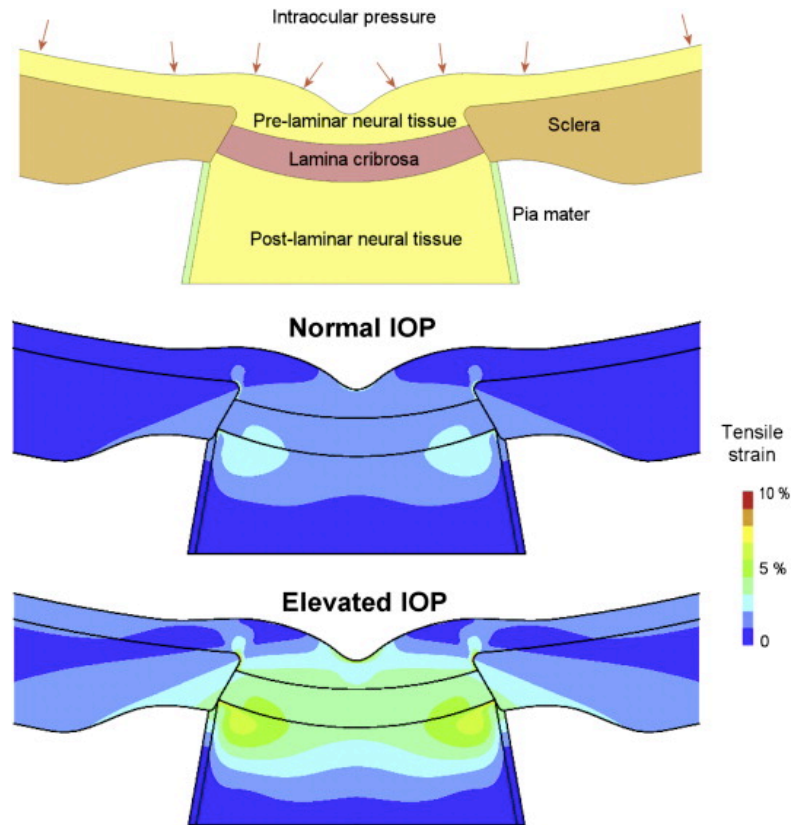
Figure 1.7 Prediction model of IOP-related tensile strain in the lamina region. The of tensile strain impact in the optic nerve head of (middle) normal IOP (12.5mmHg) and (bottom) elevated IOP (25mmHg) were predicted (Downs, Roberts et al. 2011).

The stress-strain from elevated IOP has also been shown to affect axoplasmic transport at the point that the axon passes through the lamina cribrosa (Guo, Moss et al. 2005). Early experiments in a monkey model of glaucoma showed that when IOP was elevated moderately there was an incomplete blockade of transport at the lamina cribrosa, and a complete blockade occurred when the IOP was elevated to 25mmHg (Anderson and Hendrickson 1974). With acute elevation of IOP to 30mmHg, blockade of transport was observed within 1 hour at the lamina cribrosa (Anderson and Hendrickson 1974; Quigley and Anderson 1976), indicating that flow along the axon from the brain to the retina (retrograde) was being interrupted. The retina axonal transport obstruction at the lamina cribrosa was independent of blood supply indicating that mechanical compression rather than decreased blood flow was responsible for the changes was observed (Minckler, Bunt et al. 1977; Geijer and Bill 1978). Further experiments showed that there was an interruption to axonal transport in both

orthograde and retrograde directions (Minckler, Bunt et al. 1977). Significantly there was a lack of movement of neurotrophin from the brain to the retina. Neurotrophin has an essential and potent effect on neurons survival (Almasieh, Wilson et al. 2012). In particular, brain derived neurotrophic factor (BDNF), transports retrogradely to the RGCs and has been shown to have a protective role in RGCs survival under axonal insult (Quigley, McKinnon et al. 2000; Almasieh, Wilson et al. 2012). BDNF was found to be deprived in the ONH and superior retina when exposed to 40mmHg IOP for 7days (Johnson, Deppmeier et al. 2000). Overexpression of BDNF in the rat glaucomatous model using gene therapy, promoted RGC survival compared to untreated group (Martin, Quigley et al. 2003). Therefore, BDNF deprivation as a result of mechanical stress at the optic nerve head may play an important role in IOP induced RGCs death.

1.13.2 Vascular factors

Abnormalities of retinal blood flow are associated with glaucoma (Yanagi, Kawasaki et al. 2011) and the age-related decrease in perfusion to the brain and the eye has been identified as an important risk factor for glaucoma (Guo, Moss et al. 2005; Agarwal, Gupta et al. 2009). Reduction of retinal blood flow can occur directly via changes to retinal perfusion or indirectly due to IOP elevation. Due to the high oxygen requirement of the retina, it requires a large amount of blood flow, supplied from the central retinal artery and choriocapillaris (Figure 1.8). The ocular blood flow provides nutrients and oxygen to meet the metabolic requirement of the retina. Therefore a reduction in blood flow will limit this supply. In addition, interruption of blood flow also causes accumulation of metabolic waste (Osborne, Casson et al. 2004). These factors are all proposed to contribute to RGC death in glaucoma.
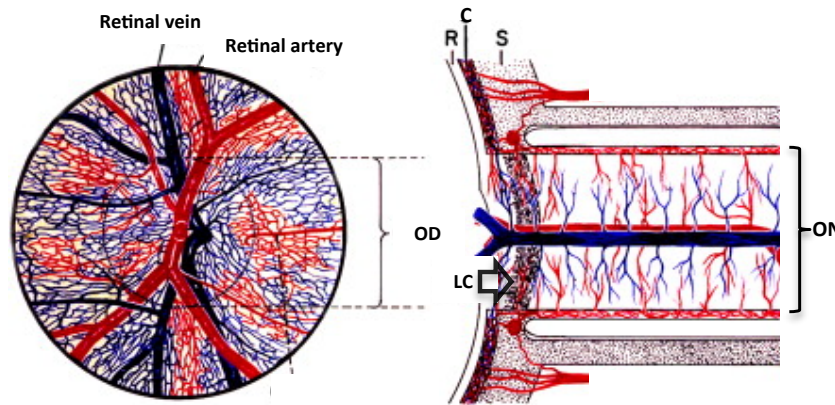
Figure 1.8 Diagram of retinal blood supply showing distribution to the retina, optic disc and optic nerve. OD, optic disc; LC, lamina cribrosa; R, retina; C, choroid; S, sclera; ON, optic nerve (Hayreh 2008).

Reduced retinal blood flow can be caused by IOP induced lamina cribrosa deformation. The central retina vessels pass through the lamina cribrosa, therefore, retinal vessels will be compressed when the lamina cribrosa is strained by elevated IOP (Hayreh 2008). Furthermore, IOP elevation also can reduce blood flow by impacting of perfusion pressure. Clinically, ocular perfusion pressure (OPP) is down-regulated with increased IOP and up-regulated by increased mean blood pressure (BP_m). The equations are shown below (BPd = diastolic blood pressure; BPs = systolic blood pressure) (Okuno, Sugiyama et al. 2004).

$$BP_m = BP_d + 1/3(BP_s - BP_d)$$

$$OPP = 2/3BP_m - IOP$$

There has been much research into the effect of ischemia on the retina. Experimental studies of retinal ischemia in vivo are mostly induced by IOP elevation or retinal artery ligation. It has been shown previously that the retina can tolerate relatively short periods of acute ischemia without irreversible damage (Sohan and Thomas 1980; Selles-Navarro, Villegas-Perez et al. 1996). However for more extended periods of ischemia RGC death is observed over the following reperfusion period. Elevating IOP to induced retinal ischemia (Nucci, Tartaglione et al. 2005; Huang, Fileta et al. 2010; Biermann, van Oterendorp et al. 2012) has

shown pathological features which are similar to those that occur in glaucoma patients (Nucci, Tartaglione et al. 2005). Inducing retinal ischemia in the rat by elevating IOP for 60min followed by 10 days reperfusion caused retina ganglion cell number to reduce with some inner retinal layer thinning compared with the outer retinal layers (Osborne, Ugarte et al. 1999). This suggested that RGCs are vulnerable to ischemic stimulation. Using the same rat model it has also been shown that the RGC number was reduced significantly and the cell loss was increased as the reperfusion time was prolonged (Selles-Navarro, Villegas-Perez et al. 1996; Nucci, Tartaglione et al. 2005). This may suggest that there is a secondary loss of following the initial ischemic insult. In human retinal explants, it has also been shown that simulated ischemia (oxygen/glucose deprivation) leads to RGC death (Niyadurupola, Sidaway et al. 2011). Experimental evidence therefore indicates that retinal ischemia causes RGC death supporting the hypothesis proposing a vascular contribution to glaucoma pathophysiology.

1.13.3 Excitoxicity

Glutamate is the most common excitatory neurotransmitter in the retina and necessary for neural communication in the retina (Thoreson and Witkovsky 1999). However, it is neurotoxic in concentrations that are higher than the normal physiological level (Choi and Rothman 1990). It has been shown to be released excessively by retinal cells under conditions that simulate the pathological situation (Osborne, Melena et al. 2001). For example, in retinal ischemic insult, glutamate level was shown to increase drastically (Neal, Cunningham et al. 1994; Osborne, Ugarte et al. 1999) and excessive glutamate has been shown to be toxic to RGCs (Vorwerk, Lipton et al. 1996; Yasumasa, Wei et al. 1998; Martin, Levkovitch-Verbin et al. 2002).

It has been shown that retinal ganglion cells highly express both NMDA receptor as well as non-NMDA glutamate receptors (Chen and Diamond 2002; Shen, Liu et al. 2006; Zhang and Diamond 2006). NMDA receptors are the primary glutamate receptors relevant to excitoxicity which is triggered by increased glutamate level (Agarwal, Gupta et al. 2009). NMDA receptors are non-selective cation channels and are highly permeable to Ca^{2+} and Na^+. The excessive extracellular glutamate leads to NMDA receptors being over stimulated, which result in prolonged calcium influx, which in turn mediates cell death (Ikeda, Dawes et al. 1992).

Mg^{2+} is a voltage-dependant ion blocker for NMDA receptors (Zeevalk and Nickias 1992; Osborne, Casson et al. 2004). During retinal ischemia, the energy failure, and spatial loss of ATP, leads to decrease activity of the Na^+/K^+-ATPase consequently affecting membrane potential, causing the cells to remain depolarized. In depolarized cells, the Mg^{2+} block of the NMDA receptor is lifted, further contributing to NMDA receptor action during retinal ischemia (Almasieh, Wilson et al. 2012). In addition, depolarization is caused by non-NMDA glutamate receptors, lifting the Mg^{2+} block and contributing to over-activation of the NMDA receptor to induce excitotoxicity.

The glutamate transporting system has also be shown to be affected during the retinal ischemia (Barnett, Pow et al. 2001). Glutamate uptake was predominantly by Müller cells, which have a major role in maintaining glutamate at low levels under normal physiological conditions in the retina (Barnett, Pow et al. 2001; Casson 2006). However, the function of Müller cells is also compromised when exposed to excessive extracellular glutamate. The process of Müller cell uptake of glutamate is dependent on the level of ATP, since it is driven by the Na^+ and K^+ gradient which is maintained by the Na^+/K^+-ATPase (Casson 2006). During retinal ischemia, ATP deficiency will therefore further elevate glutamate levels due to the loss of activity of the transport mechanisms. As the failure of Na^+/K^+-ATPase, intracellular Na^+ concentration will rise which reverses the glutamate uptake transport into Müller cell (Napper, Pianta et al. 1999; Barnett, Pow et al. 2001).

One of the important mechanisms of excitoxicity induced cell death in retinal cells is increase Ca^{2+} influx which causes intracellular Ca^{2+} overload and death of neurons (Osborne, Ugarte et al. 1999). NMDA receptors are highly calcium permeable (Osborne, Casson et al. 2004) and therefore when they are activated by excessive glutamate and allow massive calcium influx (Choi and Rothman 1990), that will stimulate calcium dependent and related processes consequently which eventually lead to cell death .

1.13.4 Mitochondrial dysfunction and oxidative stress

The mitochondria is a crucially important organelle in maintaining cellular homeostasis and can be described as an "energy factory" which produces ATP by oxidative phosphorylation, and supplies the majority of ATP requirements for cell fucntion. It also has other roles to play including regulation of intracellular Ca^{2+} concentration, which will be described in the

following section. Moreover, mitochondria involved in cell apoptosis by generating reactive oxygen species (ROS), and releasing apoptotic proteins into the cytosol, such as cytochrome C (Cheung, Yip et al. 2003; Osborne 2010).

Mitochondria dysfunction has been hypothesized as an important factor in glaucoma progression. Glaucoma is an age-related retinal neurodegeneration (Mitchell, Smith et al. 1996; Kong, Van Bergen et al. 2009), and mitochondrial function declines in efficiency as age increases (Chan 2006). Moreover, it is proposed that disruption to mitochondrial function by retinal ischemia or elevated IOP leads to the loss of supply of ATP to the RGCs (Osborne 2010). This has been observed in the mouse optic nerve, where a decrease in ATP content was seen with age, and this decrease was promoted by elevated IOP and is proposed to contribute to RGC axonal loss (Baltan, Inman et al. 2010).

The depletion of ATP also impacts the ATP-dependent ion transport, such as the sarco(endo)plasmic reticulum Ca^{2+}-ATPase (SERCA) and Na^+, K^+-ATPase. Approximately 60% of energy in the brain is consumed by cation transport through Na^+, K^+-ATPase and SERCA under the physiological conditions (Ames 2000). Ion homeostasis is essential for neuronal cell function.

Further to this, ROS are generated constantly by normal metabolic activities in the mitochondia, such as oxidative phosphorylation and redox reactions (Brasnjevic, Hof et al. 2008). They are removed by antioxidant enzymes, like catalase and glutathione peroxidase, which are necessary to keep physiological homeostatic conditions. Some primary antioxidant enzymes have been found to have decreased activities in peripheral blood of patients with POAG (Majsterek, Malinowska et al. 2011), which resulted in accumulation of ROS.

Above all, regardless of the primary insult, calcium is an important intermediary to determine cell life or death. Elevation of calcium influx is one of the crucial factors mediating cell death (Figure 1.10).
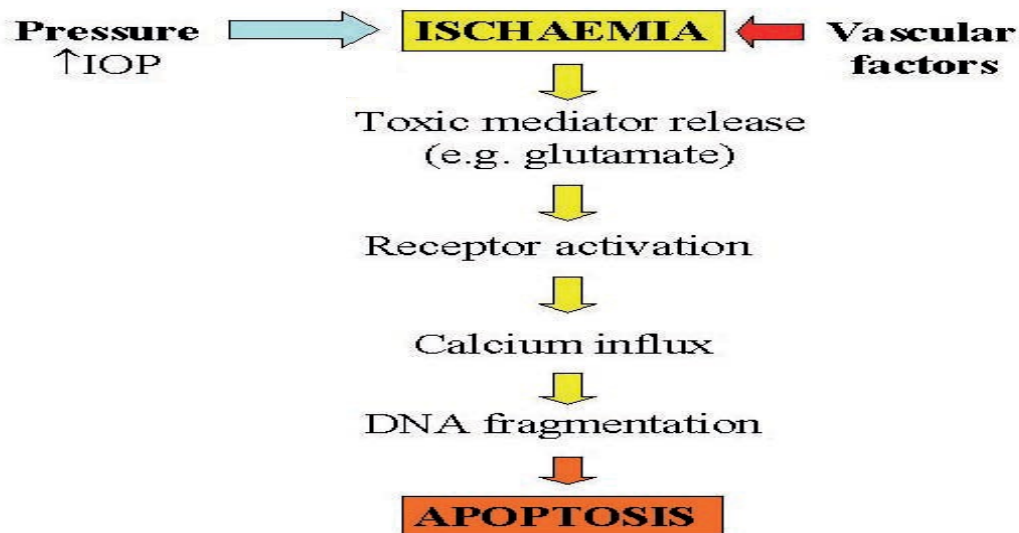
Figure 1.9 The pathology of glaucoma (Williams 2007).

1.14. Calcium

Calcium is an essential element in maintenance of normal physiological function of cells (Berridge 2004). It is a versatile and universal messenger regulating intracellular physiological processes, such as fertilization, proliferation, metabolism and secretion (Berridge, Bootman et al. 1998; Berridge, Lipp et al. 2000). Disruption of cellular homeostasis of calcium therefore impacts directly on physiological function, which in turn could lead ultimately to cell death. Calcium regulation is therefore of great interest in relation to the pathophysiology of numerous diseases, including glaucoma.

1.14.1. Mechanisms of intracellular calcium homeostasis and signaling
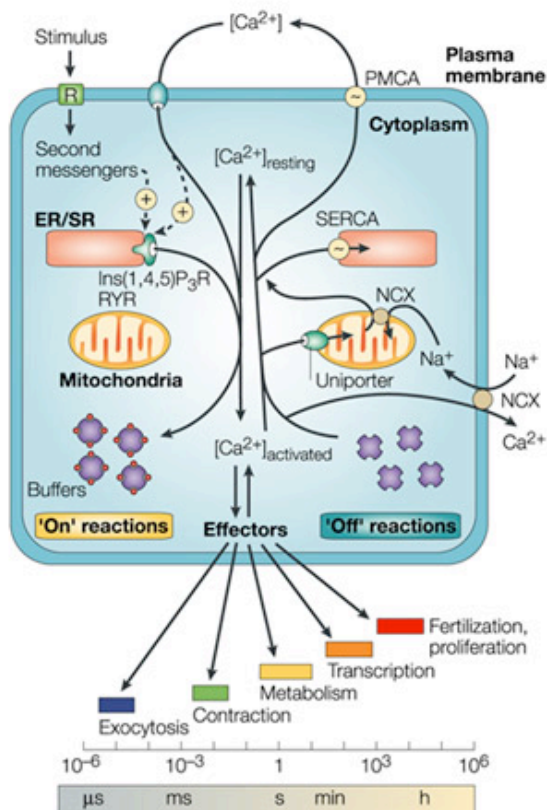
Figure 1.10 Intracellular calcium regulation and cell signaling. ER/SR: endoplasmic/sarcoplasmic reticulum, NCX: Na^+/Ca^{2+} exchanger, PCMA: plasma-membrane Ca^{2+}- ATPase, SERCA: sarco(endo)plamic reticulum Ca^{2+}- ATPase. Image from Berridge, 2003.

In the normal physiological situation, the intracellular calcium ion concentration is typically 0.1-1μM in the resting cell, which is around 10,000 times lower than the extracellular concentration (Hernandez-Fonseca and Massieu 2005). The cell is able to maintain the large electrochemical gradient, which in turn enables calcium signaling, due to the cooperation of Ca^{2+} pumps, exchangers and channels, which are present on the plasma membrane and membranes of the intracellular organelles (Figure 1.10).

1.14.2. The "off " reactions

In order to maintain intracellular Ca^{2+} homeostasis, there are a number of processes which remove Ca^{2+} from the cytoplasm (shown as the "off reaction" in Figure 1.10). The Na^+ / Ca^{2+} exchanger (NCX) and the plasma membrane Ca^{2+}-ATPase (PMCA) play principal roles in exporting Ca^{2+} from the cytoplasm against its electrochemical gradient to prevent Ca^{2+}

overload in cytoplasm (Guerini, Coletto et al. 2005). The NCX is a low affinity exchanger but has high Ca^{2+} transporting ability. NCX typically exchanges 3 Na^+ for 1 Ca^{2+}. Because the exchanger is driven by the Na^+ gradient, the rate of extrusion of Ca^{2+} by the NCX is reduced when the intracellular Na^+ concentration is increased (Guerini, Coletto et al. 2005). ATP levels and low cellular pH will also affect the exchanger because they will increase intracellular Na^+ concentration (Lee, Yu et al. 1994)). Importantly, the NCX can switch directions and allow Ca^{2+} influx once a critical concentration of Na^+ is reached.

In mammalian cells, the Na^+/Ca^{2+} exchanger comprises three isoforms, NCX1-3. It has been observed that NCX2 and NCX3 are highly expressed in the rat CNS (Lee, Yu et al. 1994). It has been reported that NCX1 is expressed throughout all the mouse retinal layers with higher density in the RGCL and IPL (Inokuchi, Shimazawa et al. 2009). Extraordinarily, the exchanger in the retinal rods and cones cells has been shown to import 4 Na^+ and extrude one Ca^{2+} and one K^+ (Cervetto, Lagnado et al. 1989; Prinsen, Szerencsei et al. 2000).

The plasma membrane Ca^{2+}-ATPase (PMCA) has a high Ca^{2+} affinity but low Ca^{2+} transporting capacity. PMCA can transport 1 Ca^{2+} when 1 molecule of ATP is hydrolyzed. PMCA is mainly regulated by calmodulin via the C-terminal region of the pump which contains a calmodulin-binding domain (Guerini, Coletto et al. 2005). When the level of intracellular Ca^{2+} is raised, Ca^{2+} combines with the calmodulin, which then binds to the calmodulin-binding domain, and the pump is activated. The C-terminal region also contains many others regulatory domains, such as phosphorylation sites for protein kinase A (PKA) and protein kinase C (PKC).

There are four isoforms of PMCA (PMCA1-4). PMCA1 and 4 are extensively expressed in human tissue, but PMCA2 and 3 are selectively expressed in the brain and heart (Guerini 1998). In the mammalian retina, all the PMCA isoforms were detected (Koulen, Fletcher et al. 1998; Krizaj, Demarco et al. 2002). Both PMCA2 and 3 highly stain the RGCL, IPL and inner side of INL (Krizaj, Demarco et al. 2002).

There are two stores for Ca^{2+} inside the cell: the endoplasmic reticulum (ER) and the mitochondria. The ER store is the most dynamic and is the principle source of intracellular Ca^{2+} used in Ca^{2+} signaling. The sarco(endo)plasmic reticulum Ca^{2+}-ATPase (SERCA) and

the mitochondrial Ca^{2+} uniporter remove free Ca^{2+} from the cytosol. The hydrolysis of ATP provides power to the SERCA pump to transport $2Ca^{2+}$ ions into the ER store against its electrochemical gradient. There are three isoforms of SERCA that have been identified, SERCA-1, SERCA-2 and SERCA-3.

In the mammalian retina, there has been shown to be no expression of SERCA-1 isoforms, whilst SERCA-2 isoforms are highly expressed in most mammalian retinal neurons, compared to SERCA-3 which is mainly expressed in the cone photoreceptors (Krizaj 2005).

The mitochondrial uniporter plays a significant role in modulating Ca^{2+} signaling. It is found in the inner membrane of the mitochondria (Kirichok, Krapivinsky et al. 2004; Raffaello, De Stefani et al. 2012) and is a highly selective calcium ion channel which enables uptake of Ca^{2+} from the cytosol down the Ca^{2+} electrochemical gradient (Kirichok, Krapivinsky et al. 2004). Ca^{2+} with calmodulin and in the cytosome are able to activate the mitochondrial uniporter.

1.14.3. The "on" reactions

Mechanisms which increase intracellular Ca^{2+} (shown as the "on" response in Fig 1.10) are mainly associated with the ER store and Ca^{2+} influx through plasma membrane. The release of Ca^{2+} from the ER store is mainly modulated by inositol 1,4,5-trisphosphate receptors (IP$_3$R) and ryanodine receptors (RyR). Both of these are calcium selective channels. Also both enable Ca^{2+}-induced Ca^{2+} release (CICR) which creates a positive feedback circuit to accelerate the increase in intracellular Ca^{2+} during Ca^{2+} signaling (Berridge 2009). In relation to the IP$_3$R, phospholipase C (PLC) hydrolyzes PIP$_2$ into Inositol 1,4,5-trisphosphate (IP$_3$) and diacylglycerol (DAG). Both DAG and IP$_3$ are second messengers. IP$_3$ activates the ER store IP$_3$Rs to release Ca^{2+} from the intracellular stores, whereas, the DAG (as well as Ca^{2+}) activates Protein Kinase C. The RyR is another type of calcium-releasing channel which is found on the ER membrane. There are two different mechanisms regulating calcium release by the RyR: CICR and DICR (depletion induced Ca^{2+} release). There are three isoforms of RyR (RyR1-3), which can be activated by low cytoplasmic Ca^{2+} concentration. In addition, Cyclic ADP-ribose (cADPR) can act as an endogenous stimulus at RyRs to induce Ca^{2+} release. In retinal cells, the RyR2 has been found was more widely expressed than other

RyRs (Shoshan-Barmatz, Zakar et al. 2007). In addition the IP_3Rs and RyRs, a number of TRP channels are suggested to play a role in Ca^{2+} release from the intracellular store, for example TRPP2 (Nilius, Owsianik et al. 2007).

At the plasma membrane Ca^{2+} influx is driven by the huge electrochemical gradient across the membrane, which is an effective way to increase the intracellular Ca^{2+}. Ca^{2+} enters the cells through different types of calcium channels, which include voltage-operated channels (VOCs), receptor-operated channels (ROCs), second messenger operated channels (SOCs) and store-operated channels (SOCs) (Figure 1.11). VOCs are expressed in most excitable cells; they are divided into two types, low-voltage-activated (also called T-type-transient) and high-voltage-activated (also called L-type-long-lasting). When depletion of the Ca^{2+} store occurs, SOCs will open and allow Ca^{2+} entry from the extracellular compartment to refill the ER (Nedergaard, Rodriguez et al. 2010). The transient receptor potential channels (TRP) are proposed to be an important kind of store-operated channel which can be activated by the depletion of ER Ca^{2+} store. ROCs respond to stimulation by neurotransmitters (Berridge, Bootman et al. 1998), include NMDA receptors (Berridge, Bootman et al. 2003) and $P2X_7$ receptors (McFadzean and Gibson 2002) which enable Na^+ as well as Ca^{2+} to pass through them when the receptors are activated. In relation to retinal neurons, the most important ROCs are NMDA and P2X receptors which respond to glutamate and ATP, respectively. SOCs regulate Ca^{2+} influx when the Ca^{2+} intracellular store is depleted.
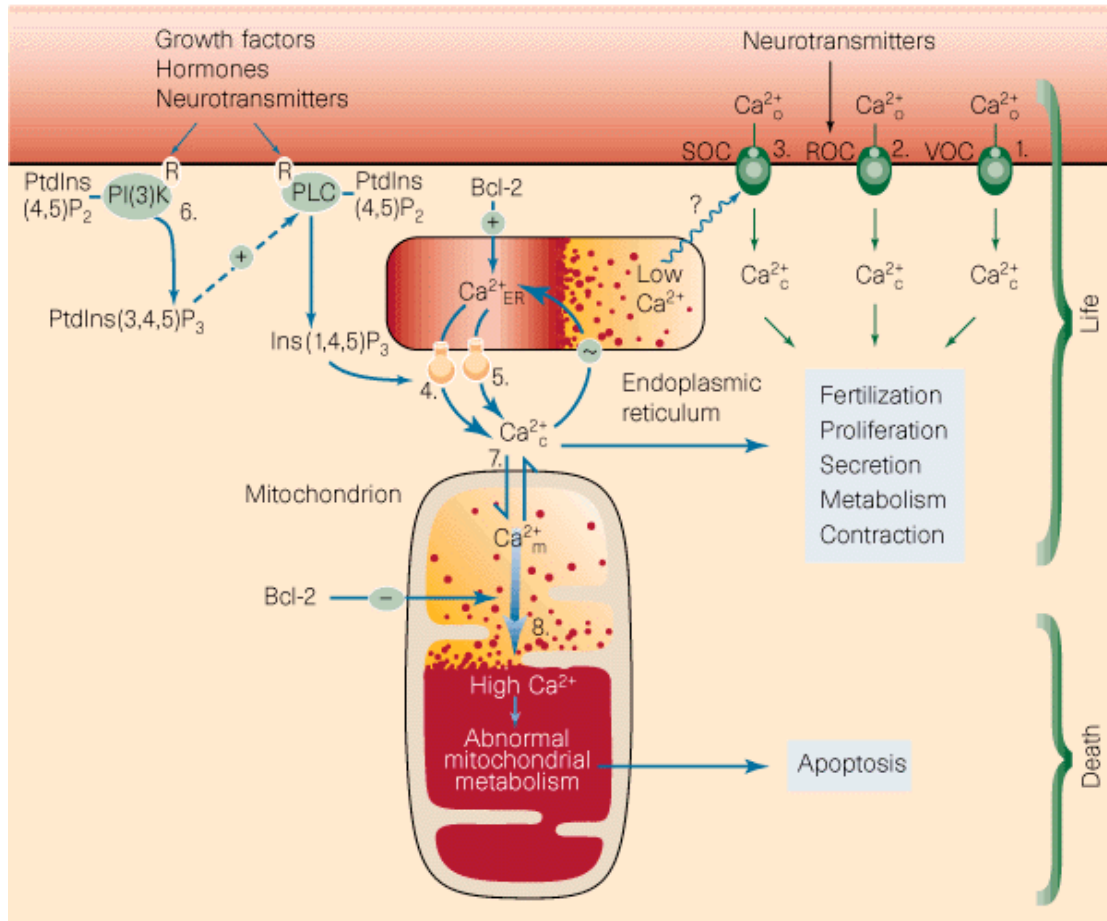
Figure 1.11 Mechanisms of cytoplasmic Ca^{2+} increase (Berridge, Bootman et al. 1998). Ca^{2+} ion can enter cell through store-operated calcium channels (SOC) (1), receptor-operated calcium channels (ROC) (2) and voltage-operated calcium channels (VOC) (3). Ca^{2+} also can be released from the intracellular store, ER, when it is activated by Inositol 1,4,5-trisphosphate (Ins(1,4,5)P3) (4), and also ryanodine receptors (5). Overload of the mitochondria can trigger cell death.

1.14.4. Calcium in retinal pathophysiology

As well as signaling in processes essential for life, Ca^{2+} signaling is one of the critical messengers in mediating cell death (Berridge, Bootman et al. 1998; Berridge, Bootman et al. 2003). Increasing intracellular Ca^{2+} beyond the physiological level, compromises neurons survival and results in neurons degeneration (Mattson 2007; Duncan, Goad et al. 2010). In the brain, excessive [Ca^{2+}]$_i$ associates with cell death induced by ischemic insult (Li, Inoue et al. 2011). The retina is part of the CNS, therefore they share similar mechanisms of neurodegeneration (Crish and Calkins 2011).

Intracellular calcium is mainly derived from two sources: release from intracellular stores and influx through Ca^{2+}-permeable channels in the membrane. Retinal ischemia initially results in ATP depletion and leads to membrane depolarization, which enhances influx of Ca^{2+} through VOCs and ROCs, as well as inhibition of ATP-dependent pumps (Osborne, Ugarte et al. 1999; Osborne, Casson et al. 2004; Crish and Calkins 2011) (Figure 1.11). At the same time other ions, including Na^+ and Cl^- enter the cell along with H_2O leading to cell swelling (Osborne, Casson et al. 2004; Bringmann, Uckermann et al. 2005). In addition, the increase in concentration of cytosolic Ca^{2+} has been shown to lead to activation of the mitochondrial uniporter and subsequent mitochondrial Ca^{2+} overload, which in turn leads to apoptotic cell death (Raffaello, Stefani et al. 2012).

Neuron cell membrane depolarization has effects on the glutamate releasing and uptake system causing glutamate to accumulate. Excessive glutamate will over-activate its receptors and further increase Ca^{2+} influx. These events will eventually cause intracellular Ca^{2+} overload and result in cell death through calcium-dependent or related pathways induced by $[Ca^{2+}]_i$ elevation activates proteases, phosphatases, lipases and endonuclease (Szydlowska and Tymianski 2010). Their over-activity induced by Ca^{2+} will disrupt the structure of the plasma membrane and organelles (Szydlowska and Tymianski 2010; Momeni 2011), which further perpetuates the cellular damage. $[Ca^{2+}]_i$ elevation also leads to an increase in generation of ROS (Carriedo, Sensi et al. 2000; Abramov, Scorziello et al. 2007; Feissner, Skalska et al. 2009), which mediates further damage.
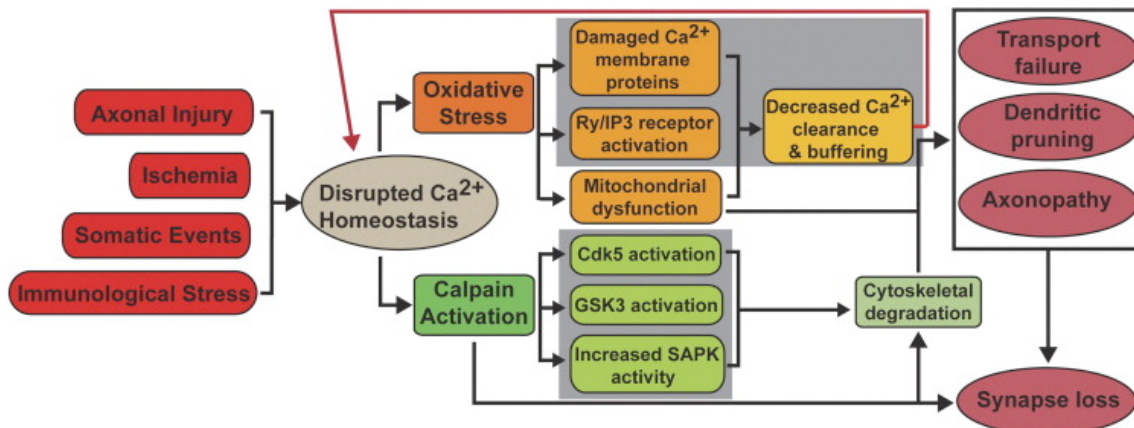
Figure 1.12 Mechanisms of Ca^{2+}disruption proposed to be involved in glaucomatous neurodegeneration (Crish and Calkins 2011). Multiple glaucomatous stressors disrupte Ca^{2+}homeostasis and consequently increase oxidative stress and simulated calpain activity.

1.15 Calpain

The calpains are a family of Ca^{2+} dependent, cytoplasmic cysteine proteases. Calpain activation has been proposed to be one of the most significant events involved in RGC death in glaucoma (Paquet-Durand, Johnson et al. 2007; Huang, Fileta et al. 2010). Calpain was first described in the rat brain by Guroff G (1964). To date, there are known to be 15 calpain genes in human (Sorimachi and Ono 2012). Calpain-1 (μ-calpain) and calpain-2 (m-calpain) are ubiquitous and are the most extensively studied calpain isoforms. They have similar characteristics but are activated by different Ca^{2+} concentration, micro-molar and milli-molar cytoplasmic Ca^{2+} respectively (Perrin and Huttenlocher 2002).

1.15.1. Calpain activation

Calpain has a critical role in physiological processes, such as signal transduction and gene transcription (Goll, Thompson et al. 2003). In transgenic mice knocking out calpain-1 and calpain-2, is embryo lethal (Arthur, Elce et al. 2000). Calpain-3 is a muscle-specific calpain, and deficiency of calpain 3 results in pathological changes related to muscular dystrophy (Topaloğlu, Dinçer et al. 1997; Richard, Roudaut et al. 2000). Uncontrolled calpain activation can lead to neuronal degeneration when [Ca^{2+}]$_i$ has become pathologically elevated, which leads to cell death through apoptosis or necrotic mechanisms (Huang and Wang 2001; Artal-Sanz and Tavernarakis 2005; Azuma and Shearer 2008).

Calpain activation is one of the significant event during cell apoptosis and necrosis (Perrin and Huttenlocher 2002). The most extensively studied consequence of calpain activation is proteolysis of cytoskeletal proteins. There are over 30 cytoskeletal proteins vulnerable to calpain activation (Nemova, Lysenko et al. 2010), including alpha-spectrin, tubulin and all three members of neurofilament family (Goll, Thompson et al. 2003). Uncontrolled calpain activity also damages Ca^{2+} channels and receptors of the plasma membrane and organelles (Momeni 2011), for example RyR (Rardon, Cefali et al. 1990) and inositol 1, 4, 5 triphosphate receptor (Magnusson, Haug et al. 1993).

Calpain activity can be regulated by several factors. The major regulating factor is cytoplasmic Ca^{2+} concentration and proteolysis is stimulated as the intracellular concentration of Ca^{2+} rises. The calcium requirement for half maximal activity of calpain-1 and calpain-2 is 3–50μM and 400–800μM, respectively (Goll, Thompson et al. 2003). Under normal condition, calpain activity is modulated by calpastatin, which is an endogenous and specific inhibitor of calpain (Goll, Thompson et al. 2003). This inhibition will be removed when intracellular Ca^{2+} becomes overloaded. Furthermore, calpastatin is degraded by caspase-3 and possibly as also by calpain itself (Orrenius, Zhivotovsky et al. 2003). Calpain also undergoes autolysis, which decreases the Ca^{2+} requirement for activation. Calpain activation has been shown in relation to many human diseases, for example stroke and neurodegeneration (calpain-1 and 2) (Rami 2003), muscular dystrophy (calpain-3) (Topaloğlu, Dinçer et al. 1997; Huang and Wang 2001; Azuma and Shearer 2008), and cataract (calpain-1 and 2) (Huang and Wang 2001).

1.15.2. Calpain inhibitors

The most common way to identify the involvement of calpain in models of disease is by use of calpain inhibitors. The addition of a calpain inhibitor, MDL 28170, in cerebral ischemia prevented infarct formation in rat (Markgraf, Velayo et al. 1998). In addition, MDL 28170 significantly protected cardiac function from injury caused by Ca^{2+} overload (Bi, Jin et al. 2012). Calpain inhibition was also shown to slow down cataract development in various models (Biswas, Harris et al. 2004; Morton, Lee et al. 2013).

1.15.3. Calpain activitation in retina

Calpain-1 and 2 are both expressed in the rat retina, although the mRNA for calpain-2 was 12 times higher than that of calpain-1 in rat retina (Tamada, Nakajima et al. 2005). Furthermore, calpain-1 was found to be expressed in relatively high amounts in RGC bodies in the rabbit retina (Croall and Demartino 1991). In addition to these two calpains, a further calpain isoform has been found in the rat retina, Rt88. This is a retina-specific calpain, which is a splice variant of calpain-3 (Azuma, Fukiage et al. 2000).

Loss of Ca^{2+} homeostasis is regarded as an important factor in RGC loss in glaucoma and there is increasing evidence to suggest that calpain activation plays an important role in the glaucoma (Azuma and Shearer 2008). For example, in a model using retina ischemia-reperfusion injury in rat, the calpain inhibitor SJA6017 was found to reduce RGC loss (Sakamoto, Nakajima et al. 2000). Also, in an experimental model of glaucoma with elevated IOP, calpain was be activated and was involved in mediation of retinal cell death (Nakajima, David et al. 2006; Huang, Fileta et al. 2010).

1.16 Aim of this thesis

The aim of this research was to develop a novel retinal planar sectioning technique to determine gene profiles in the retina and specifically in the retinal ganglion cell layer and to apply the information derived to investigation of Ca^{2+} dysregulation in the human retina in relation to glaucoma. A planar cryosectioning technique which separated RGCL from the retina was successfully developed. Using this technique together with gene array technology, the transcriptome of human RGCs was investigated. In addition the mRNA distribution for selected Ca^{2+}-signaling related proteins was determined in the human retina. Furthermore, the role of selected Ca^{2+}-signaling related proteins in retina ischemia induced RGC death were assessed using HORCs model.

Chapter 2

Materials and Methods

2.1 Materials

2.1.1 Human eye tissue

Human eyes were obtained from the East Anglian Eyebank (Norfolk & Norwich University Hospital, Norwich, UK) with ethical approval and under the tenets of the Declaration of Helsinki for human research. Eyes were donated for corneal transplant. Following removal of the cornea, globes were stored in Eagle's minimum essential medium (EMEM) (Sigma-Aldrich, Pool, UK) supplemented with 50 μg/ml gentamicin (Sigma-Aldrich, Poole, UK) and 10 μg/ml antibiotic/antimycotic solution (10,000 units/ml penicilin G, 10,000 μg/ml streptomycin sulphate and 25μg/ml amphotericin B) (Invitrogen, Paisley, UK). The retinal tissue was used within 24 hours post-mortem. Donor information included age, gender, cause and time of death, past ophthalmic history and medical history including current medication. In the research presented in this thesis 66 pairs of donor eyes were used with an age range of 37- 92. All the eyes used in this research were without retinal disease.

2.1.2 Eye dissections

Using sterile technique, the lens was removed from the globe by other group members. In order to dissect the retina, an incision of about 0.5 cm was made at the edge of the sclera. A circular scleral incision was cut around the edge of eyecup. The retina was dissected circumferentially just below the ora serrata. Following this, the neural retina was dissociated carefully from the RPE except at the optic nerve head. Using sharp scissors, the retina was removed from the eyecup by cutting around the optic nerve head. The neural retina was placed in a sterile cell culture dish and the vitreous humour removed. Due to the hemispherical shape, about four nicks of approximately 0.5 cm were made in order to allow the retina to flatten, before further samples were removed.

2.2 Planar section process

2.2.1 Preparation of macular samples for planar Cryo-sectioning

From each retina, a sample (4x4 mm) was taken from the macular region (Figure 2.1) using a surgical knife. This was identified by the yellow pigment of the macula lutea, and the position between the superior and inferior temporal vessels. Before mounting the sample, a cryo-sectioning block mould was pre-prepared in the following way. Optimal cutting temperature (OCT) medium (SAKURA, Leicestershire, UK) was placed on the surface of the cold block. Once frozen a flat surface was cut using Hacker Bright OTF5000/LS-003 cryostat (Bright Instruments, Huntingdon, UK). The sample was carefully floated onto a flat piece of filter paper with the photoreceptor cell layer uppermost. Excess fluid was removed by blotting with filter paper and the sample was placed, filter paper downwards, onto the pre-prepared block. When the sample had frozen, fresh OCT medium was poured on top and allowed to freeze. Mounted samples were stored at -80⁰C until required.
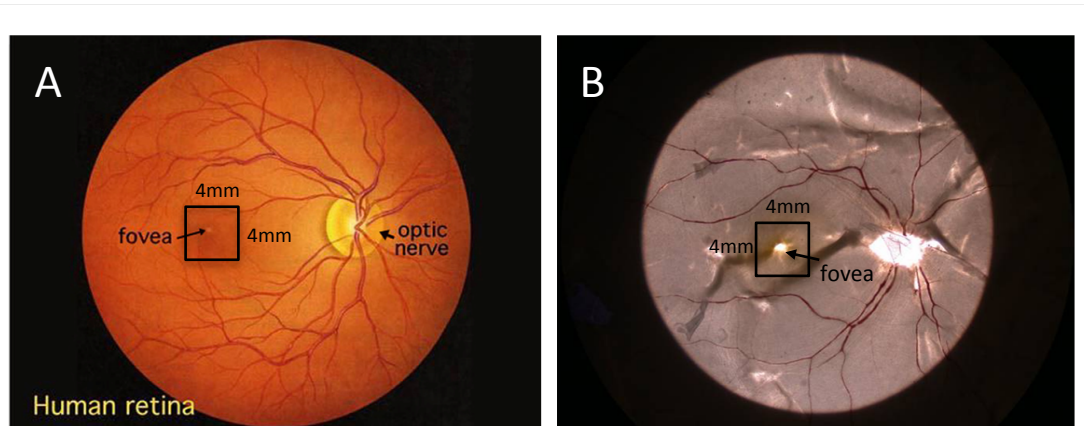
Figure 2.1 (A) Fundus image taken in vivo with an ophthalmoscope. The position of the fovea is indicated. B, Equivalent image of human retina following dissection, showing the position of the foveal sample.

2.2.2 Retinal planar cryo-sectioning

The pre-prepared macula sample was mounted in the cryo-sectioner and samples were sectioned in the horizontal plane. Surplus frozen OCT medium was removed by cutting sections until the sample was revealed. Sections (20 µm) were then placed on glass slides and examined for cells under the microscope. Slices containing retinal tissue were collected

serially and individually in pre-cooled, labeled Eppendorf tubes and stored at -80 ^{o}C until they were processed for RNA extraction.

2.3 Quantitative real-time polymerase chain reaction (QRT-PCR)

2.3.1 RNA extraction

RNA extraction from retinal samples was carried out using the Qiagen Rneasy Micro Kit (Qiagen, Crawley, UK). Kits were used according to their manufacturer's instructions. All the reactions were performed at room temperature, including centrifugation (Fisher Scientific, Loughborough, UK) (set at 16 ^{o}C). The samples were incubated in RLT lysis buffer which contained 10 µl/ml β-Mercaptoethanol (Sigma-Aldrich, Poole, UK) and aspirated 5 times through a 20-gauge needle (0.9 mm) to homogenise the tissue. The homogenate was then centrifuged at 13,000 rpm for 3 minutes and the supernatant collected. 70% ethanol was then added to the supernatant. Each sample was transferred to an RNeasy column and centrifuged for 15 seconds at 13,000 rpm. The flow through was discarded. RW1 wash buffer was added to the column and centrifuged for 15 seconds at 13,000 rpm and the flow through again discarded. Then DNase solution (Qiagen, Crawly, UK) was then added to the column and incubated for 15 minutes at room temperature to remove any DNA. The column was then washed with buffer RW1 and centrifuged for 15 seconds at 13,000 rpm and the flow through discarded. The column was transferred to a new collection tube. An 80% ethanol/20% RPE buffer (Qiagen, Crawly, UK) was added to the column and centrifuged, and the flow through discarded. In order to dry the column, 80% ethanol was added and centrifuged at 13,000rpm for 2 minutes. The column was transferred to a new 2 ml collection tube and the column was centrifuged at 13,000 rpm for 5 minutes to dry spin column membrane, to ensure no ethanol would be eluted later. Finally, the column was transferred to a 1.5 ml collection tube. 12 µl RNase free water was added to the column membrane and incubated for 1 minute, then centrifuged for 1 minute at 13,000 rpm to elute the RNA. The RNA was stored at -80 ^{o}C.

2.3.2 First strand cDNA synthesis

The concentration of RNA was measured using a Nanodrop ND-1000 spectrophotometer (NanoDrop Techologies, Wilmington, USA). The sample was then diluted with RNase free

water to give a concentration of 30-100 ng in10μl. Random primers (1 μl) (Invitrogen, Paisley, UK) and deoxyribonucleoside triphosphate (dNTP) Mix (consisting of equal concentration of dATP, dGTP, dTTP, dCTP) (1 μl) (Bioline, London, UK) were then added to the RNA sample (10 μl) to give a total volume of 12 μl. The sample was heated to 65 $^{\circ}$C for 5 minutes using a Thermocycler DNA engine (PTC-200, MJ Research, Minnesota, USA). After this, the sample was chilled rapidly on ice. 4 μl of 5X First-Strand Buffer (Invitrogen, Paisley, UK), 2 μl of 0.1 M dithiothreitol (DTT) (Invitrogen, Paisley, UK) and 1 μl of RNase inhibitor (Invitrogen, Paisley, UK) were then added to the sample, which was then incubated at 25 $^{\circ}$C for 10 minutes and 42 $^{\circ}$C for 2 minutes. Following this, 1 μl of the reverse transcriptase enzyme Superscript^{TM} II (Invitrogen, Paisley, UK), was added to the sample and incubated at 42 $^{\circ}$C for 50 minutes and 70 $^{\circ}$C for 15 minutes to synthesise the cDNA. cDNA was then stored at -20 $^{\circ}$C until use.

2.3.3 Quantitive real-time polymerase chain reation (QRT-PCR)

Taqman^{TM}QRT-PCR is an accurate method to quantify the expression levels of genes of interest. The specific primers target and amplify a region of the genes of interest from the cDNA. A specific probe binds to the gene of intrest. This is an oligonucleotide which has a fluorophore at the 5'- end and quencher at the 3'- end (Figure 2.2). The quencher quenches the fluorescence emission of the reporter fluorophore when they are in close proximity. As the amplification process occurs, the probe is released from the cDNA and exonuclease activity causes cleavage of the probe from the fluorophore and it is therefore no longer quenched. The fluorescence is detected by the system and accumulation of the fluorescent signal is proportional to the expression of the gene of interest.
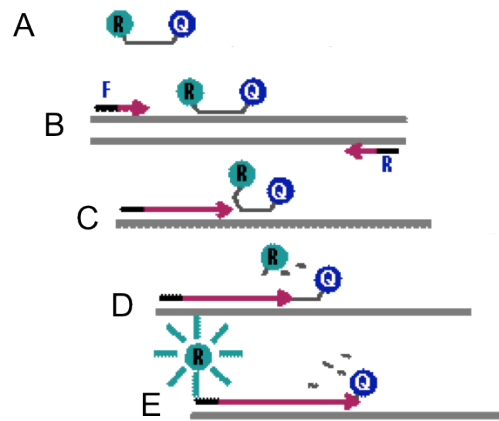
Figure 2.2 The principle of Taqman™ quantitative real-time PCR. When the probe is intact, the reporter fluorophore is quenched (A). During PCR, the double stranded DNA is heated and separated into single stranded and the probe hybridises with target gene sequences (B and C). As synthesis occurs, the reporter (R) is separated from the quencher (Q) (D). The fluorophore is measured cycle by cycle (E). The fluorescence is proportional to the amplification of the target gene. Adapted from http://netclass.csu.edu.cn/JPKC2010/CSU/weishengwuxue/jiaoxueshijian/

Taqman™ QRT-PCR used a 96-well plate. Wells were loaded with 5 ng cDNA (in 10 µl nuclease free water), 12.5 µl of Mastermix (Applied Biosystems, Warrington, UK), 1.25 µl primer/probe mix (Applied Biosystems, Warrington, UK) and 1.25 µl of nuclease free water to make a total volume of 25 µl and primer and probe concentration of 200 mM. All the primer and probe sets used are given in Table 2.1. The Mastermix contains all the components required for a PCR reaction: Taq polymerase, buffer, $MgCl_2$, KCl, deoxy-ribonucleoside triphosphate (dNTPs) and stabilizer. The PCR was performed using the ABI Prism 7700 Sequence Detection System (Applied biosystems, Warrigton, UK). The amplification step used was firstly 50 °C for 2minutes then 95 °C for 10 minutes, followed by 40 cycles of 15 seconds at 95 °C and 1 minute at 60 °C for each amplification cycle.

The cycle threshold (C_T) value was determined using the 7500 Fast System Software 1.1.1 (Applied Biosystems, Warrington, UK). This is the cycle number at which the signal becomes statistically greater than background and is proportional to the number of copies of mRNA for the target gene. Using a standard curve for the gene, the relative expression is calculated. The expression of the gene of interest in each section is calculated relative to the section with the highest expression. There was no control gene was used to analyze the data

of interesting genes, as the reason of there is multiple cell types through the retina and each of these cell types has different expression ability to the control genes.

Table 2.1 The probes/primers used for Taqman^{TM} QRT-PCR.

Probes & primers	Official full name	Part number	Supplier
THY-1	Thy-1 cell surface antigen	Hs00174816-m1	Applied Biosystems, Warrington, UK
POU4F1	POU class 4 homeobox 1	Hs00366711-m1	Applied Biosystems, Warrington, UK
RCVRN	Recoverin	Hs00610056-m1	Applied Biosystems, Warrington, UK
P2X7	Purinergic receptor P2X, ligand-gated ion channel, 7	Hs00175721-m1	Applied Biosystems, Warrington, UK
TRPC-1	Transient receptor potential cation channel, subfamily C, member 1	Hs00608195-m1	Applied Biosystems, Warrington, UK
TRPC-3	Transient receptor potential cation channel, subfamily C, member 3	Hs00162985-m1	Applied Biosystems, Warrington, UK
TRPM-2	Transient receptor potential cation channel, subfamily M, member 2	Hs00268573-m1	Applied Biosystems, Warrington, UK
TRPV-1	Transient receptor potential cation channel, subfamily V, member 1	Hs00218912-m1	Applied Biosystems, Warrington, UK
RBFOX3	RNA binding protein, fox-1 homolog (C. elegans) 3	Hs00876928-m1	Applied Biosystems, Warrington, UK
CHAT	Choline O-acetyltransferase	Hs00758143-m1	Applied Biosystems, Warrington, UK
CALB1	Calbindin 1	Hs00191821-m1	Applied Biosystems, Warrington, UK

2.4 Illumina gene array analysis

For this array analysis the retina from donors were used. The detail of these donors are given in Table 2.2. Gene array analysis was performed by Source BioScience (UK). The Bioconductor package (http://www.bioconductor.org) in R (http://www.r-project.org) was used to process array data obtained from RGC and MAC samples. First of all, data was background corrected, quantile normalized and variance stabilized. Then, a hierarchical clustering plot was constructed to check that samples from RGC and MAC grouped together. Then, in order to compensate for false positive data, only genes presented in over 50% of each group were retained (McClintick and Edenberg 2006). The fold change of each gene was calculated, that is, the difference in average expression level of given gene between RGC and MAC.

To obtain biologically meaningful results, p values for each gene were calculated using an extension of the empirical Bayes moderated t-statistic known as TREAT (McCarthy et al., 2009). This statistic allows formal testing of the hypothesis that a gene is more differentially expressed than a given fold change (FC). Since multiple comparisons are performed, the p-value adjusted for multiple testing (q-value) is computed to control the expected likelihood of falsely identifying a gene as differentially expressed; this is known as the false discovery rate (FDR). The most "up-regulated genes" are therefore those most highly expressed in the RGC layer compared to the entire macula. The most "down-regulated genes" are those expressed most highly in the entire macula compared to the RGCL.

Table 2.2 Donor information for retina samples used in the gene array experiments. Information is given as reported on the Research Tissue Donation Form.

Sample	Age	Gender	Cause of death (as reported)	Medical history (as reported)	Medication (as reported)	Post-mortem period
RGC-1	82	Male	Pulmonary embolism	Mesothelioma Asbestosis Prostate problem	Aspirin, Co-amilazide, Lansoprazole	5 hours
RGC-2	58	Female	Brainstem stroke	Knee replacement, Chest pain,	Lansoprazole, co-codamol, Amitriptyline	5 hours
RGC-3	66	Male	Ventricular tachycardia, Cardiogenic stroke	Lung cancer Cardiomyopathy	Plavix, Lisinopril, Pravastatin, Verapamil	12 hours
RGC-4	70	Male	Cardiac arrest	Cardiac artery bypass graft, Hypertenson,	Unknown	11 hours
RGC-5	73	Male	Bladder cancer	Bladder cancer, Shoulder replacement	All medicine discontinued 16 days before died, Diamorphine/haloperidol	12 hours
Mac-1	79	Female	Ultra-cerebral bleed	Hypertension	Bendroflumethiazide, Mebeverine,	8 hours
Mac-2	84	Male	Renal cancer	Renal cancer	Simvastatin, Lisinopril, Asprin	12 hours
Mac-3	92	Male	Myocardial infaction	Hypertension Type 2 diabetes Hypercholesterolemia	Paracetamol, Clotrimazole, Gliclazide, Metformin, Pravastatin, Aspirin.	7 hours
Mac-4	50	Male	Hypoxic	Type 2 diabetes	Candesartan, Glucophage, Rosuastatin.	5 hours
Mac-5	50	Male	Hypoxic	Type 2 diabetes	Candesartan, Glucophage, Rosuastatin.	5 hours

2.5 Histological labeling and Immunolabelling

2.5.1 Paraffin-embedded sections

The macula sample was fixed in 4% formaldehyde (Sigma-Aldrich, Poole, UK) in Phosphate Buffered Saline (PBS) (Thermo Scientific, Basingstoke, UK) solution for 24h at 4 ⁰C. The tissue was then dehydrated through a graded ethanol (30%, 50%, 70%, 90% and 100% (v/v) (ethanol/water), at 4 ⁰C with 30 minutes for each step. Following this, the sample was transferred to 50% xylene/ethanol (v/v) for 30 minutes at room temperature (RT). The solution was then replaced with 100% xylene for 30 minutes at RT. The tissue was now ready to embed. It was placed in a suitable mould and incubated in 50% then 100% wax (diluted in

xylene) in the oven at 60 °C for 60 minutes for each step. Finally, the sample was taken out from the oven and allowed to cool before sectioning. The sample was sectioned into 5 μm slices and mounted on glass slides. The slide was heated at 60 °C heater until dry to allow the section to adhere to the slide.

2.5.2 Hematoxylin-eosin (H&E) staining

To remove the wax, the slide was dipped into 100% xylene for 5 minutes, and then graded ethanol from 100%, 90%, 70%, 50%, and 30% to distilled water, with 1 minute for each step. Following this, the slide was put into Hematoxylin (Sigma-Aldrich, Poole, UK) solution for 5 minutes to stain the cell nuclei. The slide was washed with distilled water, before putting the slide into 1 % acid ethanol solution (for differentiation) for 1 minute. After that, the slide was washed again with distilled water then placed into 0.25% Eosin (Sigma-Aldrich, Poole, UK) solution for 3 minutes to stain the cytoplasm. To dehydrate the sample, the slide was dipped into graded ethanol from distilled water, 30%, 50%, 70%, 90% and 100% (V/V) (ethanol/ distilled water) 1 minute for each step, and then the slide was transferred to 100% xylene to improve cell transparency. Finally the slide was mounted in Hydromount medium (National Diagnostics Ltd, Hull, UK) sealed using a coverslip (VWR International, Lutterworth, UK), and left to dry overnight. Images were obtained using Nikon TE200 Eclipse Microscope (Nickon industries, Tokyo, Japan) with Nikon Coolpix 950 digital camera and MDC lens (Nickon industries, Tokyo, Japan).

2.5.3 Immunohistochemistry of paraffin-embedded sections

Slides were immersed in 100% xylene for 5 minutes to remove the wax, then dehydrated in graded ETOH (100%, 90% and 70%) for 1 minute, before washing with distilled water for 2 minutes.

The sample was gently washed in PBS (10 minutes for 3 times) before permeabilization in blocking solution which contained 5% goat serum (Sigma-Aldrich, Poole, UK) and 0.2% Triton X100 (Sigma-Aldrich, Poole, UK) in PBS. Following this, the slide was washed three times in PBS. The primary antibody (Table 2.3) was diluted in blocking solution and 50 μl added per sample and incubated overnight at 4 °C.

Table 2.3 The primary antibodies were used for immunohistochemistry of paraffin-embedded sections.

Target protein	Epitope	Host species	Dilution	Supplier and Product code
NeuN	Vertebrate neuron-specific nuclear protein	Mouse	1:200	MAB377, Millipore, Watford, UK
TRPM-2	Human transient receptor potential cation channel, subfamily M, member 2	Rabbit	1:50	NB500-242, Novus Biologicals, Cambridge, UK
AHNAK2	AHNAK nucleoprotein 2	Mouse	1:300	AB70053, Abacam
βIII-Tubulin	C-terminus of βIII tubulin	Mouse	1:2000	G7121, Promega
THY-1	Thy 1.1 antigenic determinant	Mouse	1:200	MAB1406, Millipore
HSPA1	Heat shock 70kDa protein 1A/B	Rabbit	1:50	10995-1-AP, Proteintech

To remove the antibody, the slide was washed three times in PBS before adding 50 μl per sample of secondary antibody solution (Table 2.4), diluted 1:1000 and incubated for 2 hours in the dark at RT. The following steps were carried out in the dark. The slide was washed 3 times in PBS to remove the extra secondary antibody, then 0.5 μg/ml of 4',6-diamidino-2-phenylindole dilactate (DAPI) (Invitrogen, Paisley,UK) solution in PBS was added to the slide, and incubated for 10 minutes at RT. Following the final three washes in PBS the slide was dried. A drop of Hydromount medium was pipetted onto each sample and a coverslip was placed over the section and sealed, then store at 4 ^{0}C in the dark until required.

Table 2.3 Secondary antibodies used for immunohistochemistry of paraffin-embedded sections.

Secondary antibody	Specificity	Species	Dilution	Supplier
Alexafluor 488	Mouse Ig light chains	Goat	1:1000	Invitrogen, Paisley, UK
Alexafluor 568	Mouse Ig light chains	Goat	1:1000	Invitrogen, Paisley, UK
Alexafluor 568	Rabbit Ig light chains	Goat	1:1000	Invitrogen, Paisley, UK

2.6 Systems to simulated retina ischemia in vitro

2.6.1 Human organotypic retinal cultures (HORCs) dissection

The neural retina was dissociated from the eye as described above and placed in a 60mm Petri dish (Corning, NY, USA) in 5 ml of warmed CO_2-independent medium (Gibco-invitrogen, Paisley UK). A 5-samples template (Figure 2.3) was used to ensure that para-macular samples were taken from the same position of each retina. Previous research has shown that para-macular samples taken from these positions have an equivalent number of RGCs (Niyadurupola, Sidaway et al. 2011). The macula sample was removed first using a 4mm diameter trephine (Biomedical Research Instruments, MD USA). 5 x 4 para-macular samples were then taken. Samples were cultured in 35 mm cell culture dishes (Corning, NY, USA) in serum free DMEM/F-12 medium supplemented with 50 μg/ml gentamycin and 292 μg/ml L-glutamine (Gibco-invitrogen, Paisley, UK) at 35 °C, buffered to pH 7.4 with 5% CO_2.
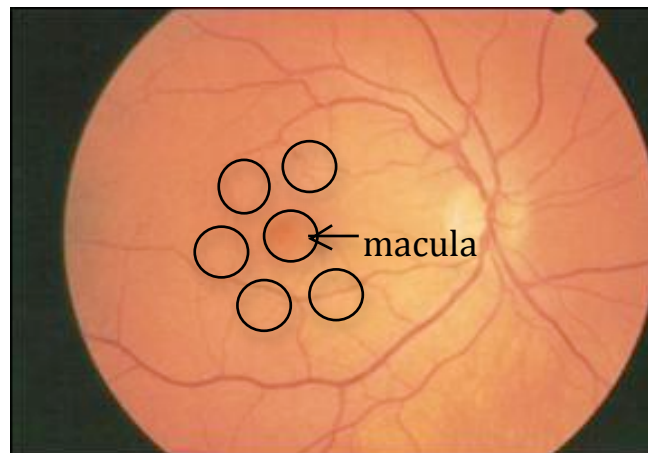
Figure 2.3 Template for the 5 para-macular samples. The macula region was removed first, and then used position the template to allow consistent positioning of the paramacular samples.

2.6.2 Simulated ischemia (oxygen glucose deprivation, OGD) in HORCs

HORCs to be exposed to the OGD protocol was placed in 2 ml of serum and glucose free Dulbecco's modified Eagle medium (DMEM) (Gibco-Invitrogen, Paisley, UK) (with 50 μg/ml gentamycin and 292 μg/ml L-glutamine). Following this, the dishes containing the HORCs were placed into a modular incubator chamber (Billups-Rothenburg, CA, USA) and

the chamber was gassed with 95% N_2/5% CO_2 for 10 minutes to deplete O_2. The inlet and outlet pipes were then sealed and the chamber incubated at 35 °C for required time. Following the ischemia culture of OGD, the HORCs were then switched to pre-warmed serum free DMEM/HamF-12 medium (Gibco-Invitrogen, Paisley, UK) for a total of 24 hours in culture including simulated ischemic culture at 35 °C in a 95% O_2/ 5% CO_2 incubator. This is referred to as the reperfusion period. The control HORCs samples were processed the same operations, but however, they were cultured in serum free DMEM but with glucose (Gibco-Invitrogen, Paisley, UK) with the same culture time as ischemia group, which was cultured at 35 °C in the incubator with 95% O_2 air /5% CO_2 in the same incubator as the ischemia chamber. After the simulated ischemia this period, the HORCs were transferred back to serum free DMEM/HamF-12 containing glucose, referred as reperfusion period.

2.6.3 Simulated Ischaemia with inhibitors

N-(p-amylcinnamoyl)anthranilic acid (ACA) and calpain inhibitor III, MDL28170 (carbobenzoxy-valylphenylalanial; Z-Val-Phe-CHO), were used and purchased from MerckMillipore (Watford, UK). There were some inhibitors were investigated with the stimulated ischemia HORCs in this thesis, they are ACA and MDL28170. Inhibitors were initially dissolved in DMSO to make a 20 mM stock solution. Inhibitor/DMSO was added to OGD or control medium to give a final concentration of 20 μM. Media without inhibitor contained DMSO added to the same concentration as when the inhibitor was present (vehicle control). The inhibitor was present at both the OGD and reperfusion stages.

2.7 Lactate dehydrogenase (LDH) assay

LDH release is a measurement used to assess cell death. Cytosolic enzymes, including LDH, are released through damaged cell membrane into the cell culture medium, and measurement of LDH activity in the medium is therefore related to the number of damaged cells. The biochemical basis of the assay is shown in Fig. 2.4. The HORC culture medium was collected and stored at 4 °C until used. The medium was centrifuged at maximum speed for 5 minutes. The Cytotoxicity Detection Kit (LDH) (Roche Products Limited, Welwyn Garden City, UK) was used according to the manufacturer's instruction. The LDH kit contains 2 solutions, catalyst solution and dye solution. The reaction solution requires 1 part catalyst to 45 parts of dye solution. These were mixed together, and then were added to 100μl of medium in a 96-

well plate. The plate was incubated in the dark at 37 °C for 10 minutes. The absorbance at 490 nm was measured using a FLUOstar Omega (BMG-LABTECH, Aylesbury, UK).
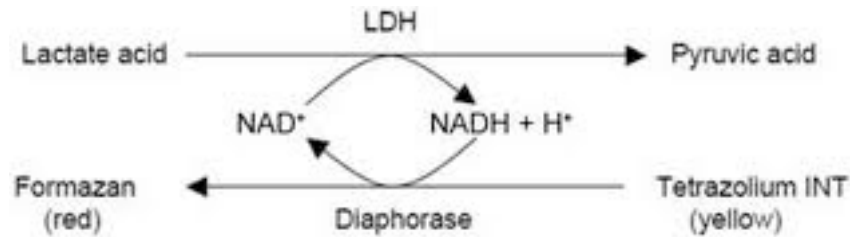
Figure 2.4 Principle of the LDH assay. LDH catalyses the conversion of lactate to pyruvate and during the reaction NAD$^+$ is reduced to NADH. The NADH is then involved in a reaction catalyzed by diaphorase to generate a coloured formazan product. The formazan produced is therefore proportional to the amount of LDH in the culture medium. http://www.beyotime.com/c0016.html

2.8 Cryosetioning of HORCs and Immunohistochemistry

2.8.1 Transverse cryosectioning of HORCs

HORCs were fixed in 4% formaldehyde for 24 hours, and then dehydrated in 30% sucrose (Fisher Scientific, Loughborough, UK) which dissolved in PBS for 24 hours. The samples were then placed into cryostat block cups filled with OCT medium and frozen on dry ice. They were stored at -80 °C. The retinal sample was cut into 13 μm slices by cryosectioning, and three pieces of slices from each sample were collected onto one slide (Sigma-Aldrich, Poole, UK). The slide was previously coated with 3'aminopropyl-triethoxyl silane (Sigma-Aldrich, Poole, UK). The immunohistochemistry was carried out following the same processes as described in section 2.4.3, starting from first PBS washing step.

2.8.2 Terminal deoxynucleotidyl transferase UTP nick end labeling (TUNEL) assay

The TUNEL assay is a method to detected cellular apoptosis through labeling of the fragments of DNA nuclear generated as a result of the apoptotic process. One of the most significant characteristics of apoptosis is that double-stranded DNA is digested by endogenous endonucleases that cleave the DNA into fragments initiated by nicks in the DNA backbone. In the TUNEL assay, the exposed 3'-OH end combines with fluorescein-12-dUTP by the action of terminal deoxynucleotidyl transferase (TdT) (Figure 2.5). All the TUNEL

assay reagents were supplied by Promega Life Science DeadEnd™ Fluorimetric TUNEL System (Southampton, UK), and the kit was used according to the manufacturer's instructions.
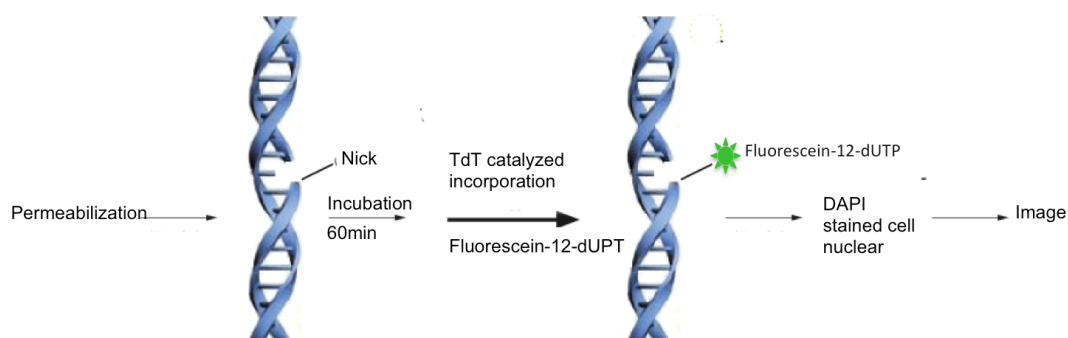
The HORC sections were washed with PBS (5 minutes for 3 times). Following the wash, 0.2% Triton X-100 in PBS solution was added to cover the retinal sections for 5min at room temperature to permeabilize the cell membrane. They were then treated with Equilibration Buffer for 10 minutes, then washed in PBS (5 minutes for 3 times). Following this, the sections were covered with 50 μl rTdT incubation buffer, which was made up from Equilibration Buffer, Nucleotide Mix and rTdT enzyme (ratio of 45:5:1, V/V/V) and incubated for 1 hour at 35 °C. This and subsequent incubations were carried out in the dark. The reaction was stopped by immersion of the slides in 2X standard saline citrate (SSC) for 15 minutes. This was followed by PBS washes (5 minutes for 3 times). Cell nuclei were stained with DAPI diluted in PBS (1:1000, V/V) for 10min at RT. Three further PBS washes of each 5 minutes, removed the excess DAPI dye. The sections were then mounted in Hydromount medium. The sections were imaged using a Zeiss Axiovert 200M upright wide-field fluorescent microscope (Zeiss, Welwyn Garden City, UK) at 10X magnification. Image capture was via a CCD camera (Zeiss AxioCam, Welwyn Garden City, UK) using Zeiss Axiovision 4.7 software.

2.8.3 Quantification of retinal ganglion cell loss

Retinal slices were labelled with NeuN antibody by immunohistochemistry to allow assessment of retinal ganglion cell number. 10 images of each HORC sample were taken at 10X magnification using a Zeiss Axiovert 200M upright wide-field fluorescence microscope. For each image, the number of NeuN positive immunolabelled cells in 200 μm was counted from three different areas of each image. All the images were randomly assigned and counted by other members of the lab in a masked manner. A mean was calculated for each HORC from each image. In sections that had also been TUNEL labeled, the number of TUNEL-positive NeuN-labelled cells was also counted.

2.9 QRT-PCR of HORCs

The process of QRT-PCR of HORCs was same as the method was given in the Section 2.3, RNA extraction, First strand cDNA synthesis and finally detected THY-1 expression using 7500 Fast System Software 1.1.1. The only exception was RNA extraction of HORCs. HORCs were extracted RNA using Qiagen Rneasy Micro Kit (Qiagen, Crawley, UK), and followed its manufacturer's instructions. After the QRT-PCR was determined, the data was normalised using two housekeeping genes, TOP-1 and CYC-1, to improve data validity. These two housekeeping genes have been found previously in the lab that they were the most stable genes of HORCs under the stimulated ischemia and were chosen for data normalization (using the GeNorm programme) (Niyadurupola, Sidaway et al. 2011). The geometric mean of expression of these 2 genes was therefore used to normalize expression data in HORCs experiments.

2.10 Kinase signaling

2.10.1 Protein extraction

All the end of the HORCs experiments, explants were transferred to 1.5 ml Eppendorf tubes, frozen immediately in liquid nitrogen and stored at -80 °C. To lyse and extract the protein from the HORCs, cell lysis buffer was used of the following composition: 10 μl/ml EDTA solution (0.5 mM) (Thermo Scientific, Cramlington, UK), 10 μl/ml Protease inhibitor (Thermo Scientific, Cramlington, UK) and 10 μl/ml phosphatase inhibitor diluted in M-PER solution (which contains 25 mM bicine buffer at pH 7.6) (Thermo Scientific, Cramlington,

UK). 200 µl of lysis buffer was added to the sample and homogenized. The samples were then incubated in the fridge for 30 minutes before being spun for 10min at 13000 rpm. The supernatant was collected and stored at -80 °C until required.

2.10.2 Bicinchoninic acid (BCA) Protein Assay

The bicinchoninic acid (BCA) protein assay (Thermo scientific, Cramlington, UK) was used to measured protein concentration from HORC samples according to the manufacturer's instructions. In this assay, the original colour appears green due to the present of Cu^{2+}. The Cu^{2+} is reduced to Cu^+ by the protein, which then binds with bicichoninic acid to produce a purple coloured compound. This can be measured by the absorbance at 562 nm. The absorbance increase at 562 nm is proportional to protein concentration. 10 µl samples were loaded into the 96 well plate in triplicate. The BCA assay reagent solution was made up with 1 part Cupric Sulphate solution and 45 parts bicichoninic acid solution. 100 µl was added to the protein samples, and incubated at 37 °C for 30 minutes. The plate was read using a plate reader (Victor, EG & G Wallace Instruments, Cambridge, UK). The protein concentration could be quantified using a calibration curve (BSA: 0-2000 ng/µl).

2.10.3 Polyacrylamide gel electrophoresis

Protein extract was diluted in distilled water to obtain equal volume of protein solution up to 4.5 µl which contained equal quantity of protein (1 µg), NuPAGE® LDS sample buffer (4.5 ul) (Invitrogen, Paisley, UK) and 1 ul NuPAGE® sample reducing agent (10X) (Invitrogen, Paisley, UK) were added to the sample, which made a total volume of 10 µl. The samples were heated at 100 °C for 5 minutes.

Samples were run using the NuPAGE® system from Invitrogen (Invitrogen, Paisley, UK). NuPAGE® Novex® 4-12% Bis-Tris gels were placed into the XCell SureLock™ Mini-Cell. NuPAGE® MOPS SDS running buffer was added. The protein samples (10 µl) and MagicMark™ XP Western protein standard (Invitrogen, Paisley, UK) were loaded onto the gel. The gel was run at 200 V for 50 minutes in the cold room (7 °C).

For transferring the protein, the gel was removed from the cell and placed into a square Petri dish with NuPAGE® transfer buffer. Polyvinylidene fluoride (PVDF) membrane (Perkin

Elmer, Cambridgeshire, UK) was cut to the same size as the gel and immersed in 100% methanol. The gel and PVDF were then sandwiched between two pieces of thick filter paper that had been immersed previously in the NuPAGE® transfer buffer. Then the gel was placed into the transfer blotter, SureLock™ Mini-Cell (Invitrogen, Paisley, UK), with gel closest to the cathode. The inside of the chamber was filled with transfer buffer and the outside filled with distilled water. The proteins were transferred at 30 V for 60 minutes at room temperature.

2.10.4 Western blot – protein detection

The membrane was placed into a square Petri dish and incubated for 1 hour at room temperature in blocking solution of following composition: 0.1% Tween®-20 (Fisher Scientific, Loughborough, UK) with 5% milk powder in PBS (PBS-T). The primary antibody was diluted with PBS-T at the required concentration (Table 2.5). The membrane was then incubated in primary antibody solution for 2 hours at room temperature or overnight at 4°C. The primary antibody was removed and the membrane washed three times for 15 minutes in PBS-T to remove unbound antibody. Following this, the membrane was incubated, with shaking, with secondary antibody (Table 2.6) diluted at 1:1250 in PBS-T for 2 hours at room temperature. The secondary antibody was then removed and the membrane washed (15 minutes for 2 times) in PBS-T, followed by one wash with PBS-T without milk powder for 10 minutes at room temperature. Bound antibody was detected using ECL reagent (GE Healthcare, Buckinghamshire, UK) according the manufacturer's instructions. ECL reagent was applied to the membrane and incubated for 5 minutes at room temperature. The membrane was placed into a film cassette (GE Healthcare, Buckinghamshire, UK).

In the dark room, the ECL reagent was removed and chemiluminescence film paper (GE Healthcare, Buckinghamshire, UK) was placed on the membrane in the film cassette. It was then removed and developed using GBX developer solution (Kodak,GBX developer) until bands appeared. The developing action was ended by the stop solution (Photosol SB80, Basildon, UK), and then fixed in the fixative (Ilford Imaging, Mobberley, UK) until the background of film was invisible. Finally, film paper was rinsed by tap water and air-dried. The bands were scanned (HP Deskjet 3050), and their band intensity quantified using Image-J (http://rsbweb.nih.gov/ij/).

Table 2.5 Antibodies were used for Western blot.

Antibody	Dilution and Resource	Supplier and product code
α-Fodrin (1st antibody)	1:1000, Mouse	Enzo Life Sciences, Exeter，UK
Calpain 2 (1st antibody)	1:1000, Rabbit	Abcam, Cambridge, UK
β-actin (1st antibody)	1:2000, Rabbit	Cell Signaling Technology, Danvers, UK
Vimentin (1st antibody)	1:1000, Mouse	Sigma, Dorset, UK
Anti-mouse IgG HRP Sheep conjugate (2nd antibody)	1:1250	GE Healthcare, Buckinghamshire, UK
Anti-rabbit IgG HRP Donkey conjugate (2nd antibody)	1:1250	GE Healthcare, Buckinghamshire, UK

2.11 Data analysis

Data is expressed as the mean ± standard error of the mean (S.E.M.) for at least 4 independent experiments. Student's t-test was used to evaluate the significance of differences between two groups. A probability of $p \leq 0.05$ was taken as significant.

Chapter 3

A novel planar sectioning technique for profiling of the human retina

3.1 Introduction:

The human retina is a highly complex tissue and contains 10 distinct layers and multiple cell types. According to their morphological and physiological characteristics, there are 5 classes of neuronal cell in the retina: photoreceptor cell, horizontal cell, bipolar cell, amacrine cell and retinal ganglion cells. There are also several non-neuronal cell types, the major one being Müller cells (Bringmann, Pannicke et al. 2009). Identification of regional expression in the retinal layers is studied largely by immunohistochemistry, but this is reliant on good quality antibodies being available. This chapter describes development and characterization of a method to section the human retina in order that mRNA profiles across the retina can be determined.

Previous reports have demonstrated that in glaucoma RGCs are severely affected and the thickness of the RGCL is greatly decreased compared with other retinal neuronal cells and retinal nuclear layers which show minimal changes in both experimental glaucoma and glaucoma patients (Kendell, Quigley et al. 1995; Osborne, Ugarte et al. 1999; Kielczewski, Pease et al. 2005). It has been identified that the death of RGCs in glaucoma seems to be by an apoptotic mechanism (Quigley, Nickells et al. 1995; Kerrigan, Zack et al. 1997). Therefore, in order to investigate the signaling pathways and changes in gene regulation that are involved in glaucoma, it is important that the genes expressed in human RGCs are identified. The techniques developed will enable the expression in the RGC layer to be studied.

Recently, several groups have investigated the RGC gene expression profiles of normal RGCs and also in the animal models of glaucoma (Ahmed, Brown et al. 2004; Ivanov, Dvoriantchikova et al. 2006; Kim, Kuehn et al. 2006; Guo, Cepurna et al. 2010). Expression in human RGCL has also recently been investigated (Kim, Kuehn et al. 2006). Typically two ways have been used to isolate the cells: immuno-panning from mixed retinal cells (Ivanov,

Dvoriantchikova et al. 2005; Hong, Iizuka et al. 2012; Siegert, Cabuy et al. 2012) and laser capture microdissection (LCM) (Kim, Kuehn et al. 2006; Guo, Cepurna et al. 2010).

Immuno-panning is a valid method to isolate large numbers of pure RGCs, which gives 90-99.5% purification of RGCs (Barres, Silverstein et al. 1988; Hong, Iizuka et al. 2012). The method uses an enzyme, such as papain, to digest the connections between the RGCs and other retinal cells, followed by purification of the RGCs by binding to the Thy-1 antibody that has usually been immobilised on a Petri dish. Cells can be used directly or plated in order to gain cultures of RGCs. The survival rate has been found to be around 85% 3h after plating (Meyer-Franke, Kaplan et al. 1995). Protocols improve cell viability and prolong cell life have also been developed, for example adding brain derived neurotropic factors or other growth factors (Ma and Taylor 2010; Zhang, Liu et al. 2010). These methods, however, have only been used for rodent retinas. Attempts have been made in our lab to use these techniques in human retina, but have not been successful.

LCM is a powerful and potentially precise way to capture cells of interest by removing the rest of retinal cells under the microscope. However, the close morphological similarity and proximity to RGCs make it potentially difficult to distinguish displaced amacrine cells from RGCs. Therefore previous studies using this technique in retina have mainly taken the entire RGC layer rather than isolating the RGCs. Even when the entire RGCL is taken, experiments using these techniques remain very time consuming. Further to this, they only yield low quantities of mRNA. Therefore, an alternative method was developed in this study.

The aim of this study was to develop novel techniques to obtain large quantities of high quality mRNA from planar retinal sections that would enable analysis of gene expression profiles in the human RGCL.

3.2 Results:

3.2.1 Histological investigation of the human retina layer from the macular region to the periphery retina

Preliminary experiments looked at thickness of the RGCL in the human retina. The retina was stained with Haemotoxylin and Eosin (H&E), to look at histological characteristics of the macular, paramacular and peripheral human retina. In terms of overall morphology, the macula region was thickest, decreasing in thickness out to the peripheral retina (Figure 3.1). The retinal ganglion cell layer in the macular region was several cells thick and was the thickest of the retinal nuclear layers (Figure3.1A). Ganglion cell number and thickness decreased from the macular to the para-macular region (Figure 3.1B). There were only a few ganglion cells localized in the RGCL in the peripheral region (Figure 3.C). Other two nuclear layers were of a similar thickness in the macular and para-macular, but not in peripheral retina. Furthermore, the three retinal nuclear layers and plexiform layers could be clearly determined in the macular and para-macular regions, but were difficult to identify in the peripheral retina. Note that these sections did not contain photoreceptor outer segments, which have been shed beyond the outer limiting membrane.

Overall these images show that the morphology of the human retina is well maintained in the samples derived from the post mortem donor eyes. They also confirmed that the RGCL is the thickest in the macular region of healthy human retina. Therefore, this was selected for further experiments to develop the sectioning technique since in this research we are most interested in determining expression in human RGCs.
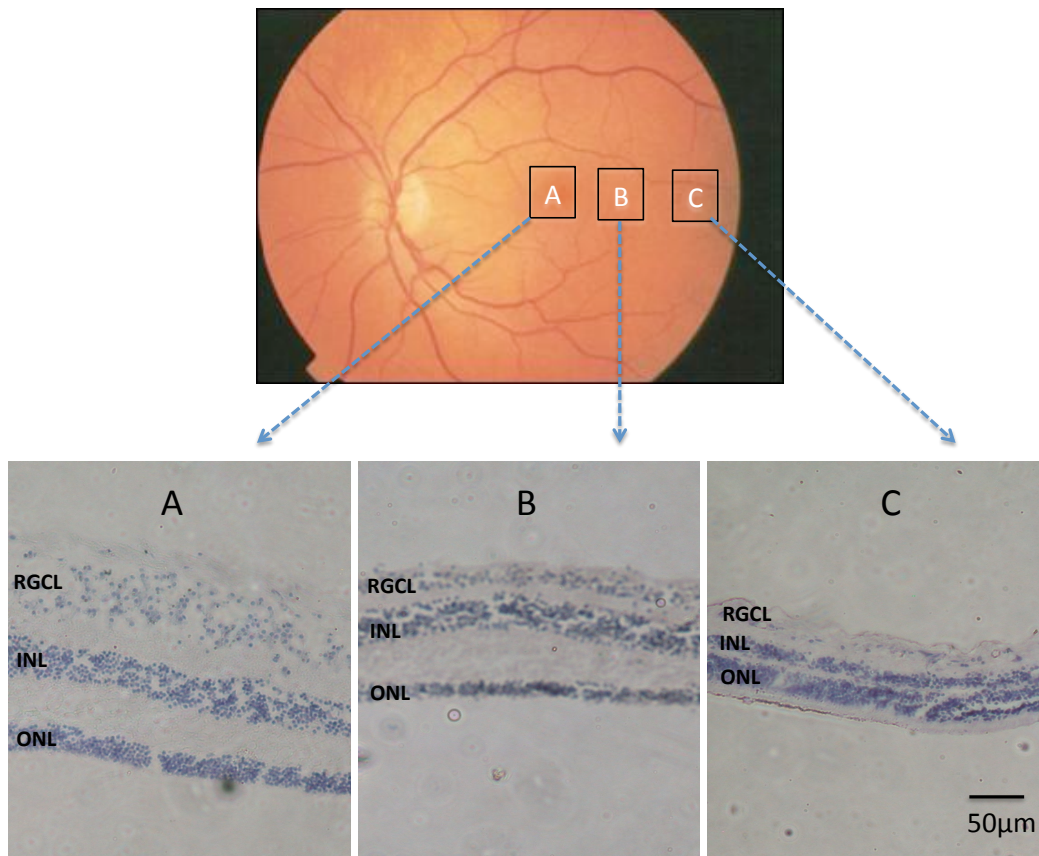
Figure 3.1 H&E staining of human retina. A, macular region; B, para-macular region; C, peripheral region. RGL = retinal ganglion cell layer, INL = inner nuclear layer, ONL = outer nuclear layer.

3.2.2 RNA was extracted from the retina planar sections.

Using the macular region, techniques were developed to section the retina in order to obtain samples from the retinal cell layers that could be used for mRNA profiling. This involved ensuring that the retina was flat so that the sample of each section was from the same layer of retina. In order to make it as flat as possible, frozen OCT medium on a metal block mould was cut using a cryosectioning machine. This provided the flat surface on which to mount the retina. The sample was carefully floated onto a piece of filter paper. Following this, the filter paper with macular sample was placed onto that flattened OCT surface, and the sample covered by liquid OCT medium prior to freezing immediately on dry ice. The macular sample was then ready for cryosectioning. The thickness of each section was set at 20μm. Macular planar sections were collected serially into respective Eppendorfs. For each macular sample, approximately 21 sections were obtained.

The serial retina planar sections were collected and extracted RNA. High yields of RNA were got from each 20 μm section, particular in the inner retina part (Figure 3.2). After the RNA extraction, over 10μl of solution was obtained from each section, which contained approximately 5-40 ng/ul. The highest concentrations were obtained from the inner retina.

RNA level of each serial retina section
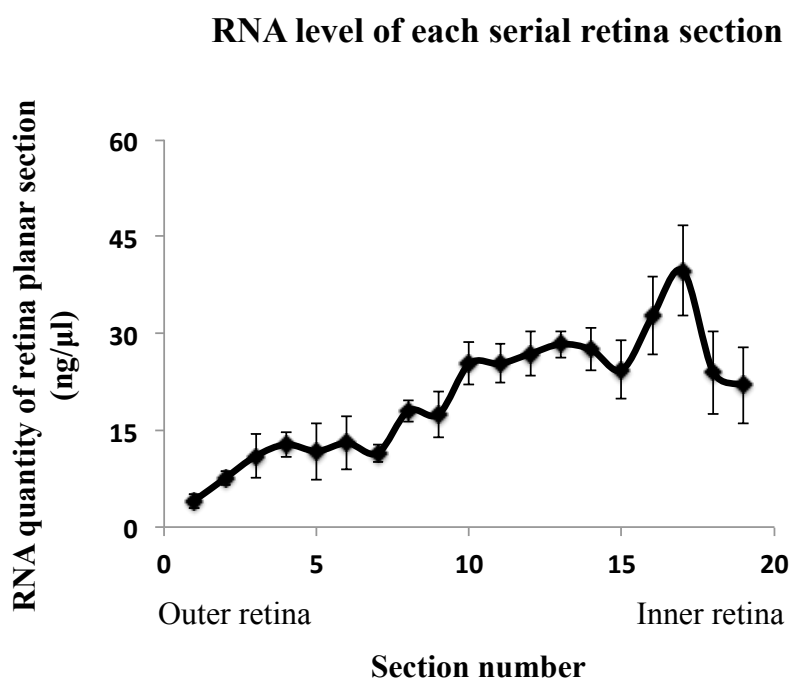
Figure 3.2 RNA level through retina planar section. Serial cryosections were taken and extracted and measured by Nanodrop. Mean ± standard error of the mean (S.E.M), n=5.

3.2.3 Expression profiles of retinal cell markers.

Gene expression of selected retinal cell markers was measured using quantitative PCR (Figure 3.3 and Figure 3.4). Markers used were recoverin (RCVRN) for photoreceptors(Dizhoor, Ray et al. 1991), calbindin (CALB) for horizontal cells (Nakhai, Sel et al. 2007), choline acetyltransferase (CHAT) for amacrine cells (Haverkamp and Wassle 2000) and Thy-1 (Barnstable and Drager 1984), NeuN (RBFOX3) and (Buckingham, Inman et al. 2008) and Brn3a (POU4F1) (Nadal-Nicolas, Jimenez-Lopez et al. 2009) for retinal ganglion cells. RCVRN expression was highest in the outermost sections and almost absent

from the inner RGC layer. Given this distinct profile, RCVRN was used to line up the sections from different retinal samples: samples were aligned at the section where RCVRN expression started to increase. The peaks for CALB and CHAT expression corresponded closely with the positions of horizontal and amacrine cells respectively. Furthermore, the known RGC markers Brn3a, Thy-1 and NeuN were most highly expressed in the innermost sections corresponding to the RGC layer (Figure.3.4). Expression profiles of the retinal cell markers were therefore highly consistent with their expected positions in the retina (Figure 3.3 A and C).
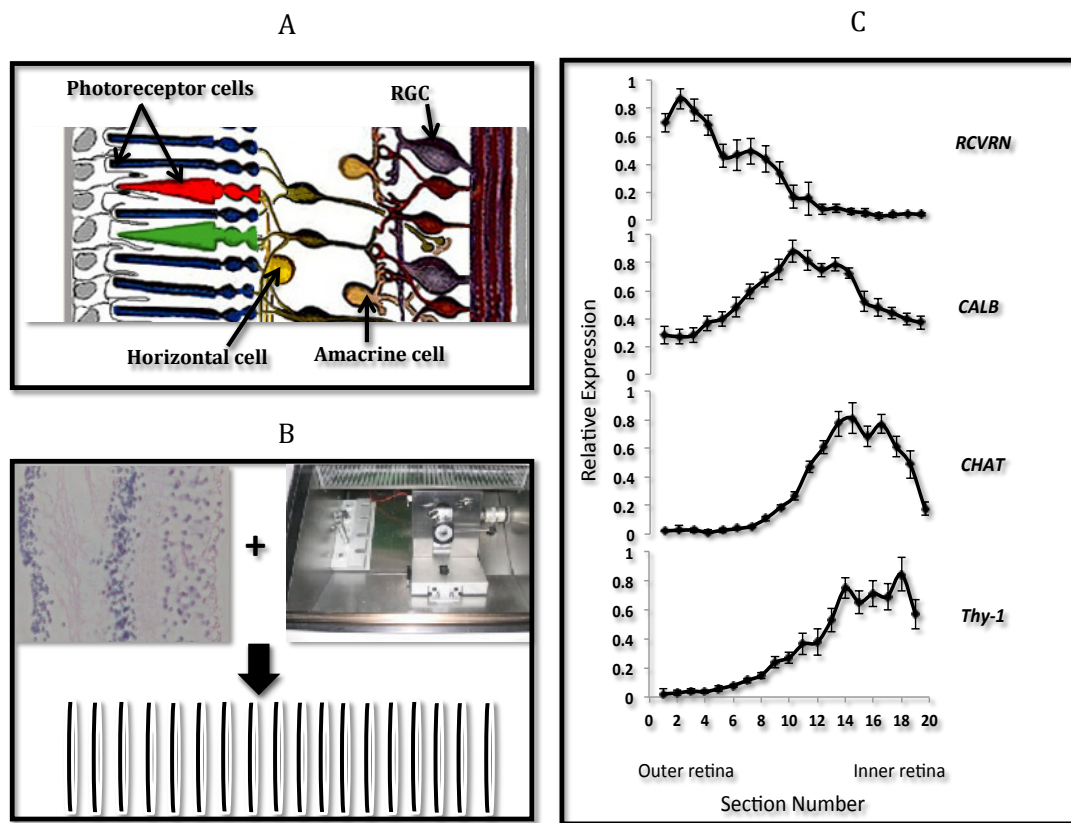
Figure 3.3 The expression profile of retinal ganglion cell markers in human retina. (A) Diagram showing the different cells of the retina. Adapted fromhttp://php.med.unsw.edu.au/embryology/index.php?title=File:Retina-layers-diagram.jpg. (B) Serial cryosections of the retina were taken from photoreceptor cell layer to the ganglion cell layer. (C) Gene expression of RCVRN, CALB, CHAT and THY-1 were measured by quantitative PCR and normalised to the highest expression. Mean ± standard error of the mean (S.E.M), n=8.
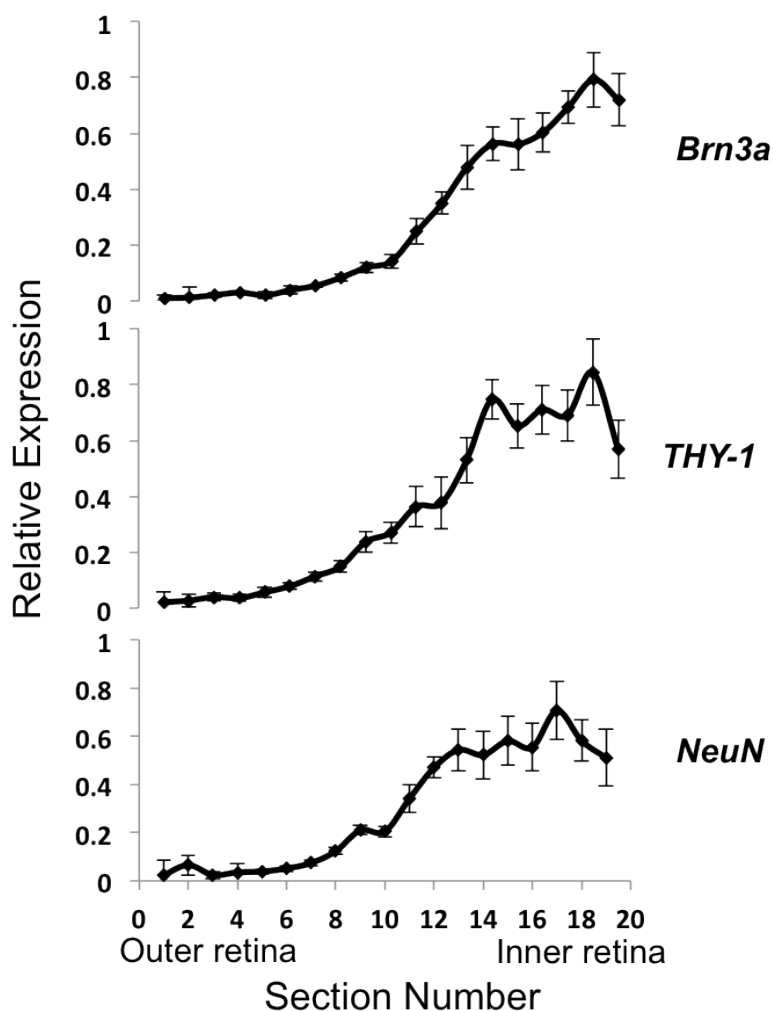
Figure 3.4 The expression profile of RGC markers in human retina. Serial cryosections were taken and gene expression was measured by QRT-PCR. Mean ± standard error of the mean (S.E.M), n=8.

To confirm the mRNA profiles, immunohistochemistry was carried out on macular transverse sections. NeuN and Thy-1 are both reliable retinal ganglion cell markers; they were therefore used to immune-label RGCs in the human macular sections. Recoverin is specific marker of both cones and rods photoreceptor cells; this was used to stain photoreceptor cells. It can be seen that NeuN and Thy-1 antibodies stain cells in the RGCL (Figure 3.5). It is notable that only a few cells displaced RGCs are seen in the inner nuclear layer. RCVRN presented an excellent immunoreaction in the outer retina (including OPL, ONL and possibly as well as

outer segment layer) (Figure 3.6). Therefore, the immunostaining presented the consistent patterns as their mRNA distribution in the retina macular.
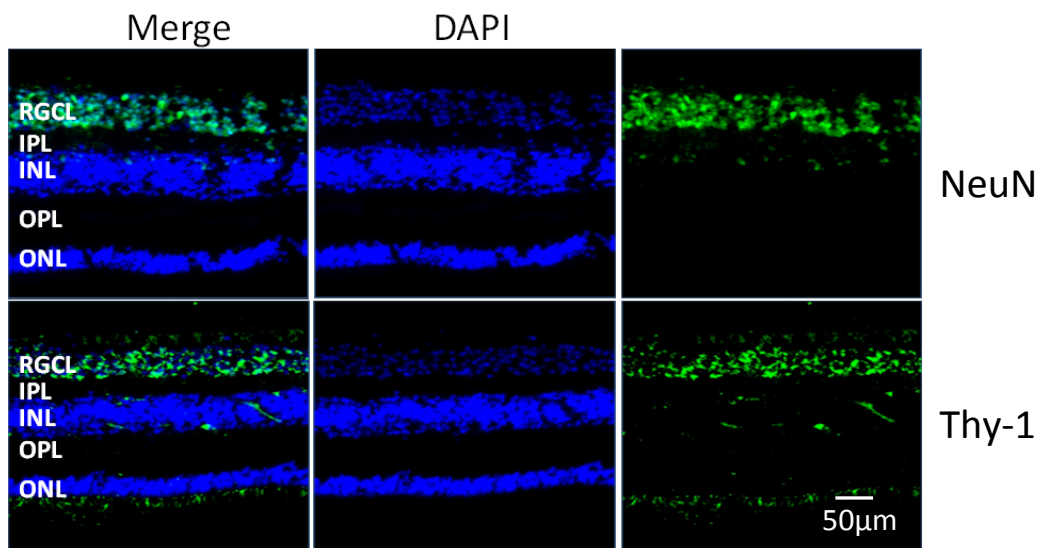
Figure 3.5 Immunohiscochemistry images of human retinal macular region. Retinal ganglion cell markers, NeuN and Thy-1 labelled ganglion cells. The cell bodies in the retinal ganglion cell layer (RGCL), inner plexiform layer (IPL), inner nuclear layer (INL), outer plexiform layer (OPL) and outer nuclear layer (ONL) were stained by DAPI (blue). NeuN and Thy-1 stained the cell body in the RGCL and a few in the INL.
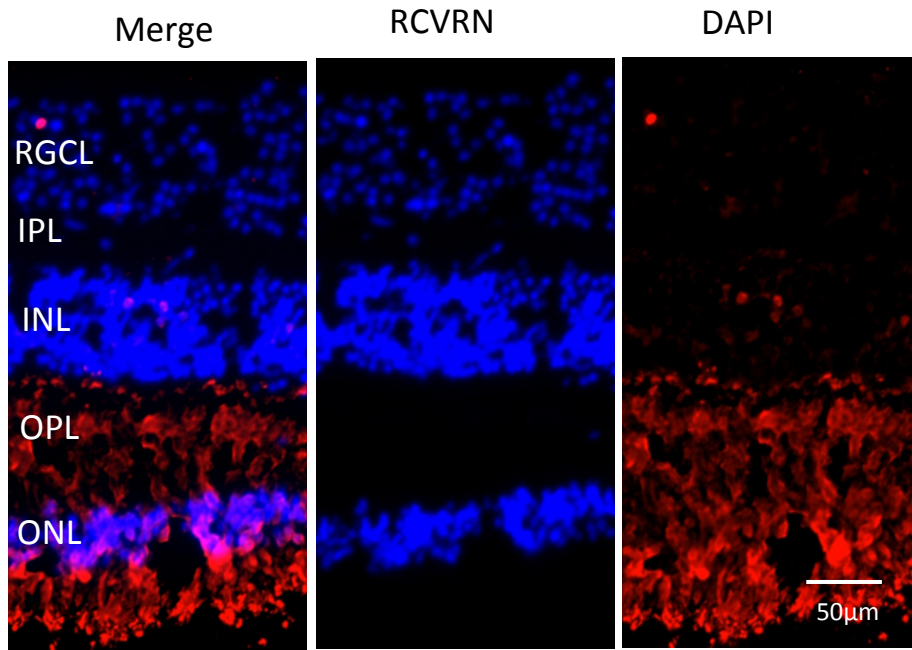
Figure 3.6 Immunohiscochemistry images of human retinal macular region. Photoreceptor cell marker, RCVRN, labelled outer retina layers. The cell bodies in the retinal ganglion cell layer (RGCL), inner plexiform layer (IPL), inner nuclear layer (INL), outer plexiform layer (OPL) and outer nuclear layer (ONL) were stained by DAPI (blue).

3.3 Discussion

Retinal morphology was retained in human retina within 24h post mortem. The retinal macular region contained abundant retinal ganglion cells compared with para-macular and peripheral regions. The central macular region is approximately 2% of the area of the whole retina, but contains over 30% of RGCs (Curcio and Allen 1990). The RGCL thickness in the central retina has been reported to be 60-80μm decreasing to 10-20μm in the periphery (Forrester, Dick et al. 2002). Our retinal macula samples with histological H&E staining verified that the retina macular region contained the thickest retinal ganglion cell layer (RGCL) and highest numbers of RGCs.

In this study a new technique has been developed, which offers a powerful and practical method to obtain relatively high quantities of mRNA from the human RGC layer. The gene expression profiles of different retinal cell markers, RCVRN, CALB, CHAT and THY-1, for photoreceptor cells, horizontal cells, amacrine cells and ganglion cells respectively (Figure 3.2 and 3.3), were highly consistent with the known structure of the retina. Furthermore, when the profiles of two further RGC markers were investigated, Brn3a (POU class 4 homeobox 1) and NeuN (RNA binding protein, fox-1 homolog (C. elegans) 3, RBFOX3) they were found to correspond with that for THY-1.

To confirm the mRNA profiles Immunohistochemistry was used. NeuN is a neuronal specific protein which labels RGCs in the RGCL and INL (Mullen, Buck et al. 1992; Wolf, Buslei et al. 1996). It was widely used to determine RGC number changes in experimental models of glaucoma (Buckingham, Inman et al. 2008; Niyadurupola, Sidaway et al. 2011; Niyadurupola, Sidaway et al. 2013). Thy-1 is a cell surface antigen which label the cell body and cell processes (Barnstable and Drager 1984). It was widely utilized in the immune-panning procedure to purify RGCs (Barres, Silverstein et al. 1988; Zhang, Liu et al. 2010; Hong, Iizuka et al. 2012). Recoverin is expressed in both rod and cone photoreceptor cell (Dizhoor, Ray et al. 1991; Haverkamp and Wassle 2000). In the human retina, NeuN and Thy-1 were seen to label RGCs in the RGCL and only a few displace RGCs in the INL; RCVN staining was seen in the ONL and OPL. These immunoreactivities supported their mRNA profiles in the human retina.

Overall, these data show that the technique developed to give horizontal planar sections of the retina was successful. Having developed the technique it can be used to study expression of genes of interest across the human retina. By isolating mRNA from the RGCL, gene arrays can be used to study gene expression in this region of the human retina.

Chapter 4

Expression profiling of genes in human retinal ganglion cells using a novel sectioning technique

4.1 Introduction:

In the research discussed in the previous chapter, a novel sectioning technique was developed, which enabled isolation of the RGCL from entire retina. This layer predominantly contains the retinal ganglion cells, which are the neuronal cells that take the visual information from the sensory retina to the brain. RGC degeneration is linked to several diseases, particular glaucoma. Previous reports have demonstrated that in glaucoma RGCs were severely affected and the thickness of RGCL is greatly decreased, both in experimental glaucoma and glaucoma patients (Kendell, Quigley et al. 1995; Osborne, Ugarte et al. 1999; Kielczewski, Pease et al. 2005). In order to enable to understand more about the cellular processes that might be involved in RGC degeneration in glaucoma, it is important that genes expressed in human RGCs are identified.

As same in all cells, genes regulate the whole life of the RGCs, from embryonic development to differentiation and to RGC apoptosis. Gene mutations have been shown to cause various retinal diseases (Siegert, Cabuy et al. 2012). For example, the absence of cytochrome P450, family 1, subfamily B, polypeptide 1 (CYP1B1) has been shown to be relevant to primary congenital glaucoma (Dimasi, Hewitt et al. 2007) and its overexpression promotes RGCs survival (Wang, Kunzevitzky et al. 2007). Deficiency of chemokine (C-X3-C motif) receptor 1 (CX3CR1) contributed to the disease progression of age-related macular degeneration (Chen, Connor et al. 2007).

Global gene expression studies have been carried out investigating the expression profile of RGCs in animal models (Farkas, Qian et al. 2004; Ivanov, Dvoriantchikova et al. 2006; Wang, Kunzevitzky et al. 2007) and also human retina recently (Kim, Kuehn et al. 2006). As the immunopanning was successfully developed to isolate RGCs in the rat, the gene expression profiling was put into practice using purified RGCs (Farkas, Qian et al. 2004; Ivanov, Dvoriantchikova et al. 2006). Gene microarray of purified rat RGCs, which

compared with the whole retina, was found out that majority of RGC markers had been included in RGC-enriched microarray list. Moreover, there was a group of genes which related to cell pro-survival, such as Nrg1, Rgn and Nrn1, was revealed highly expressed in RGCs. Unfortunately, there was few successful attempt to purify the human RGCs. However, the gene expression profiling of human RGCL was obtained using LCM, and it was compared with the rest layers of retina (Kim, Kuehn et al. 2006). Some research groups also set up experimental glaucoma models to assess the alteration of gene expression of RGCL using LCM and immunopanning (Ahmed, Brown et al. 2004; Soto, Oglesby et al. 2008; Guo, Cepurna et al. 2010).

In the previous chapter the RGCL was successfully separated from the entire retina, therefore, this technique was used to isolate RGCL mRNA in order to perform gene array analysis. Two groups of gene array data were obtained, one for the RGCL (isolated from the macular region) and the other for the entire macula (Mac). The aim of the research presented in this chapter was to compare the gene expression of the RGCL with the Mac, to find out the most expressed genes in the RGCL relative to the whole retina. This may identify genes of specific importance to the retinal ganglion cells.

4.2 Result:

4.2.1 Selection of RGCL samples for Illumina gene arrays

Retinal macular samples were sectioned and collected by our planar sectioning technique to isolate the RGCL from the retina. The mRNA samples from each macula were measured and the expression of the RGC cell marker, THY-1, was determined by QRT-PCR. Figure 4.1 shows the THY-1 expression profile for a single macula. Three sections were then chosen: the sample with the peak expression and its next-door neighbors. These three samples were combined. For the control group, RNA was isolated from the entire macula (Mac). For each eye, over 100ng of RNA was processed for gene array analysis. There were 5 samples in total from each group (RGC and Mac). These samples were send to Source Bioscience (Nottingham, UK) and processed Illumina gene microarray.
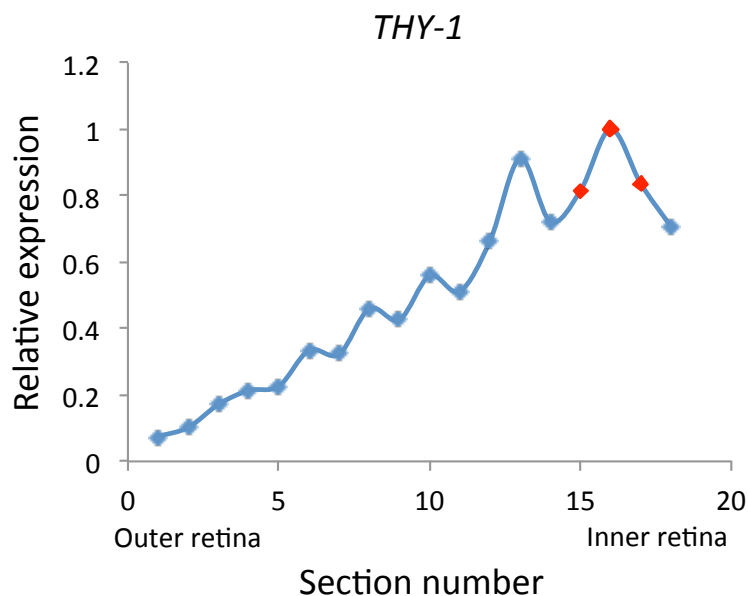
Figure 4.1 The expression of THY-1 across the retina macular sections, measured by QRT-PCR. The red dots were the sample selected as RGCL sample for array analysis. The expression was normalised to the highest expression.

4.2.2 Illumina gene arrays and analysis

Global gene expression analysis using Illumina gene arrays was carried out to identify genes expressed in human RGCL. RNA samples were either from the RGC layer (n=5) obtained by cryosectioning or from Mac samples (n=5). RNA integrity was assessed by running a small aliquot from each sample on an Agilent Bioanalyzer 2100 using RNA 6000 Nano or Pico Assay. Most samples had a high RNA integrity number (RIN > 8), apart from one where RIN was 6.9, indicating they were good quality samples with sufficient integrity to be used for further gene array analysis.

Table 4.1 RNA viability for array samples. The RNA integrity number (RIN) provides information on the presence or absence of RNA degradation products. A RIN number of 10 indicates perfect, 5 partially degraded and 1 totally degraded RNA.

Sample Name	RIN Number	Pass/ Questionable/ Fail	260/280	ng/µl	Yield (ng)
RGC-1	8.9	Pass	2.07	34.40	378.4
RGC-2	8.9	Pass	2.09	37.72	414.92
RGC-3	6.9	Questionable	1.94	18.12	199.32
RGC-4	9.1	Pass	2.09	22.40	246.4
RGC-5	8.4	Pass	2.08	16.12	177.32
Mac-1	8.0	Pass	1.98	30.88	339.68
Mac-2	8.5	Pass	2.04	33.60	369.6
Mac-3	8.9	Pass	1.92	17.48	192.28
Mac-4	9.2	Pass	1.91	28.00	308
Mac-5	8.9	Pass	1.83	33.24	365.64

The samples were grouped into different phenotypes by constructed hierarchical plot, which based on expression of 7953 genes (Figure 4.2). These two phenotypes were from RGCL and Mac, respectively. And the five RGCL samples were all closely related, indicating that sample selection was appropriate. Furthermore, when a heat-map was produced of the top 50 most expressed genes in the RGCL compared to the whole macula, it can be seen that the

individual samples are very well segregated. They also shown that the individual variation between each sample in the two groups was low: with only 2 exceptions all of the RGCL samples were red for each of these genes.
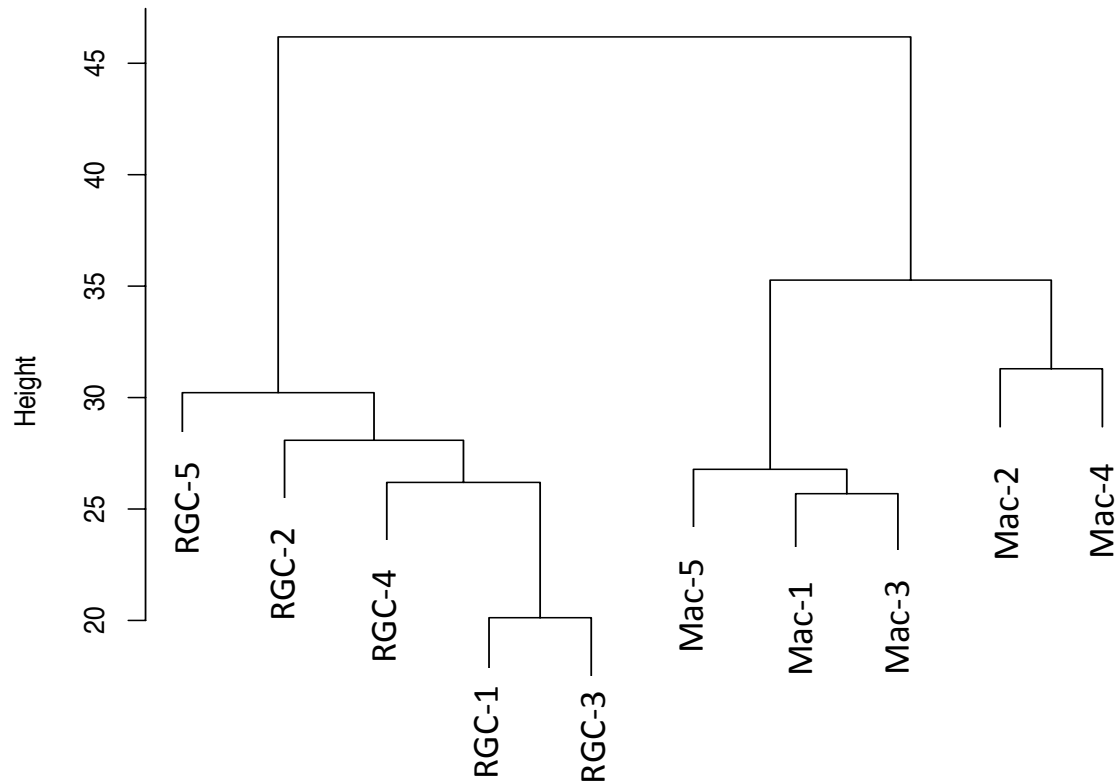
Figure 4.2 Sample relationship based on expression of 7953 genes with sd/mean >0.1. The samples were split into two groups. These samples from same phenotype were grouped together.
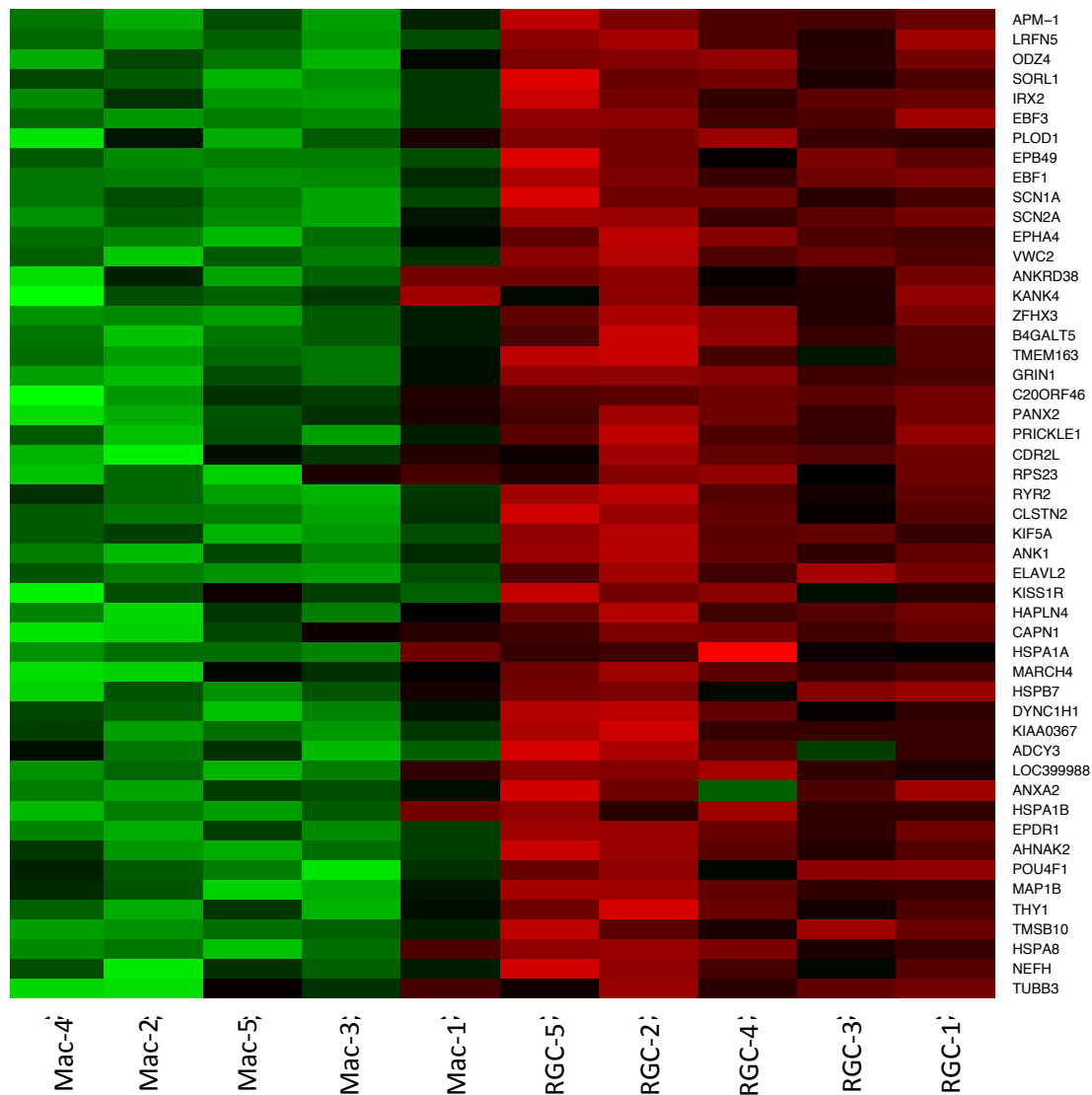
Figure 4.3 The heat map of the top 50 features of RGC. The red colour means positive correlated, the green means negative correlated.

Data analysis compared gene expression in the RGCL to whole macular samples (MAC). The 7953 genes were retained only if they were presented over 50% of one phenotype, which were further analyzed. The most "upregulated genes" are therefore those most highly expressed in the RGC layer compared to the entire macula. The most "downregulated genes" are those expressed most highly in the entire macula compared to the RGCL.

4.2.3 Gene array analysis: RGCs vs entire macula

Gene array analysis compared gene expression levels in the RGCL to the whole macula. A total 34689 gene were tested on the RGC samples and Mac samples. Expressions of 820 genes were detected as present in either RGCL or Macular samples. 359 genes were identified with higher expression (>1.3-fold enrichment) in the RGCL ($p<0.05$) compared to 461 genes (include ribosomal encoding genes, duplicate genes and uncharacterized genes) showing over 1.3-fold greater expression in the whole macula. Table 2.1 shows the most enriched genes in the RGCL compared to the entire macula (>2-fold). In these most up-regulated genes, several genes are specific to neuronal development and neurogenesis, such as ZFHX3, EBF1 and MAP1B. Heat shock protein 70KDa protein 1B (HSPA1B) and AHNAK nucleoprotein 2 (AHNAK2) were the most highly expressed two genes in the RGCL (Table 4.2), and are possible new candidates for RGC markers. Importantly the RGC and axon markers, POU4F1, TUBB3, THY-1 and NFH were included in the most expressed genes (fold change >2) in the RGL. NeuN, however, did not appear in the gene list.

Table 4.2 The genes which were most differentially expressed (>2-fold) in the RGCL compared to whole macula. These genes were placed from the biggest fold change to the smaller.

Order No. in list	Official symbol	Official full name	Fold change
1	HSPA1B	eat shock 70kDa protein 1B	3.22
2	AHNAK2	AHNAK nucleoprotein 2	2.61
3	ZFHX3	Zinc finger homeobox3	2.54
4	SCN1A	Sodium channel, voltage-gated, type 1, alpha subunit	2.48
5	EBF1	Early B-cell factor 1	2.47
6	SORL1	Sortilin-related receptor, L (DLR class) A repeats containing	2.40
7	MAP1B	Microtubule-associated protein 1B	2.36
8	KANK4	KN motif and ankyrin repeat domain 4	2.35
9	NPR3	Natriuretic peptide receptor C/guanylate cyclase C (atrionatriuretic peptide receptor C)	2.32
10	IRX2	Iroquois homeobox 2	2.25
11	RYR2	Ryanodine receptor 2	2.17
12	C20ORF46	Transmembrane protein 74B	2.16
13	DYNC1H1	Dynein, cytoplasmic 1, heavy chain 1	2.16
14	EPDR1	Ependymin related protein 1	2.15
15	POU4F1	POU class 4 homeobox 1	2.14
16	PANX2	Pannexin 2	2.13
17	EBF3	Early B-cell factor 3	2.12
18	PRUNE2	Prune homolog 2	2.11
19	ELAVL2	ELAV (embryonic lethal, abnormal vision, Drosophila)-like 2 (Hu antigen B)	2.11
20	B4GALT5	UDP-Gal:betaGlcNAc beta 1,4- galactosyltransferase, polypeptide 5	2.10
21	SCN2A	Sodium channel, voltage-gated, type II, alpha subunit	2.09
22	EPB49	Dematin actin binding protein	2.08
23	PRICKLE1	Prickle homolog 1	2.07
24	HSPA1A	Heat shock 70kDa protein 1A	2.07
25	EPHA4	EPH receptor A4	2.07
26	TUBB3	Tubulin, beta 3 class III	2.07
27	HAPLN4	Hyaluronan and proteoglycan link protein 4	2.06
28	HS.4892	EFR3 homolog B	2.05
29	KIF5A	Kinesin family member 5A	2.04
30	CDR2L	Cerebellar degeneration-related protein 2-like	2.04
31	ODZ4	Teneurin transmembrane protein 4	2.04
32	CAPN1	Calpain 1, (mu/l) large subunit	2.04
33	THY1	Thy-1 cell surface antigen	2.04
34	HSPA8	Heat shock 70kDa protein 8	2.03
35	NEFH	Neurofilament, heavy polypeptide	2.03
36	TMEM163	Transmembrane protein 163	2.02
37	RPS23	Ribosomal protein S23	2.02
38	KISS1R	KISS1 receptor	2.00
39	HSPB7	Heat shock 27kDa protein family, member 7 (cardiovascular)	2.00
40	GRIN1	Glutamate receptor, ionotropic, N-methyl D-aspartate 1	2.00

81

The genes listed in Table 4.3 were those with the highest relative expression in whole macula compared to the RGCL. Most genes in this list were involved in the phototransduction pathway. There is just one exception, RAX2, a transcription factor which has been reported to be essential in eye development and in modulating gene expression in photoreceptor cells (Wang, Chen et al. 2004).

Table 4.3 The "down-regulated genes", which were most differently expressed in the MAC compared with RGCL. These genes were placed from the biggest fold change to the smaller.

Order No. in list	Official symbol	Official full name	Fold change
1	PDE6H	Phosphodiesterase 6H, cGMP-specific, cone, gamma	17.58
2	OPN1LW	Opsin 1 (cone pigments), longwave-sensitive	17.37
3	OPN1MW	Opsin 1 (cone pigments), mediumwave-sensitive	14.64
4	ARR3	Arrestin 3, retinal (X-arrestin)	14.15
5	GNAT2	Guanine nucleotide binding protein (G-protein), alpha transducting activity polypeptide 2	10.54
6	SAG	S-antigen; retina and pineal gland (arrestin)	9.86
7	GUCA1B	Guanylate cyclase activator 1B (retina)	9.28
8	RAX2	Retina and anterior neural fold homeobox 2	8.79
9	GUCA1A	Guanylate cyclise activator 1A	8.47
10	CNGA1	Cyclic nucleotide gated channel alpha 1	8.28

4.2.4 Expression profiles of HSPA1B and AHNAK2

In order to validate the array results, QRT-PCR was used to measure expression of genes with high expression in the RGC or whole macula. The top two most highly expressed in the RGCL genes (HSPA1B and AHNAK2) (Table 4.2) and one of the genes (OPN1LW) most highly expressed in whole macula were selected to carry out QRT-PCR in samples from 4 additional retinas. These were compared to the RGC

and photoreceptor markers THY-1 and RCVRN. The distribution of AHNAK2 was closely associated with the RGC marker, THY-1 (Figure 4.4). The expression of AHNAK2 in the photoreceptor layer was negatively associated with the photoreceptor cell marker, RCVRN. AHNAK2 presented 2.61-fold enrichment in the RGCL compared to the photoreceptor layer (Figure 4.4).

HSPA1B is another gene relatively highly expressed in the RGC gene list. Its expression also associated with THY-1 and AHNAK2, but it is more variable. It was higher in the inner retina compared to the outer retina, giving a 3.22-fold enrichment in the RGCL. OPN1LW was highly expressed in the photoreceptor layer and very limited expression was detected in the inner retina. Distribution was similar to RCVRN although the profile for OPN1LW showed a steeper decline than RCVRN. Its expression was 17.37-fold greater in the photoreceptor cell compared with RGCs, whereas RCVRN was 7.34-fold (Figure 4.4).
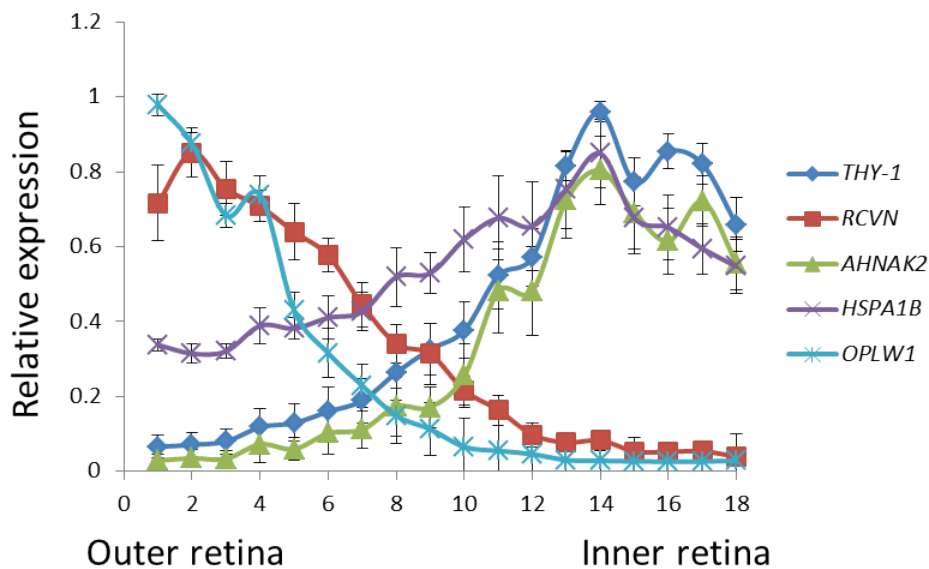
Figure 4.4 The expression profile of HSPA1B, AHNAK2 and OPLW1 in human retina compared to the selected marker genes THY-1 and RCVN. Serial cryosections were taken and gene expression was measured by QRTPCR. n=4.

4.2.5 Localisation of RGC markers in the human retina

AHNAK2 displayed highest immunoreactivity in the RGCL. It also presented very limited staining in the OPL and outer segment layer (Figure 4.5). HSP1AB staining was seen throughout the retina, although staining appeared to be most intense in the RGCL and was extensively colocalised with NeuN (Figure 4.6). RCVRN is a marker that labels both rod and cone photoreceptor cells. It exclusively stained in the OPL, ONL and outer segment layer (Figure 4.6).
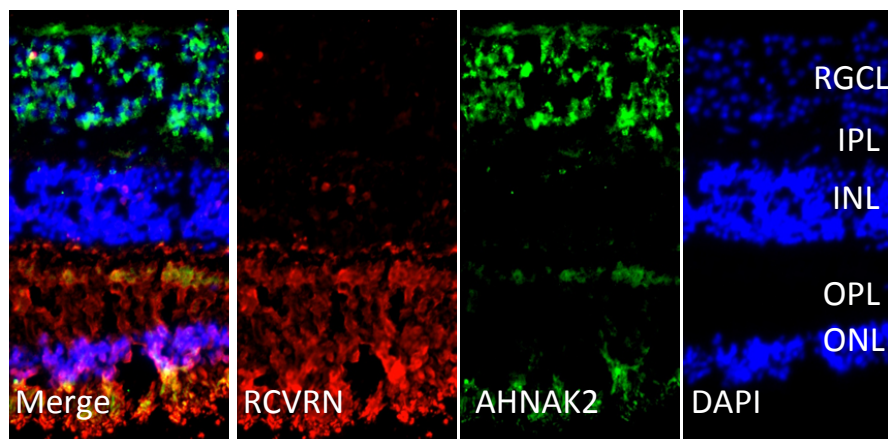
Figure 4.5 Transverse retinal sections immune-labelled with antibodies against the photoreceptor cell marker, RCVRN (red), and co-labelled with AHNAK2 (green). The cell nuclei was labelled with DAPI (blue). ONL, outer nuclei layer; OPL, outer plexiform layer; INL, inner nuclei layer; IPL, inner plexiform layer; RGCL, retinal ganglion cell layer.
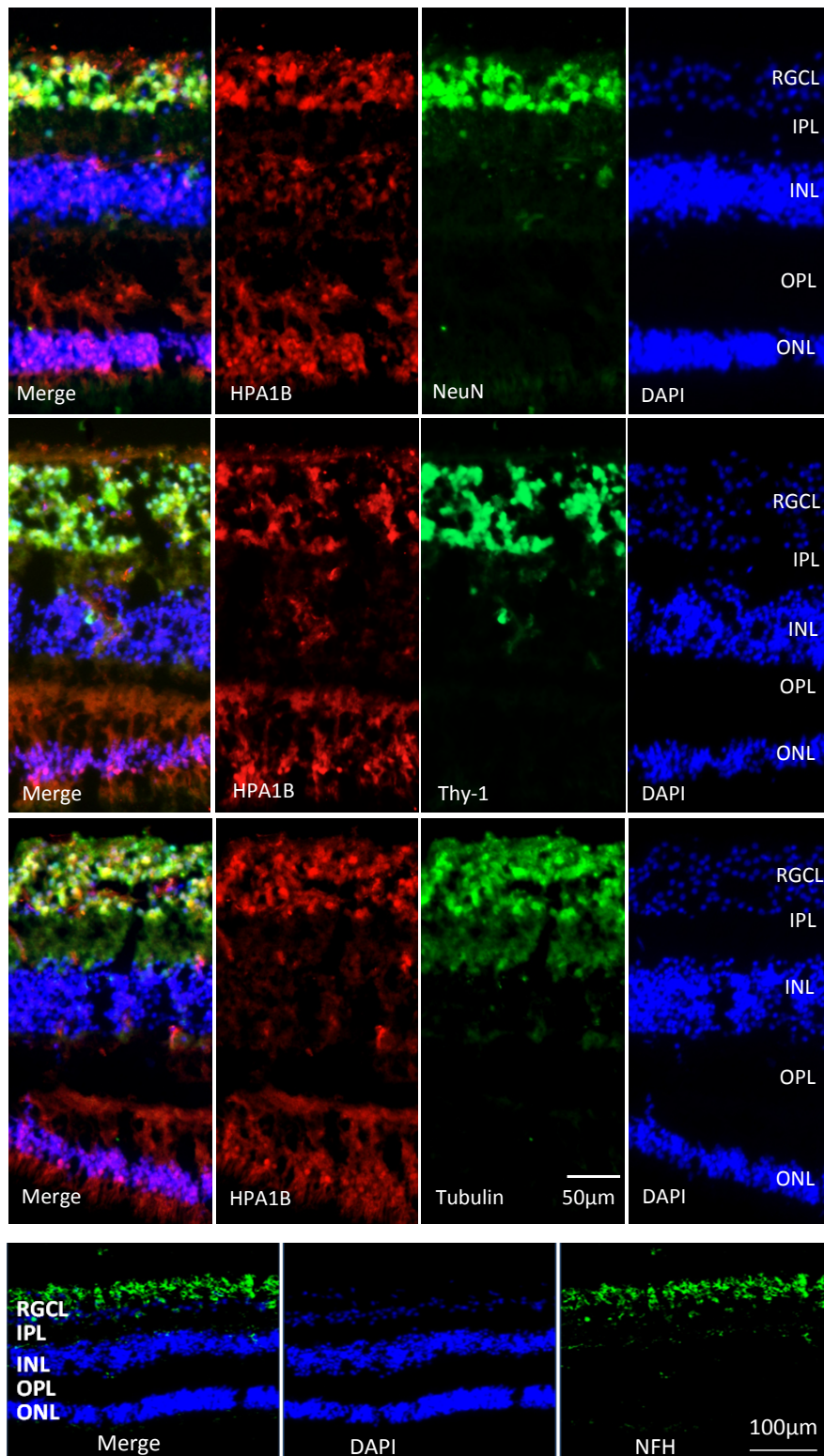
Figure 4.6 Transverse retinal sections immuno-labeled with antibodies against the RGC markers, NeuN, THY-1, Tubulin and neurofilament heavy chain (green), HSPA1B (red). The cell nuclei were labelled with DAPI (blue). ONL, outer nuclei layer; OPL, outer plexiform layer; INL, inner nuclei layer; IPL, inner plexiform layer; RGCL, retinal ganglion cell layer.

4.3 Discussion

Gene array analysis has identified a large number of genes, which were preferentially expressed in the RGC layer. Some of the genes which identified in this study have not been previously linked with RGCs. Retinal sections of entire macular were obtained with high quality RNA by using our novel planar section technique. RGCL samples were successfully isolated from the retina as they were grouped together as same phenotype, which were apart from the Mac samples. Heat map of top 50 arrays samples shown that all the sample were classified into two phenotypes, even they have individual variations as been excepted when using human tissue. The validity of Illumina gene array data was checked using three representative genes, which were highlighted by the array. They were in fact expressed in the human retina by testing both PCR and immunoreaction.

The genes identified can be separated into a number of functional groups. The most noticeable are members from heat shock protein (HSP) family. Of all RGCL enriched genes (fold change >2), 4 genes belong to the HSP family and three of these were from the 70kDa heat shock protein gene family (HSP70) (Table. 4.4). A further two HSP genes, HSP105 and HSP10, were found in the list of genes with >1.5-fold enrichment (Table 4.4).

Heat shock proteins (HSPs) are highly conserved proteins which involved in cell survival by upregulated its expression and against cell apoptosis pathway under pathological conditions (Takayama, Reed et al. 2003; Beere 2005). They are important in early immune response in tissue under environmental stress (Wax and Tezel 2009). Several reports have indicated that antibody levels to HSPs were elevated in serum, aqueous humor and the optic nerve head in glaucoma patients (Tezel, Hernandez et al. 2000; Joachim, Bruns et al. 2007a; Joachim, Wuenschig et al. 2007b).

It was observed that cultured rat RGCs increased HSP72 expression after hyperthermia (42˚C, 1h) and hypoxia (6h) treatment (Caprioli, Kitano et al. 1996). These pretreated cells were then found to have greater resistance to anoxia (6h) or glutamate treatment (6h) exposure (Caprioli, Kitano et al. 1996). It has also been

shown that the small heat shock proteins (aA- and aB-crystallin and HSP27) are elevated in glaucoma patients, and that this is greater in normal pressure glaucoma patients compared to those with primary open angle glaucoma (Tezel, Seigel et al. 1998; Wax, Tezel et al. 2000). Furthermore, in experimental glaucoma there is increased expression of HSPs, particular HSP27, in both RGCs and glial cells (Huang, Fileta et al. 2007). This may suggest that HSPs have an important role in assisting RGCs in maintenance of cell function and resisting stressful insults.

HSP70 is a group of highly conserved protein which contains 13 members, such as *HSPA1A* and *HSPA1B*. *HSPA1A* and *HSPA1B* are two stress-inducible and intronless genes that have almost identical sequences with only two amino acids different (Kampinga, Hageman et al. 2009). They were not able to be distinguished by most methods, including the protein level (Scieglinska, Piglowski et al. 2011). HSP70 functions as a chaperone molecule to supervise protein denaturation, translocation, correct folding, activation and aggregation (Takayama, Reed et al. 2003). HSP70 has a potential neuroprotective function when over-expressed and has been shown to protect some neuron cells from certain stressful insults, including oxidative stress (Yenari, Giffard et al. 1999; Kalmar and Greensmith 2009). A recent report has indicated that HSP70 is specifically expressed in RGCs and is the earliest gene was induced after optic nerve injury, crucial for RGCs survival in the zebra fish retina (Nagashima, Fujikawa et al. 2011). Heat shock 70kDa protein 8 (*HSPA8 or HSC70*), shares 85% sequence homology with HSP70 and has similar functions to the other members of HSP70 family (Liu, Daniels et al. 2012). *HSP70* and *HSC70* expressions were also enhanced after cerebral ischemia (Muranyi, He et al. 2005). Furthermore, administration of HSP/HSC70 to the neonatal mouse with traumatic injury can reduce subsequent apoptotic loss of neurons (Tidwell, Houenou et al. 2004). Thus, HSP70 and HSC70 appear to play a positive role in neuroprotection.

Table 4.4 Genes of the heat shock protein family with greater expression in the RGCL in the human retina.

Official symbol	Official full name	Fold change
HSPA1B (HSP70-2)	Heat shock 70kDa protein 1B.	3.22
HSPA1A (HSP70-1)	Heat shock 70KDa protein 1A.	2.07
HSPA8 (HSC70)	Heat shock 70kDa protein 8.	2.03
HSPB7	Heat shock 27KDa protein family, member 7.	2.00
HSPH1 (HSP105)	Heat shock 105/110 KDa protein 1.	1.79
HSPE1 (HSP10)	Heat shock 10kDa protein 1.	1.54

A second functional group of genes up-regulated in RGCL were several transcription factors (Table 4.5). *ZFHX3, EBF1* and *IRX2* were included in the top 10 RGCL genes. Both *Ebf1* and *Ebf3* have been detected in the developing retina of mouse (Davis and Reed 1996; Wang, Tsai et al. 1997; Wang, Tsai et al. 1997; Trimarchi, Stadler et al. 2007). *EBF1* has also been previously shown to be expressed in the RGCL of human retina (Kim, Kuehn et al. 2006). Knockdown of *EBF1* in mouse retinas, caused abnormal RGC axons at the optic chiasma and increased numbers of Müller glial cells in the retina (Jin and Xiang 2011). These data suggest that they are also important transcription factors in the human retina. *ZFHX3* is found in the central nervous system where it participates at an early stage in visual sensory development. It also promotes the differentiation and proliferation of neuronal cells (Watanabe, Miura et al. 1996; Jung, Kim et al. 2005; Kim, Kawaguchi et al. 2010). *ZFHX3* has been found to activate platelet-derived growth factor (PDGF) receptor b, a neuronal survival factor, considered to be a protector when cerebellar neurons suffer oxidative stress (Kim, Kawaguchi et al. 2010). This may be significant in the retina, where it has been shown the PDGF is neuroprotective (Kim, Kawaguchi et al. 2010). *IRX2* is a member of Iroquois homeobox gene family. Another closely related gene, *IRX3* (FDC=1.88), was also detected in the RGCL in this study.

Table 4.5 Transcription factor genes of with greater expression in RGCL in the human retina.

Official symbol	Official full name	Fold change
ZFHX3	Zinc finger homeobox3	2.54
EBF1	Early B-cell factor 1	2.47
IRX2	Iroquois homeobox 2	2.25
POU4F1	POU class 4 homeobox 1	2.14

A third group of genes which was upregulated in the RGCL were ion channels and ion associated proteins. Several sodium-related genes (Table 4.6) and calcium- related genes (Table 4.7) were presented. *AHNAK2* encodes a calcium-associated protein, which is an unusually large (approximately 700KDa) and propeller-like protein. It is the second most highly expressed gene in the RGCL that is first time determined its distribution in the retina. RyR2 is a ryanodine receptor calcium channel, which was found on the ER membrane and participates in Ca^{2+} from the internal store. Cyclic ADP-ribose (cADPR) can act as an endogenous stimulus at RyRs to induce Ca^{2+} release. In retinal cells, RyR2 has been found was more widely expressed than other RyRs. CAPN1 is one of ubiquitous calpains, which are calcium-dependent cysteine proteases (Johnson and Guttmann 1997; Ono and Sorimachi 2012). Calpain-1 has been shown that highly expressed in RGCs in the rabbit retina (Croall and Demartino 1991). Calpain activation has been testified that involved in ischemia/hypoxia-induced retinal cell death in both in vivo (Sakamoto, Nakajima et al. 2000; Tamada, Nakajima et al. 2005) and in vitro in animal models (Tamada, Fukiagea et al. 2002; Tamada, Nakajima et al. 2005). GRIN1 is a glutamate receptor. Glutamate receptor has been widely studied in the retina, which its activation involves in ischemia induced RGC death by increased the cellular calcium.

SCN1A was one of top 10 RGCL enriched genes. It is the alpha subunit of the Type I voltage-gated sodium channel. In addition to SCN1A, another two members of voltage-gated sodium channel, *SCN2A* and *SCN2* were also detected as having greater expressions in the RGCs. These code the alpha and beta subunits of the Type II

voltage-gated sodium channel. It would be expected that expression of voltage-gated sodium channels would be abundant in the RGCL, since the fundamental role of the RGCs is to conduct action potentials along its axons to take visual information to the brain.

Table 4.6 Calcium-related genes with greater expression in RGCL in the human retina.

Official symbol	Official full name	Fold change
AHNAK2	AHNAK nucleoprotein 2	2.61
STX1B	Syntaxin 1B, calcium-dependent cellular receptor for Synaptic transmission.	2.20
RYR2	Ryanodine receptor 2	2.17
CAPN1	Calpain 1, (mu/I) large subunit.	2.04
GRIN1	Glutamate receptor, ionotropic, N-methyl D-aspartate 1	2.00

Table 4.7 Sodium-related genes with greater expression in RGCL in the human retina.

Official symbol	Official full name	Fold change
SCN1A	Sodium channel, voltage-gated, type 1, alpha subunit	2.48
SCN2A	Sodium channel, voltage-gated, type II, alpha subunit.	2.09
SCN2B	Sodium channel, voltage-gated, type II, beta subunit	1.91

The rest of the RGCL enriched genes encode genes for cytoplasmic components, membrane structural proteins or RNA binding proteins. Some have interesting connections to neurodegenerative disease. *SORL1* expression associates with Alzheimer's disease as it regulates activities of amyloid precursor protein (Klinger, Glerup et al. 2011; Lao, Schmidt et al. 2012). *MAP1B* is a member of microtubule-associated protein that promotes microtubule assembly and is up-regulated during axonal growth of developing neurons and in regeneration in the CNS (Bates, Trinh et al. 1993; Tymanskyj, Scales et al. 2012). *NPR3* codes one of the natriuretic peptide

receptors. These have previously been shown to be widely expressed in the CNS, including in the retina (Cao and Yang 2008). *NPR3* has also been shown to be expressed in the human retina, (Rollín, Mediero et al. 2004) and in rat has been detected in RGC membranes (Xu, Tian et al. 2010).

In this study a new technique has been developed, which offers a powerful and practical method to obtain relatively high quantities of high quality mRNA from the human RGC layer. Using Illumina gene array technology the genes that are most highly expressed in the RGCL from the macula compared to the whole macula in human retina. Several genes were identified which may have crucial contributions for retinal ganglion cell functions. Furthermore, the data has identified new candidates for specific markers of retinal ganglion cell, especially *AHNAK2*. Finally, our study has identified targets that warrant further research in relation to targeting RGC degeneration in glaucoma. There are several interesting genes were highlighted in the RGCL up-regulated list, whereby, most interesting ones were calcium- related group. Glutamte is excitotoxicity which lead to $[Ca^{2+}]_i$ overload. Consequently, the calcium-depend cellular pathways will be activated and stimulated cell death. In the following chapter, calpain, which has been found by gene array will be identified in greater detail, and investigate its role in relation to neurodegeneration in the human retina.

Chapter 5

Calpain activation and retinal ganglion cell death in HORCs induced by retina ischemia

5.1 Introduction:

In the previous chapter, several calcium-related genes presented greater expressions in the RGCL which included one of calpain member. Calpain activation contributed to neural cell death under the ischemia condition (Rami 2003). The causes of RGC death in glaucoma remain unclear, but retinal ischemia is proposed to play an important role (Osborne, Casson et al. 2004). During retinal ischemia, calcium homeostasis is breakdown (Crish and Calkins 2011).

Excitotoxicity by glutamate has been proposed as the mechanism by which retinal ischemia leads to Ca^{2+} overload and subsequent RGC death (Goll, Thompson et al. 2003; Chiu, Lam et al. 2005). In an ischemia/reperfusion experimental model, glutamate has been measured at the retinal surface during the retinal ischemia and following reperfusion (Louzadajunior, Dias et al. 1992). Glutamate levels increased as a result of ischemia, but greater levels were seen after reperfusion. Release of glutamate causes over-activation of both NMDA and non-NMDA glutamate receptors. NMDA receptors, are inotropic glutamate receptors, which are highly permeable to Ca^{2+} and Na^+ allowing these ions to enter the cells (Szydlowska and Tymianski 2010). Activation therefore leads to Ca^{2+} influx and elevated $[Ca^{2+}]_i$. Isolated rat RGCs show increased $[Ca^{2+}]_i$ when treated with glutamate (Miao, Dong et al. 2012) and MK801, an antagonist of NMDA, has been shown to protect the retina following ischemic insult (Lam, Siew et al. 1997). The NMDA receptor is extensively expressed in the retina, including in RGCs (Yin Shen 2006). Furthermore, the NMDA receptor subunit GRIN1 was one of the genes identified as being enriched in the human RGCL (Chapter 4). The increase in intracellular Ca^{2+} caused by excitotoxic mechanisms could, in turn, lead to activation of calcium-activated enzymes, such as calpain. The large subunit of calpain 1 was also one of the genes identified as being enriched in the human RGCL (Chapter 4).

5.1.1 Calpain-1 and calpain-2

The calpains are a family of calcium-dependent cysteine proteases (Johnson and Guttmann 1997; Ono and Sorimachi 2012). Calpain-1 (μ-calpain) and calpain-2 (m-calpain) are ubiquitously distributed and the most extensively studied isoforms of calpain. They have similar characteristics, but are activated by different Ca^{2+} concentrations, with calpain-1 being activated at lower concentrations than calpain-2. Calpains have a number of substrates, but key substrates are cytoskeletal proteins, such as spectrin, tubulin, vimentin (Goll, Thompson et al. 2003). Spectrin is a cytoskeletal protein that is proteolsed both by calpain and caspase-3. A 145-kDa fragment is specifically generated by calpain and 150-kDa fragments are produced by both calpain and caspase-3 in apoptotic cells (Nath 1996; Huang, Fileta et al. 2010). Both of these fragments are generated under the pathological conditions, and are early markers of neurodegeneration (Huang, Fileta et al. 2010).

5.1.2 Calpain activation and neurodegeneration in the retina

Calpain activation has been well studied in brain ischemia, where degeneration of cytoskeletal proteins by calpain led to neuronal cell death (Yamashima 2000; Huang and Wang 2001; Rami 2003). In the retina, it has been found that calpain activation is involved in ischemia/hypoxia-induced retinal cell death in both in vivo (Sakamoto, Nakajima et al. 2000; Tamada, Nakajima et al. 2005) and in vitro in animal models (Tamada, Fukiagea et al. 2002; Tamada, Nakajima et al. 2005). Activation has also been observed in an experimental model of glaucoma (Huang, Fileta et al. 2010). In addition, calpain-1 activation showed a time dependent increase after the rat retina was subjected to intravitreal injection of NMDA (Chiu, Lam et al. 2005). Calpain-2 and spectrin breakdown products (SBDPs) were also increased after exposure of rat RGCs to glutamate in isolated rat retinal neurons, and the formation of SBDPs was inhibited by glutamate receptors antagonists (Miao, Dong et al. 2012). There is therefore good evidence that calpain can be activated in the retina in models of glaucoma.

5.1.3 Calpain inhibitors

There are numerous different calpain inhibitors and several of them have been used to investigate neuroprotection in the retina (Paquet-Durand, Johnson et al. 2007; Azuma and Shearer 2008). Calpain inhibitor II, N-Acetyl- Leu-Leu-Met-CHO (ALLM), has been shown to protect RGCs against NMDA induced excitotoxicity (Chiu, Lam et al. 2005). Other inhibitors produced by the company Senju Pharmaceutical Co., Ltd, have also been investigated, for example SNJ-1945 and SJA6017. SNJ-1945 was found to prevent RGC death following axonal damage (Ryu, Yasuda et al. 2012), and SJA6017 partially protected RGCs from IOP induced hypoxic-injury (Nakajima, David et al. 2006). MDL28170 (also known as calpain inhibitor III; Z-Val-Phe-CHO) is a potent inhibitor of both calpain-1 and calpain-2. It has been shown to exhibit a neuroprotective role in excitotoxicity by glutamate in in vitro (Brorson, Marcuccilli et al. 1995; Bi, Jin et al. 2012), and in vivo model of brain ischemic injury (Lia, Howlett et al. 1998). In fact, administration of the drug 7 hours after global brain ischemic insult was still able to offer neuroprotection in the rodent (Lia, Howlett et al. 1998). It has not previously been used to investigate neuroprotection in the retina.

The aim of the research presented in this chapter was to investigate (1) whether simulated ischemia could induce calpain activation in HORCs; (2) whether MDL 28170 could prevent calpain-mediated proteolysis and protect RGCs from ischemia induced death.

5.2 Results:

5.2.1 The profiling of calpain-1 and calpain-2 in the human retina

In order to assess whether calpain-1 or calpain-2 are expressed in human retina and the expression profile across the retinal layers, cryo-sectioning together with QRT-PCR (as described in chapter 3) were used. The pattern of Calpain-1 (CAPN1) expression was very similar to that of THY-1, starting low at the baseline in the outer retina sections and increasing to peak expression in the inner retinal sections. The peak of CAPN1 expression coincided with peak of THY-1, although was higher than THY-1 in the mid-retina layers (Figure 5.1 A). The pattern of Calpain-2 (CAPN2) expression showed relatively higher expression in the inner retina but was more evenly distributed than CAPN1, with the expression seen also in the outer retinal sections. The total amount of mRNA for CAPN1 and CAPN2 is shown in Figure 5.1 B. The results show that both of these two genes were present predominantly in the inner retina, with CAPN1 having a more differential distribution through retinal different layers. This was in accordance with the gene array analysis. The heat map showed that CAPN1 had different expression in the macular samples (Mac1-5) and retinal ganglion cell layer sections (RGCL1-5) (Figure 5.2.A), and the analysis documented that there was a 2.03-fold change (Figure 5.2.B). For CAPN2 differential expression could not be detected by the arrays.
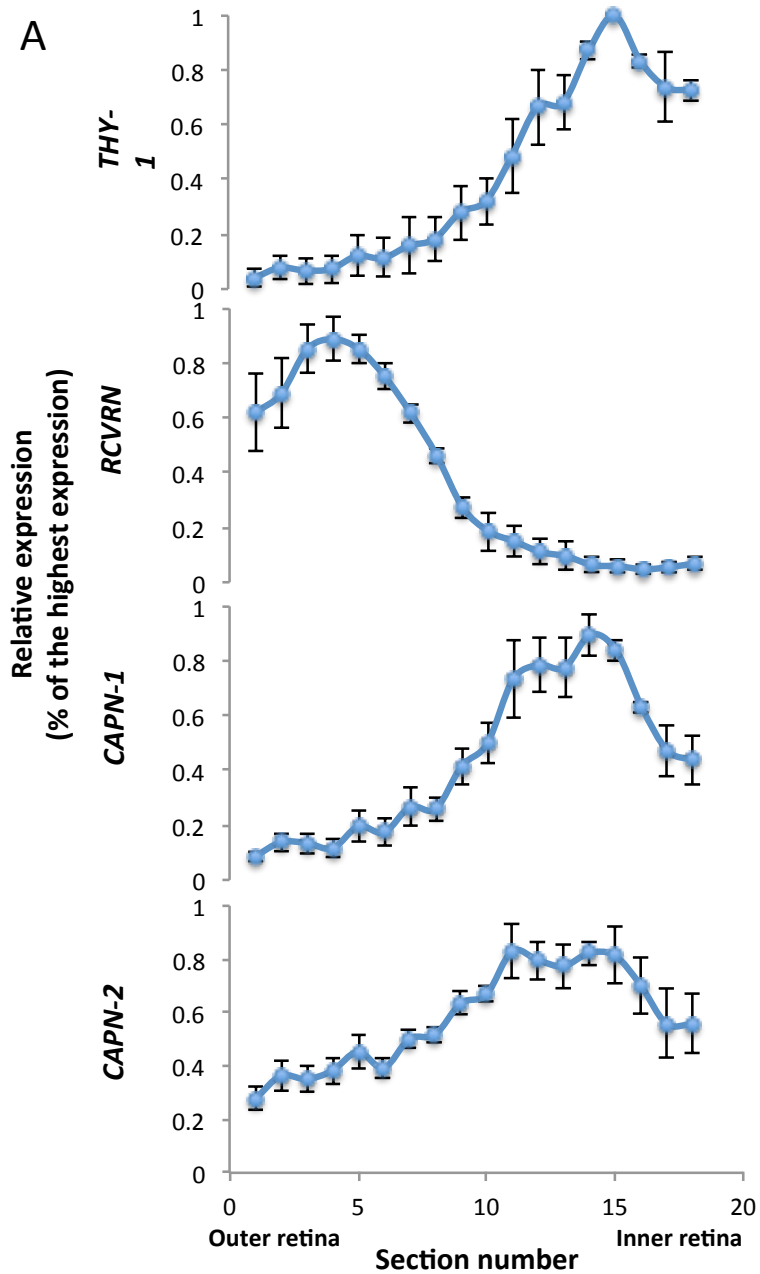
Figure 5.1 (A). Calpain-1 (CAPN1) and calpain-2 (CAPN2) mRNA expression across the retina (mean ± S.E.M.) expressed as a percentage of the highest value (n=4 donor eyes). RCVRN -photoreceptor cell marker; THY-1 - RGC marker. **(B) The average amount**

of mRNA for CAPN1 and CAPN2 present in the sections with peak RCVRN and THY-1 expression in planar retinal sections.
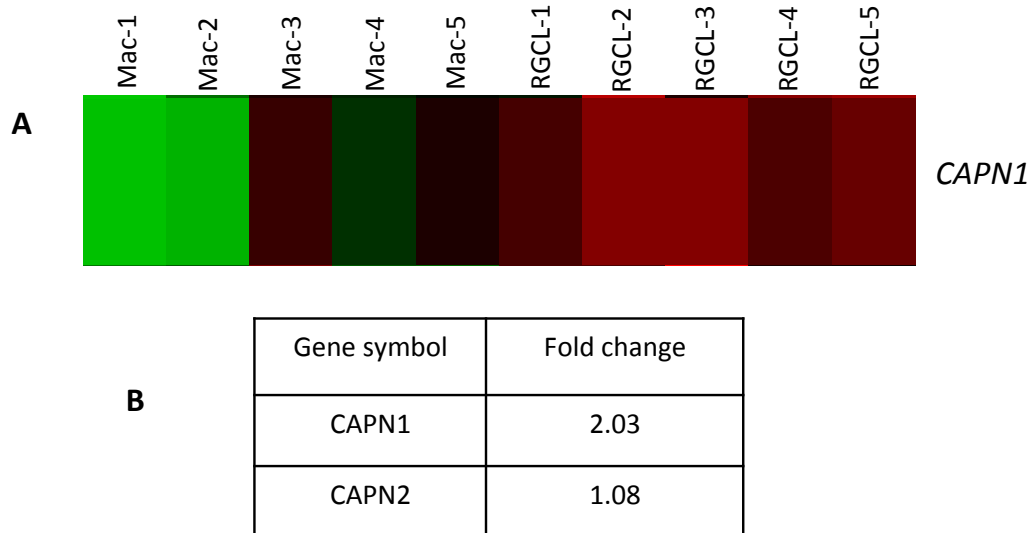
Figure 5.2 (A) Heat map of CAPN1 expression in entire macular (Mac 1-5) samples and retinal ganglion cell layer sections (RGCL1-5) samples. Red = higher expression; Green = lower expression. (B) Fold-change from Illumina gene arrays analysis of calpain-1 (CAPN1) and calpain-2 (CAPN2).

Further investigation of the distribution of calpain-1 and -2 in the retina was carried out by immunohistochemistry. CAPN1 immunostaining mainly the existed in the RGCL but also appeared in the outer retina, plexiform layer (OPL), and there was some staining apparent in the outer nuclear layer (ONL) (Figure 5.3.A). CAPN2 expression was associated with NeuN labeling of neuronal cells in the RGCL, but was nearly absent in the outer retina (Figure 5.3.B). These images suggested that both calpain-1 and 2 expressed in the human retina, and that calpain-2 was predominantly in the RGCL, whereas, calpain-1 was found in both inner and outer retinal layers.

A
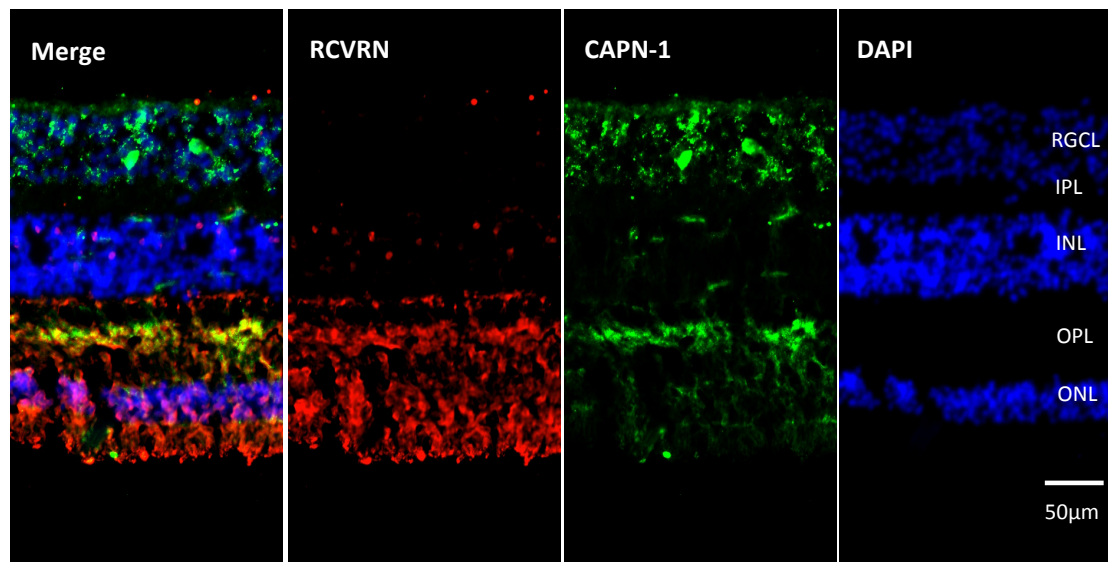
B
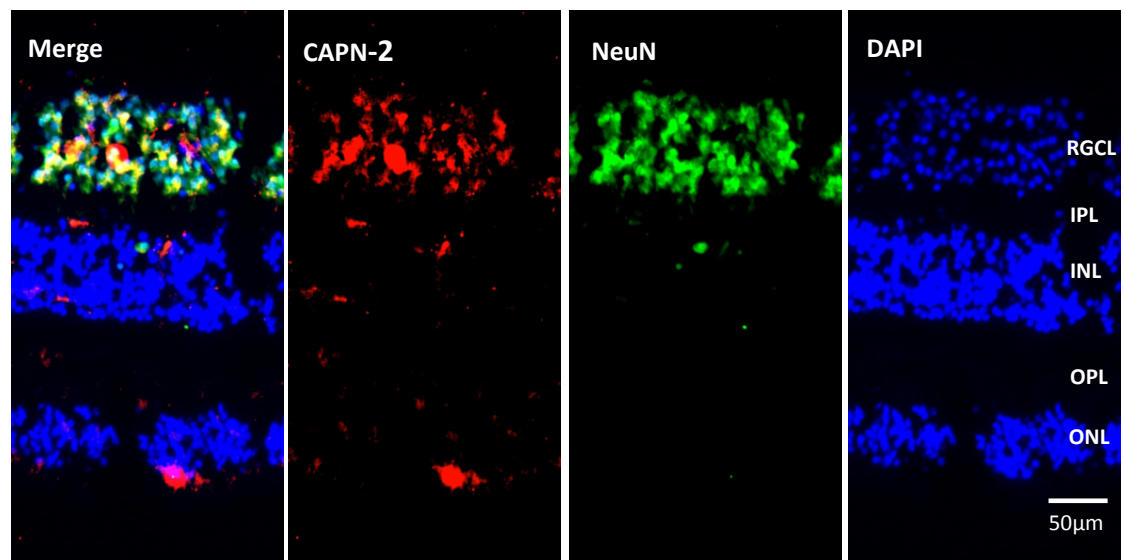
Figure 5.3 (A) Macular retinal section labelled with RCVRN (red), CAPN1 (green) and DAPI (blue) using immunohistochemistry. (B) Macular section labelled with CAPN2 (red), NeuN (green) and DAPI (blue) using immunohistochemistry. RGCL, retinal ganglion cell layer; IPL, inner plexiform layer; INL, inner nuclear layer; OPL, outer plexiform layer; ONL, outer nuclear layer.

5.2.2 Simulated ischemia induced retinal cell death and calpain activation in HORCs

In order to verify whether the calpain was activated in simulated ischemia, the oxygen glucose deprivation (OGD) model in human organotypic retinal cultures (HORCs) was used (Niyadurupola et al 2011). Using this model, it has been shown the OGD leads to a loss of RGCs in human retina. α-spectrin and spectrin breakdown products (SBDPs) were measured by Western blot analysis as an assessment of calpain activation. HORCs were cultured in OGD for 5 time periods: 0 hour, 3 hours, 12 hours, 18 hours, or 24 hours, then incubated in control medium for a further period (the "reperfusion" period), ending the experiment at 24 hours. The data was normalised by β-actin expression. The data shown that OGD induced the proteolysis of α-spectrin (Figure 5.4). Loss of full-length spectrin was detected at 3 hours and by 12 hours approximately 80% was lost compared with the control (Figure 5.4A). SBDPs increased with OGD, showing an approximate doubling with 12 hours, 18 hours and 24 hours OGD treatment (Figure 5.4B).
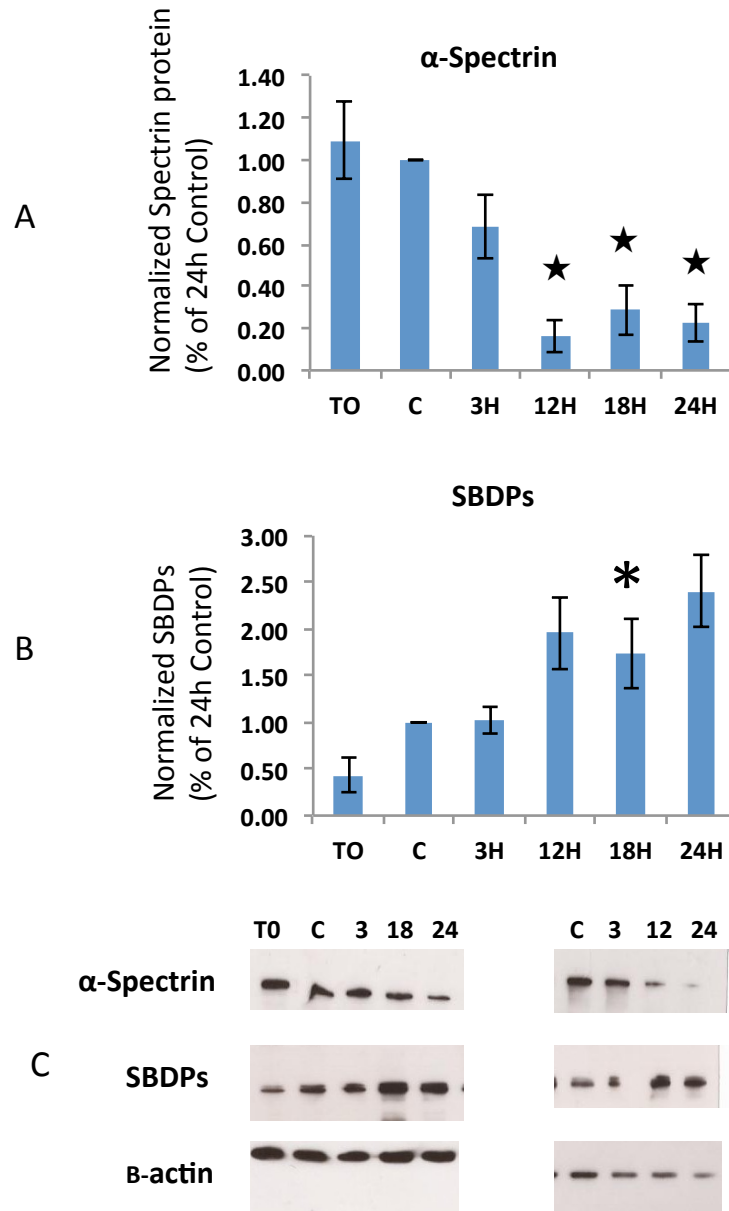
Figure 5.4 α-Spectrin proteolysis following simulated ischemia in HORCs with different time points. Western blots analysis of α-Spectrin (A) and SBDPs (B). Level is measured by densitometry and expressed relative to β-actin (mean ± S.E.M; n=3 donors eyes). Representative blots are shown in (C) (★ p≤ 0.005; * p≤0.05;).

The effects of simulated ischemia leaded to LDH leakage into the medium was measured for 3 hours and 12 hours OGD. LDH leakage gives an overall measurement of cell death in the retina. For the 3 hours OGD treatment, there was a significant increase (about 1.36 fold) in LDH leakage after at the end of the 24 hours period (Figure 5.5A). For the 12 hours OGD treatment, there was an increase of

approximately 5 fold, both in the first 12 hours (when exposed to OGD) and in the subsequent 12 hours of reperfusion (Figure 5.5. B and C). This indicated that cell death had occurred as a result of simulated ischemia, with increased cell death following a longer exposure to OGD.
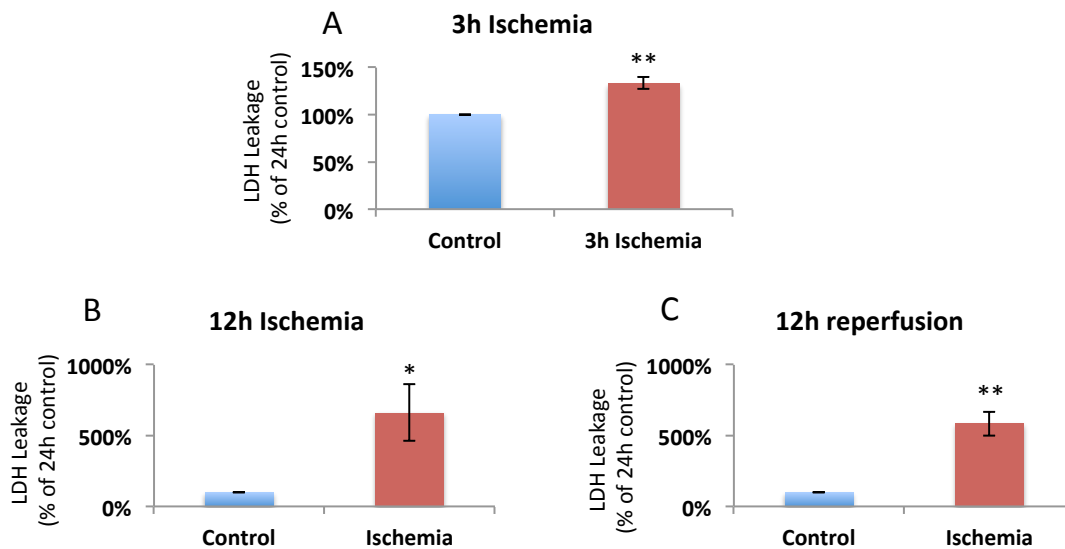
Figure 5.5 LDH release from HORCs following simulated ischemia. (A) LDH release from HORCs following 3 hours OGD/21 hours reperfusion. Measurement was from the medium sampled at the end of the reperfusion period (n=5 donor eyes, mean ± S.E.M.). (B) LDH release from HORCs during a 12 hours OGD compared to control (n=3 donor eyes, mean ± S.E.M.). (C) LDH release during the 12 hours reperfusion period following 12 hours OGD (n=3 donor eyes, mean ± S.E.M.). * P<0.05 VS control, ** P<0.01 VS control.

To further investigate retinal cell death with simulated ischemia in HORCs, immunohistochemistry in conjunction with TUNEL staining was carried out. Following both 3 hours OGD/21 hours reperfusion and 12 hours OGD/12 hours reperfusion in HORCs, retinal cell number decreased in all the layers (Figure 5.6). After 12 hours OGD the majority of cells in all retinal layers were TUNEL positive. Furthermore, with 12 hours OGD/12 hours reperfusion, the retina showed an overall loss of structure.
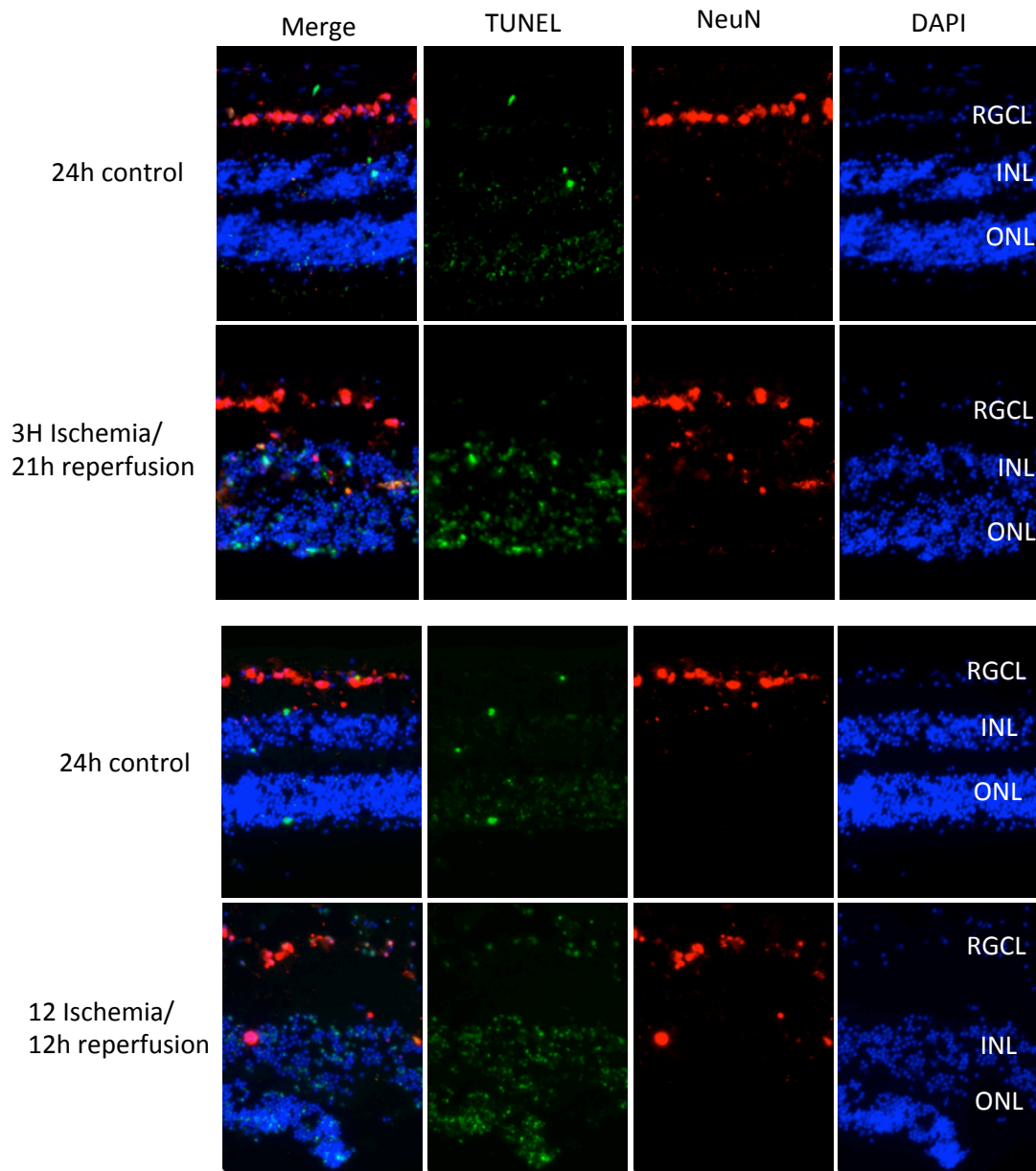
Figure 5.6 Immunohistochemistry of 3 hours/21 hours and 12 hours/12 hours OGD/reperfusion. HORCs were stained with TUNEL (green), NeuN (red) and DAPI (blue). RGCL, retinal ganglion cell layer; INL, inner nuclear layer; ONL, outer nuclear layer.

Taking the data from the proteolysis, LDH leakage and immunohistochemistry, 3 hours OGD/21 hours reperfusion was taken as an appropriate protocol to investigate the effect of calpain inhibitors since this increased cell death and also proteolysis of spectrin, without causing extensive destruction.

5.2.3 Effects of the calpain inhibitor on proteolysis in HORCs with simulated ischemia.

In order to verify whether the proteolysis of the cytoskeletal protein, α-spectrin, was via calpain activation, the inhibitor MDL-28170 was used, which inhibits both calpain-1 and calpain-2 activations (Kunz, Niederberger et al. 2004). 3 hours OGD/21 hours reperfusion caused a loss of α-Spectrin (Figure 5.7). There was also an increase in SBDPs (both 145 and 150kDa), which were clearly separated in the gels (Figure 5.7A). These breakdown products are both generated by calpain, but the band at 145kDa is specifically produced by calpain, whereas the 150kDa band can also be produced by caspase-3 (Nath 1996). Simulated ischemia caused an increased in both products (lane I). The presence of the calpain inhibitor (lane I+i) protected against the loss of full-length spectrin and also decreased the amount of both of the SBDPs. Interestingly, there were higher level of spectrin and lower amounts of SBDPs with 20μM MDL28170 compared to control (Figure. 5.7). These data give good evidence that calpain is activated by simulated ischemia 3 hour OGD/21 hours reperfusion and that calpain inhibiton can inhibit this activation.
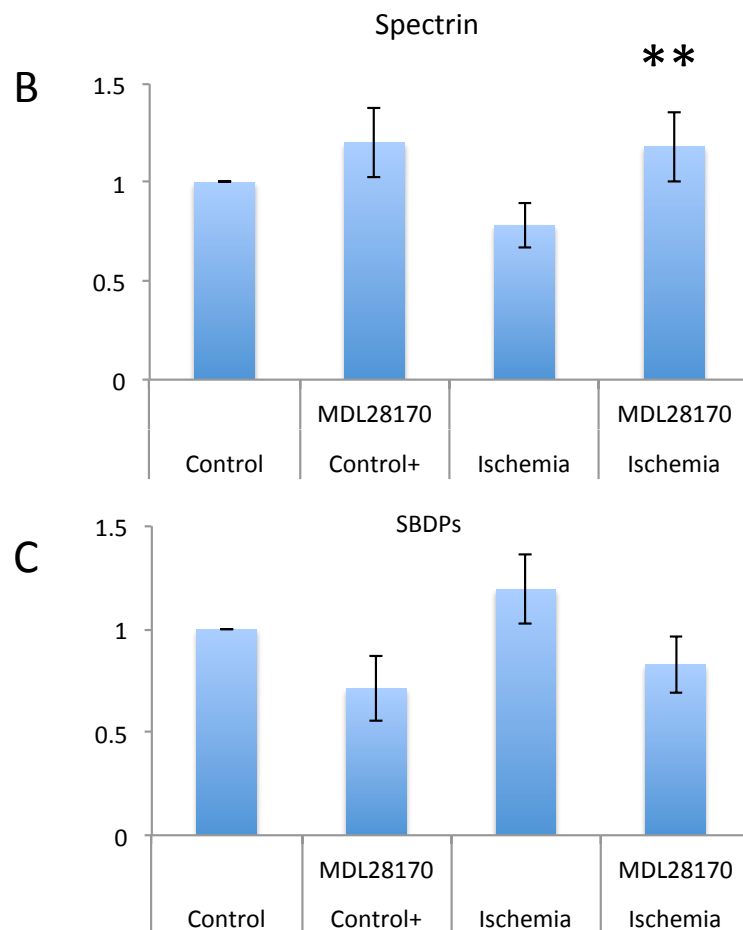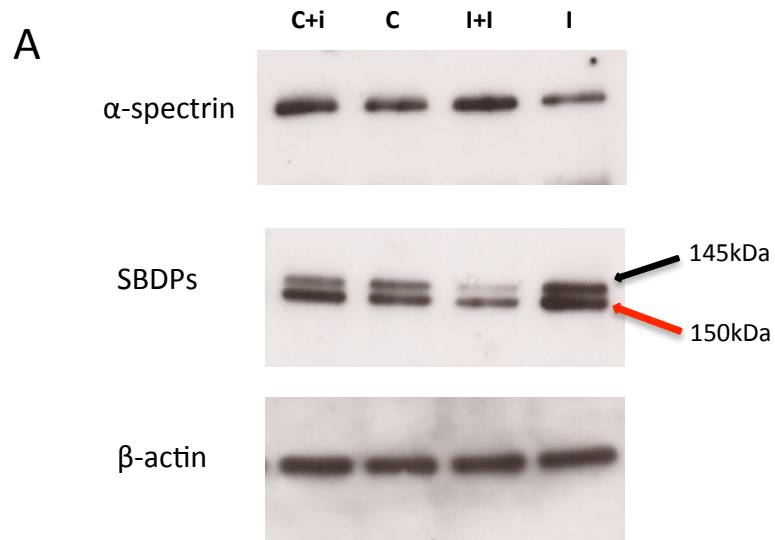
Figure 5.7 (A) Representative Western blots of α-spectrin and its breakdown products from HORCs with simulated ischemia in the presence or absence of MDL28170. The HORCs were treated with either 3 hours OGD with (I+i) and without 20μM MDL28170 (I), or control with (C+i) and without MDL28170 (C). The black arrow points to the spectrin breakdown product of 150 kDa and the red arrow points to the breakdown product of 145

kDa. **(B and C) Quantification (mean ± S.E.M.) of α- Spectrin expression (B) and SBDPs (C) in the HORCs (n=7 donor eyes).** ** P<0.01.

5.2.4 Role of calpain in simulated ischemia induced retinal cell death in HORCs

The role of calpain activation in simulated ischemia-induced cell death was investigated by measuring LDH leakage. The HORCs were exposed to the inhibitor MDL28170 during both the OGD and the reperfusion phase. Exposing the HORC to the inhibitor did not increase the level of LDH release indicating that the inhibitor was not toxic to the retina. HORCs exposed to OGD showed a significant increase in LDH (approximately 30%) leakage compared to control. This was not inhibited by 20 μM MDL28170. This suggested that MDL28170 was unable to protect the retina from simulated ischemia.
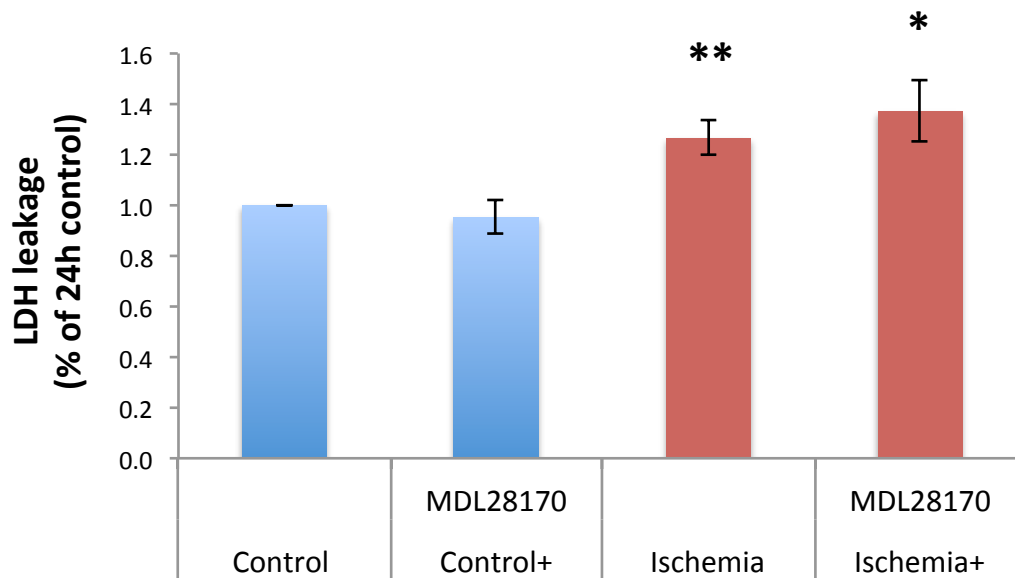
Figure 5.8 LDH release from HORCs in simulated ischemia in the presence and absence of MDL28170. LDH levels in the medium from the reperfusion phase in control HORCs with/without 20 μM MDL28170 (Blue) and 3 hours/21 hours OGD/reperfusion with/without MDL28170 (Red) (n=5 donor eyes, mean ± S.E.M.). ** P< 0.01, control vs ischemia, and *P< 0.05, control +MDL28170 vs ischemia + MDL28170.

5.2.5 Calpain-induced RGC death in simulated ischemia in HORCs

In order to investigate whether inhibition of calpain protected RGCs, immunohistochemistry was carried to assess the number of NeuN-labelled neuronal cells in the RGCL in HORCs exposed to simulated ischemia (3 hours OGD-21 hours reperfusion). In addition, TUNEL labelling was used to assess the level of apoptosis. In the presence of 20 μM MDL28170 alone, NeuN staining suggested that there was an increased number of RGCs compared to controls (Figure 5.9). When the number of cells was counted, there appeared to an increase, although this was not statistically significant (Figure 5.10). With simulated ischemia, there was a loss of NeuN positive RGCs (Figure 5.9 and Figure 5.10) and TUNEL staining increased. The calpain inhibitor 20 μM MDL28170 did not dramatically protect against the loss of RGCs and the small protection seen when the number of RGCs was counted, it was not found to be significant.
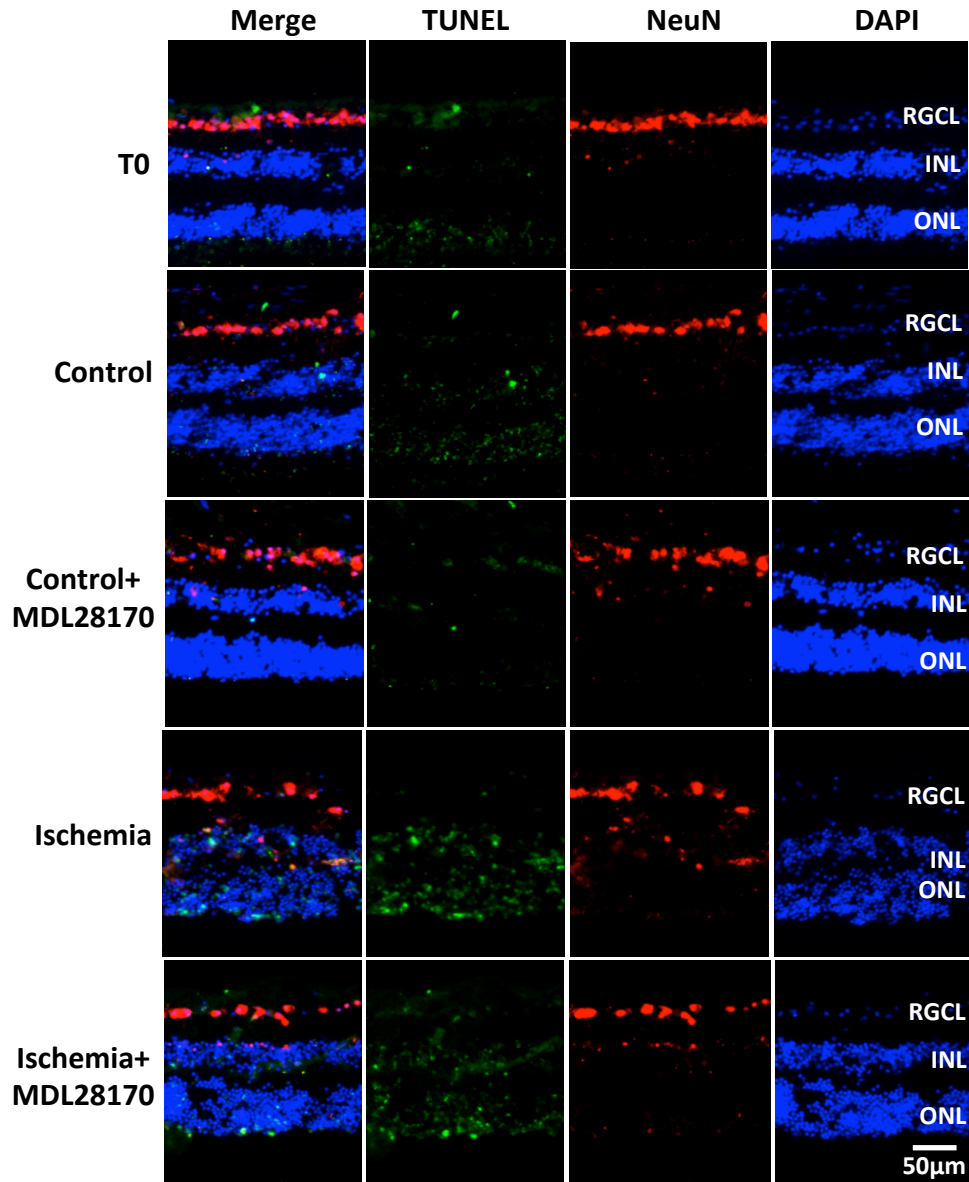
Figure 5.9 Representative immunohistochemical images of HORCs with simulated ischemia in the presence and absence of MDL28170. RGCs were labelled with antibody to NeuN (Red), TUNEL staining for apoptosis is shown in Green, and nuclei are stained with DAPI (blue). IPL, inner plexiform layer; INL, inner nuclear layer; OPL, outer plexiform layer; ONL, outer nuclear layer.
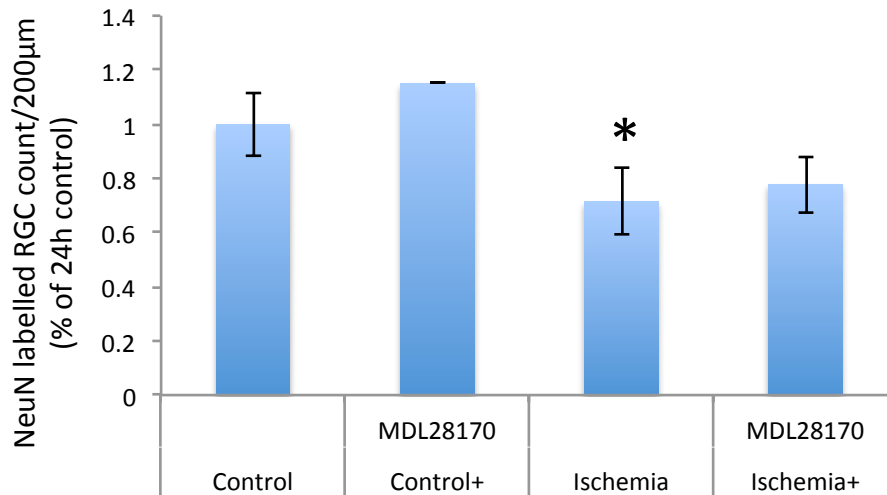
Figure 5.10 Counts of NeuN labelled cells in the RGCL in the control with and without 20 μM MDL28170, 3h/21h OGD/reperfusion with and without 20 μM MDL170 (mean ± S.E.M.; n=4 donor eyes). * p<0.05 vs control.

Levels of THY-1 mRNA were also examined to further determine whether MDL28170 inhibited RGC death THY-1 mRNA in control was significant higher than in the 3 hours OGD/21 hours reperfusion HORCs (Figure 5.11). 20 μM MDL28170 alone had similar THY-1 expression to control. The addition of 20 μM MDL28170 did not increase THY-1 mRNA in the 3 hours OGD/21 hours reperfusion HORCs.
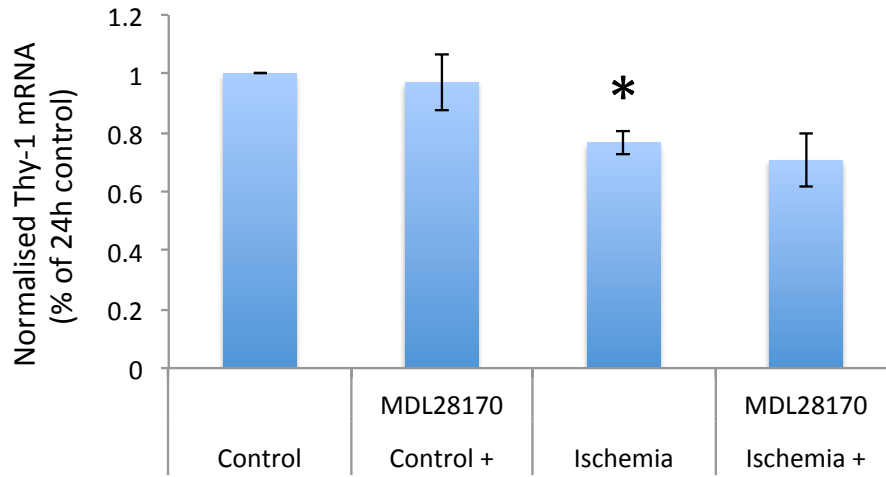
Figure 5.11 THY-1 level in 3 hours/21 hours OGD/reperfusion treated HORCs in the presence and absence of 20 μM MDL28170 THY-1 mRNA expression was normalised to geometric mean of TOP-1 and CYC-1 mRNA expression and expressed relative to control, (mean ± S.E.M.; n= 4 donor eyes). * $p < 0.05$ vs control.

5.3 Discussion

Although calpain-1 and calpain-2 are ubiquitously expressed and they are the major members of the calpain family these are active in the human (Nakajima, David et al. 2006; Ono and Sorimachi 2012). Calpain-1 has been shown to have relatively high expression in RGCs in the rabbit retina (Croall and Demartino 1991). However, it has also been observed that overall, calpain-2 mRNA was 12 times higher than calpain-1 mRNA in the rat retina (Tamada, Nakajima et al. 2005). In the human retina, calpain-1 and calpain-2 were both detected at the mRNA and protein level. Calpain-1 overall had higher mRNA levels compared to calpain-2 in the inner retina. Both were relative highly expressed in the inner retina, compared to the outer retina, although the fold difference was much greater for calpain-1 suggesting that the mRNA is much higher in the RGCs compared to the photoreceptors. This was also indicated by gene arrays analysis, which showed that calpain-1 had a significantly higher expression (2.03 fold) in the RGCL samples compared to entire retinal macular region.

Interestingly, when calpain-1 was investigated using immunohistochemistry, it distributed throughout the retina, from the OPL to the RGCL. This is not inconsistent with the mRNA profile data, which showed a wider expression than THY-1 indicating localization in the INL. The immune-staining in the OPL could result from expression in cells whose nuclei are located in the INL, but synapse in the OPL, specifically the amacrine and bipolar cells. It also may be present in Müller cells. Note that mRNA for the protein would be associated with the cell body, independently of where the protein is expressed. For calpain 2, the assessment of the antigen in the human retina displayed exclusively staining in the RGCL, This is surprising and is not consistent with the mRNA profile data, which indicates that there is expression in all layers, including in the photoreceptors. Further work would need to be done here to look into this inconsistency in more detail.

It has been proposed that retinal ischemic insult leads to an excessive increase in extracellular glutamate, which results in a sustained activation of glutamate receptors and followed by greater Ca^{2+} entry into cells (Osborne, Casson et al. 2004). In addition, it has been shown in the human retina, that simulated ischemia leads to activation of $P2X_7$ receptors, which would also lead to increased calcium in the RGCs

(Niyadurupola, Sidaway et al. 2013). Therefore, the calcium-dependent proteases, such as calpain, could be activated. There is good evidence that increased Ca^{2+} indeed causes RGC death (Hartwick, Hamilton et al. 2008; Araie and Mayama 2011) and apoptosis has been observed (Osborne, Wood et al. 2004; Sappington, Sidorova et al. 2009; Crish and Calkins 2011). Also, calpain-2 activation has been observed in rat retinal neurons treated with glutamate (Miao, Dong et al. 2012).

In our experiments presented in this chapter, both 3 hours and 12 hours OGD protocols significantly increased LDH release compared with their control samples. Therefore, this simulated ischemia-reperfusion model in HORCs led to retinal cell damage. To show that proteolysis was induced in this model, α-spectrin and SBDPs were assessed at different OGD exposures. Proteolytic activities were greater as the OGD time increased with intact spectrin levels decreasing and levels of spectrin breakdown products increasing as the severity of the simulated ischemia increased.

Since it was been found that both calpain-1 and 2 were mainly expressed in the inner retina, and particular in the RGCL this was consistant with a possible role for these enzymes in the RGC cell death observed with simulated ischemia. MDL28170 is an inhibitor of both calpain-1 and 2 and was chosen to examine its protective effects in the OGD model in HORCs. It has been identified that MDL28170 is a highly cell-permeable molecule, which has been shown to inhibit ischemic damage in the brain (Lia, Howlett et al. 1998; Markgraf, Velayo et al. 1998; Brana, Benham et al. 1999; Rami, Agarwal et al. 2000; Kawamura, Nakajima et al. 2005). Specially, it reduced infarct volume in rat cerebral ischemia, and its protective activity extended after the induction of ischemia, still being effective if applied 6 hours after the brain initial ischemia (Markgraf, Velayo et al. 1998). Its pharmacodynamic half-life was around 2 hours and peak reaction was obtained after 30min (Markgraf, Velayo et al. 1998). Its neuroprotective role is achieved by inhibiting cell apoptosis and necrosis (Kawamura, Nakajima et al. 2005).

In HORCs, MDL28170 significantly inhibited spectrin degradation of both the 145 kDa and 150kDa fragments. The 145 kDa fragment is produced specifically by calpain activation, so these results suggested that calpain was indeed activated in the HORC simulated ischemia model. LDH release following 3 hours OGD/21 hours

reperfusion was increased compared to control, but MDL28170 failed to prevent the retinal cell damage from the ischemia insult. The number of NeuN-labeled neuronal cells in the RGCL and THY-1 mRNA were used to determine the effect of MDL28170 specifically in relation to the RGCs. RGC number was significantly reduced after 3 hours ischemia and followed by 21 hours reperfusion and THY-1 mRNA level decreased. The inhibitor slightly prevented RGCs lost but this did not reach significance. THY-1 mRNA did not enable detection of any protection of MDL28170. These data would indicate that calpain-induced proteolysis was not part of the mechanism mediating RGC death in simulated ischemia, although this is unexpected and it would be important to carry out further work to confirm this. It is possible that other signaling pathway activated by Ca^{2+} are more significant in ischemia-induced cell death, including caspase-mediated pathways (Wang 2000).

Therefore, both calpain-1 and 2 are confirmed to be present in the human retina. Our simulated ischemia model of human retina culture can stimulate their action. Calpain activity appeared to be inhibited by 20 μM MDL28170 in the 3 hours simulated ischemia insult of HORCs. However, RGC death was not significantly reduced by experimental inhibition of calpain activity, and it therefore remains inconclusive whether calpain activity involved in the RGC death observed in this model.

Chapter 6

TRP channels in the human retina and role in ischemia-mediated RGC death

6.1 Introduction

The previous chapter has identified that calpain activation was stimulated by 3 hours OGD in HORCs, which was suggested $[Ca^{2+}]_i$ was elevated prior to calpain activation. TRP channels are a large group of ion channels containing seven subfamilies (Nilius, Owsianik et al. 2007; Dadon and Minke 2010). They play a crucial role in modulation of the cytosolic Ca^{2+} concentration but are also implicated in the pathophysiology of numerous diseases (CLAPHAM 2005; Clapham 2007; Nilius, Owsianik et al. 2007; Venkatachalam and Montell 2007).

The TRP superfamily is divided into subfamilies based on their structure and function: TRPC (canonical), TRPV (vanilloid), TRPM (melastatin), TRPP (polycystin), TRPML (mucolipin), TRPA (ankyrin) and TRPN (NOMPC) (Clapham 2005). These are further subdivided giving 28 different subtypes.

Expression of all 28 TRP channels has been demonstrated in the mammalian retina (Gilliam and Wensel 2011) indicating their importance to retinal physiology. The distribution of TRP channels in the human retina has not been studied, but the expression of different TRP subunits has been shown to vary in different cell types of the rodent retina (Crousillac, Lerouge et al. 2003; Gilliam and Wensel 2011). There are some members from the TRPC and TRPV families that have been proposed to play a significant role in glaucoma (Sappington, Sidorova et al. 2009; Ryskamp, Witkovsky et al. 2011; Pan, Capó-Aponte et al. 2012). TRPC-6 was found to have a RGC protective role against ischemia/ reperfusion early injury when the channel was activated prior to ischemia (Wang, Teng et al. 2010). TRPV-1 and TRPV-4 activities contribute to RGC apoptosis (Sappington, Sidorova et al. 2009; Ryskamp, Witkovsky et al. 2011).

The TRPC family is the one of the most widely studied TRP channels. It includes seven members, TRPC1 -7 (Table 5.1). Except TRPC-2, which is a pseudo gene, the rest of the TRPC channels are extensively expressed in brain where they play critical roles in neuronal cell differentiation, proliferation and survival (Dadon and Minke 2010; Shapovalov, Lehen'kyi et al. 2011). Their activities are also implicated in neuronal degeneration diseases, such as Parkinson's Disease, Alzheimer's Disease and Cerebellar Ataxia (Selvaraj, Sun et al. 2010). TRPC channels are nonselective cation channels, which are permeable to Ca^{2+} and Na^+(Nilius, Owsianik et al. 2007). The TRPC channels are mainly activated by the PLC pathway, via G protein–coupled activation (PLC-β) or receptor tyrosine kinase (RTK) activation (PLC-γ). IP3 and DAG can also regulate calcium influx through some TRPC channels (Selvaraj, Sun et al. 2010).

The TRPM (melastatin) family of TRP channels has 8 members (TRPM1-8). TRPM-1 was the first member of TRPM family to be identified in mammalian retina. It was found that TRPM-1 is involved in on-pathways in the human retina, being expressed in ON-bipolar cells and at the synaptic ribbons of some rods (Klooster, Blokker et al. 2011). Mutation of TRPM-1 in the human retina leads to night blindness (Genderen, Bijveld et al. 2009). The role of TRPM-2 in brain ischemia has been widely investigated, and it has been suggested that inhibition of TRPM-2 has the potential to protect against neuronal cell death in ischemic conditions (Simard, Tarasov et al. 2007; Szydlowska and Tymianski 2010). However, its role in RGC death has not been studied.

TRPC-3 (Miller 2006) and TRPM-2 are both activated by cellular oxidative stress (Herson and Ashford 1997; Smith, Herson et al. 2003) and both lead to raised intracellular Ca^{2+} concentration when they were activated. Oxidative stress is one of important reasons contributes to ischemic neuronal injury (Verma, Quillinan et al. 2012) and there is increasing evidences suggest that oxidative stress involves in RGC death in glaucoma (Qu, Wang et al. 2010; Crish and Calkins 2011; McElnea, Quill et al. 2011) and there are parallels drawn between neurodegeneration following ischemia in the brain and RGC degeneration in glaucoma.

In summary, there have been several papers relating to the role of TRP channels in RGCs (Crousillac, Lerouge et al. 2003; Sappington, Sidorova et al. 2009; Wang, Teng et al. 2010; Pan, Capó-Aponte et al. 2012). They play a major role in Ca^{2+} homeostasis and are gated by mechanisms that relate to the pathophysiology of glaucoma, including mechanical stress and oxidative stress (Pan, Capó-Aponte et al. 2012). Therefore, although they were not identified from the gene array data, a series of experiments were carried out to look at these in more detail in the human retina. In this chapter the methods described in the previous chapter were used to investigated the expression of the TRP channels TRPC-1, TRPC-3 and TRPM-2. In addition, a TRP inhibitor (N-(p-amylcinnamoyl) anthranilic acid; ACA) was used to see if it could inhibit RGC death in a human model of retinal ischemia.

6.2 Result:

6.2.1 mRNA levels of TRPM-2, TRPC-1 and -3 in the human macula.

The cryosectioning technique, described in Chapter 3, was used to assess expression of the TRP channels TRPC-1, TRPC-3 and TRPM-2. TRPC-1, TRPC-3 and TRPM-2 mRNA were all expressed in the human retina (Figure 6.1). Compared to the other two TRP channel mRNA investigated, TRPC-1 had a relatively low expression. It was expressed throughout the retina, with a slightly higher expression in the outer retina compared to the inner retina. Its lowest level was in the innermost four sections, which were the sections showing highest expression of THY-1. The distribution of TRPC-3 and TRPM-2 showed almost identical expression patterns. They were both most highly expressed in the inner retina sections and nearly absent in the outer retina. Their expressions associated closely with THY-1 expression indicating that expression may be exclusive to RGCs.
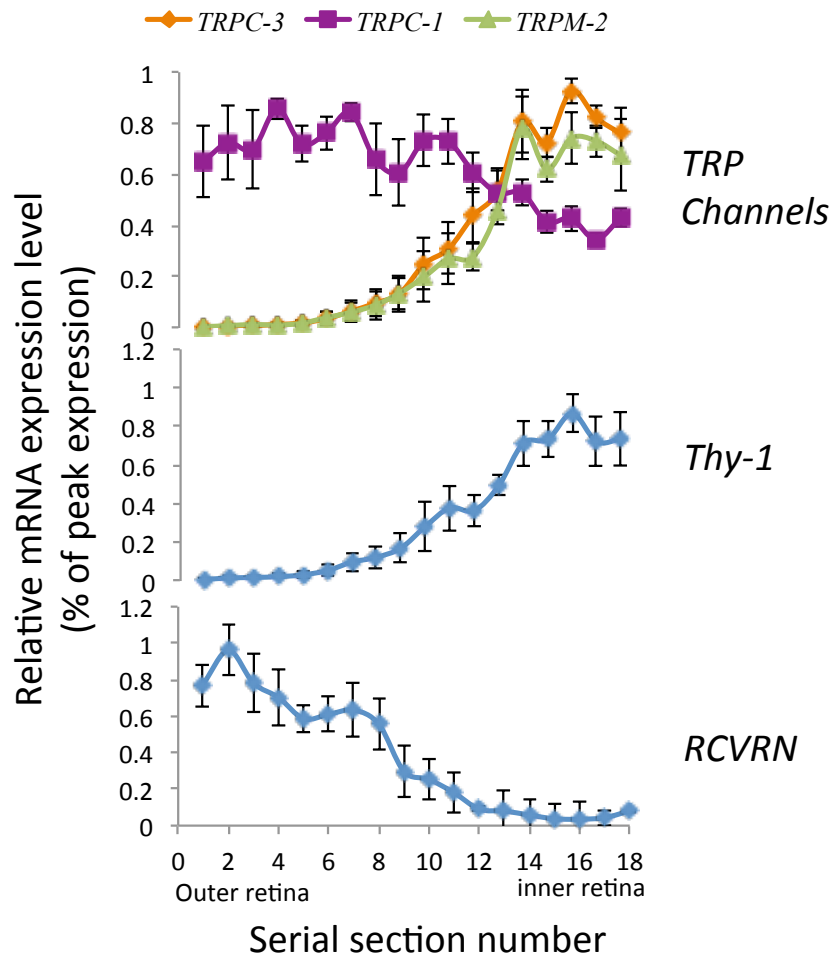
Figure 6.1 Relative mRNA expression of TRPC-1, TRPC-3 and TRPM-2 in serial sections of human retina. Data was normalized relative to the section with the highest mRNA (n= 5 donor eyes, mean± S.E.M.)

6.2.2 Immunoreactivity of TRPM-2 in the retina

The distribution of TRPM-2 was assessed in the human retinal macula by immunohistochemistry. To verify TRPM-2 distribution, NeuN was used to compare with the TRPM-2 expression. TRPM-2 immunoreactivity was observed that it exclusively occurred in the RGCL, and staining coincided with that for NeuN (Figure 6.2). This provided further evidence that TRPM-2 channel mainly or specially existed in the human RGCL and that human RGCs express TRPM-2.

| Merge | TRPM-2 | NeuN | DAPI |

(DAPI panel labels: RGCL, IPL, INL, OPL, ONL; scale bar 50µm)
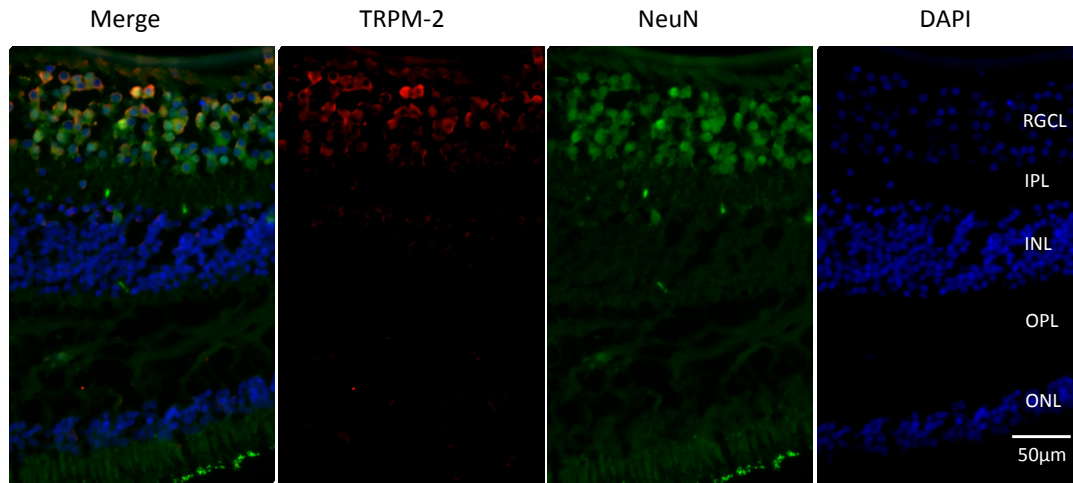
Figure 6.2 Photomicrographs of immunohistochemistry of the human macula with NeuN and TRPM-2 staining. Section was co-labeled with RGC marker, NeuN (green), and TRPM-2 (red), and the nuclear was stained with DAPI (blue).

6.2.3 Simulated ischemia induced cell death in HORCs and treated with the TRP inhibitor, ACA

HORCs were incubated under condition of oxygen and glucose deprivation (OGD) for 3 hours followed by a 21 hours "reperfusion" in normal medium. Initial experiments measured LDH leakage into the medium. This is a measure if overall cell death caused by simulated ischemia.

HORCs exposed to 3 hours OGD-21 hours reperfusion caused a significant increase in LDH leakage compared to control (Figure 6.3). This was not inhibited by 20 µM ACA. However, 20 µM ACA alone caused a small but statistically significant increase in LDH release compared with control. This suggested that 20 µM ACA might be toxic to the human retina. LDH release gives information about cell death, but does not indicate which cells are involved. It is known that simulated ischemia causes a loss of RGCs. Furthermore, TRPM-2 and TRPC-3 appear to be the expressed exclusively in RGCs. It was therefore of interest to look specifically at the effect of 20 µM ACA on RGC survival.
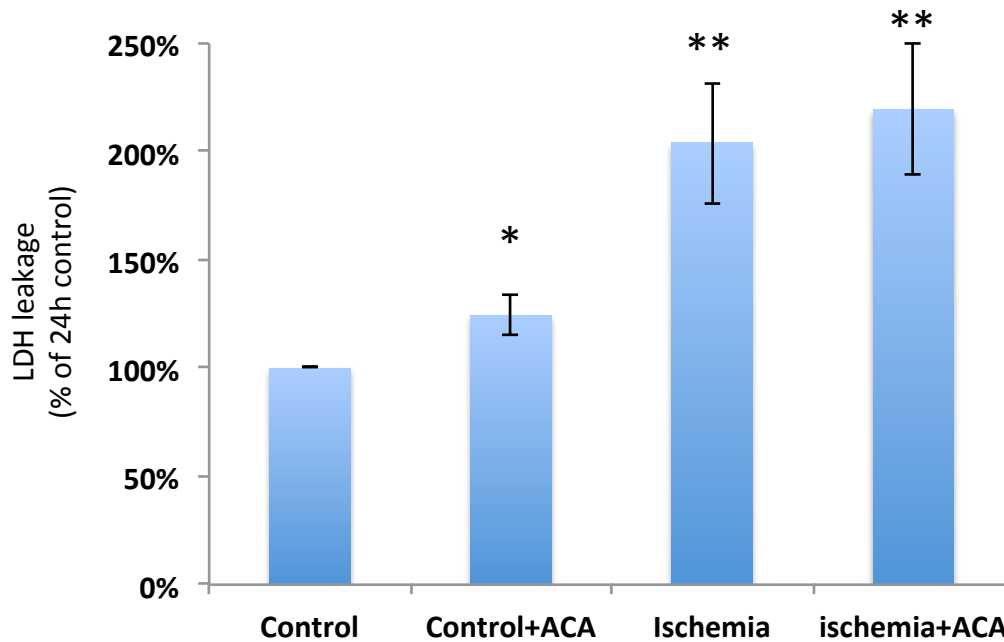
Figure 6.3 LDH release from HORCs in simulated ischemia in the presence and absence of 20 μM ACA. LDH levels in the medium from the reperfusion phase in control HORCs with/without 20 μM ACA and 3 hours/21 hours OGD/reperfusion with/without 20 μM ACA (n=5 donor eyes, mean ± S.E.M.). ** P<0.01, * P<0.05 vs control.

6.2.4 Involvement of TRP channels in simulated ischemia induced RGC death in HORCs

In order to investigate whether the TRP inhibitor, ACA, protected RGCs against simulated ischemic insults, NeuN immunohistochemistry was carried out to assess RGC number in RGCL after the HORCs were exposed to 3 hours OGD/21 hours reperfusion. Immunohistochemical images showed that the number of NeuN-positive cells in the RGCL was decreased when HORCs were exposed to 3 hours OGD/21 hours reperfusion compared to 24 hours control (Figure 6.4). Cell counts showed a significant decrease in NeuN-positive cells in the RGCL of simulated ischemia HORCs, compared to the 24 hours control (Figure 6.4B). In the presence of 20 μM ACA alone, NeuN-positive cell number was slightly increased compared with control (Figure 6.4B), although this increase was not significant. Furthermore, with application of ACA, the numbers of NeuN-positive cells were slightly increased, although again they were not found to be significant (Figure 5.5A and B).
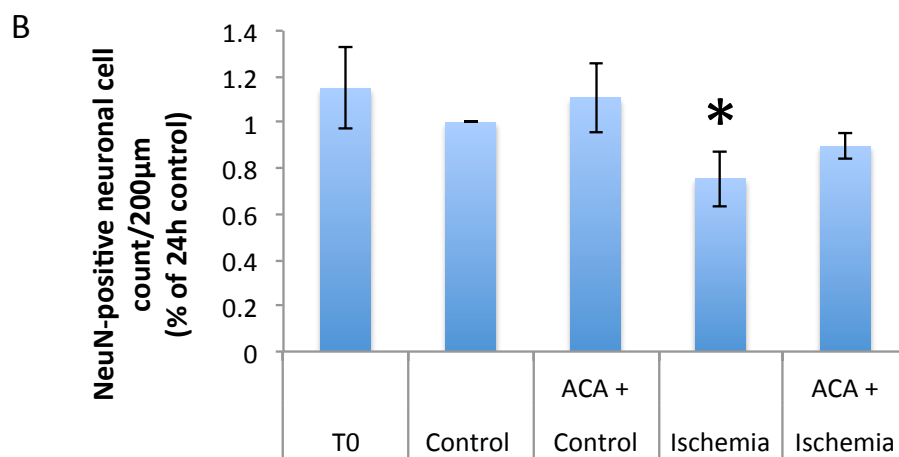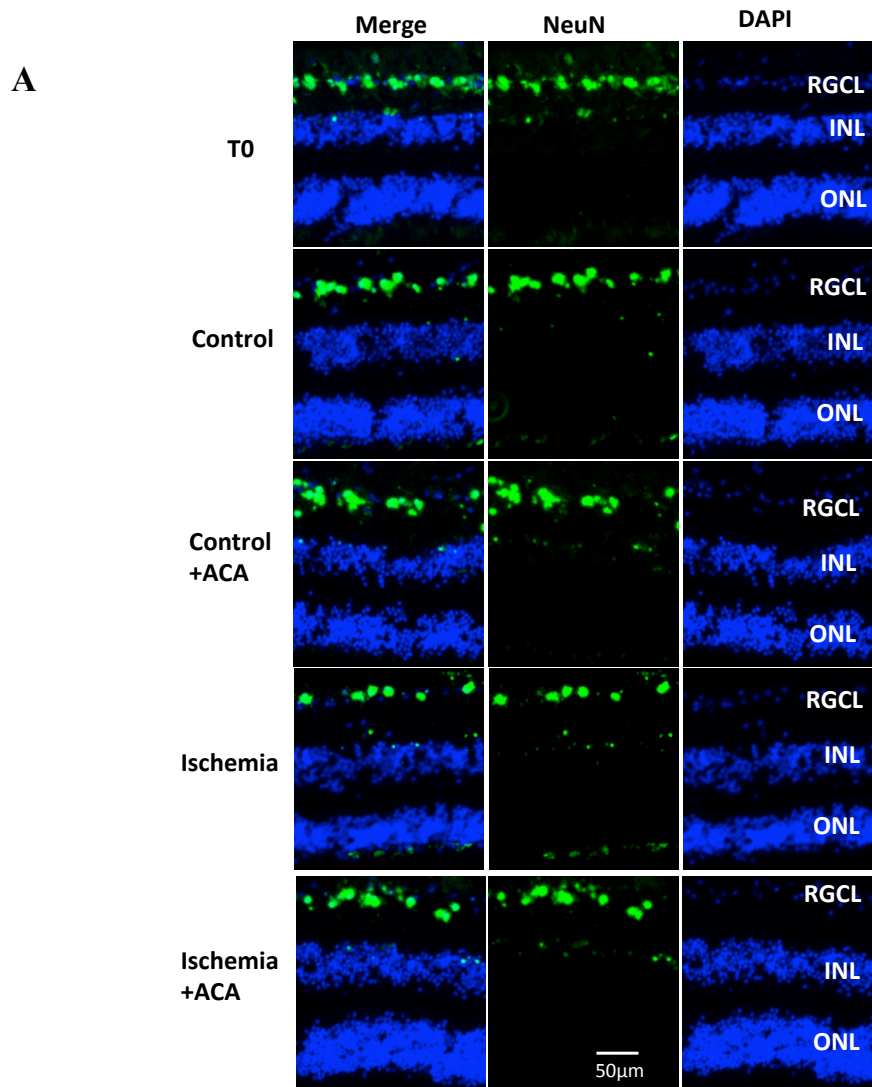
Figure 6.4 (A) Representative immunohistochemical images of HORCs with simulated ischemia in the presence and absence of 20 μM ACA. RGCs were labeled with antibody to NeuN (Red), TUNEL staining for apoptosis is shown in Green, and nuclei are stained with DAPI (blue). IPL, inner plexiform layer; INL, inner nuclear layer; OPL, outer plexiform layer; ONL, outer nuclear layer. (B) Counts of NeuN labelled cells in the RGCL in the control with

and 20 µM ACA, 3 hours/21 hours OGD/reperfusion with and without 20 µM ACA (mean ± S.E.M.; n=4 donor eyes). * p<0.05 vs control.

RGC number was also assessed by measuring THY-1 mRNA. Exposure of HORCs to 3h OGD-21h reperfusion led to a significant decrease in THY-1 mRNA compared with the 24h control (Figure 6.5). The addition of 20µM ACA alone increased THY-1 mRNA level in the control HORCs. In addition, 20µM ACA added to HORCs with 3h OGD-21h reperfusion treatment, caused an increased THY-1 mRNA expression, although again this was not statistically significant.
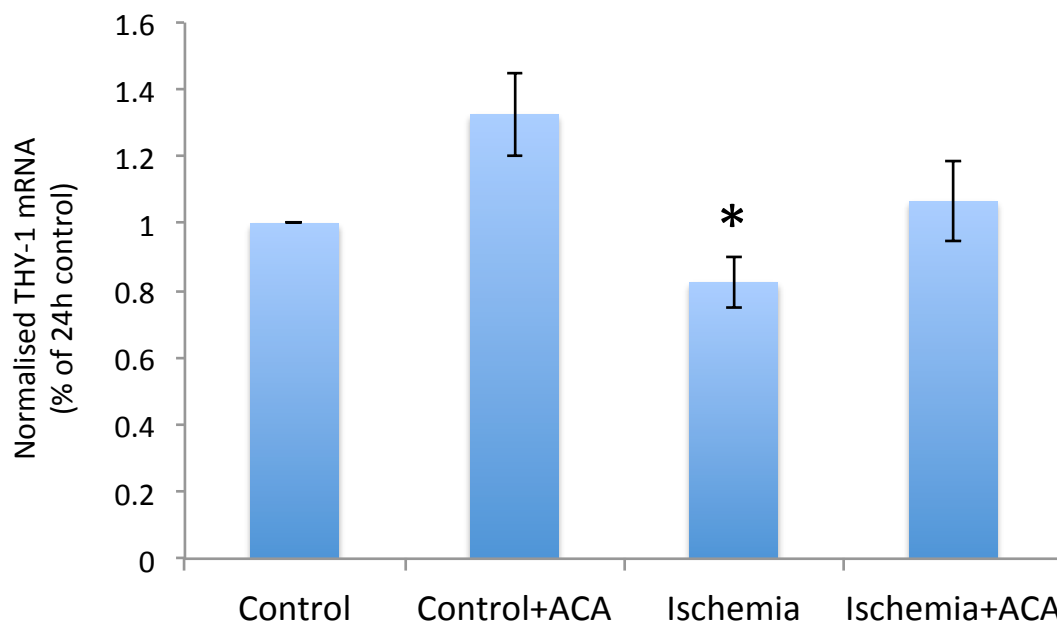
Figure 6.5 THY-1 level in 3h/21 h OGD/reperfusion treated HORCs in the presence and absence of 20µM ACA. THY-1 mRNA expression was normalised to the geometric mean of TOP-1 and CYC-1 mRNA expression and expressed relative to control, (mean ± S.E.M.; n= 4 donor eyes). * p<0.05 vs control.

6.3 Discussion

Although IOP is the main risk factor of glaucoma, there is more and more evidence indicating that reduced blood supply is involved in the pathophysiology of glaucoma (Flammer, Orgul et al. 2002; Grieshaber and Flammer 2005; Yanagi, Kawasaki et al. 2011). Reduced blood flow in the retina will consequently result in ischemia, a deficit of oxygen and glucose (OGD) in the retina, which has a close link with RGC death (Osborne, Casson et al. 2004; Kaur, Foulds et al. 2008; Osborne 2010). There are multiple factors involved in pathological processes, deregulation of Ca^{2+} homeostasis is one of the critical events contributes to RGC death.

Disruption of Ca^{2+} homeostasis is a frequent phenomenon induced by the anoxic condition which leads to neuronal cell death and increasing evidence suggests that TRP channels have a significant contribution to that process (Venkatachalam and Montell 2007). TRPC-1, TPRC-3 and TRPM-2 are highly expressed in the brain, however, their distribution in the retina is not clear. For the initial experiments the expression profile of mRNA of these three TRP channels was investigated. The data indicated that TRPC-3 and TRPM-2 were highly expressed in the RGCL with no evidence of any expression in the photoreceptors. TRPC-1 was expressed throughout the retina, with higher amounts in the outer retina, which is similar as the observation in the mouse retina (Gilliam and Wensel 2011). Immunohistochemistry data further verified TRPM-2 localization, with TRPM-2 immunoreaction appeared to be exclusively located in RGCL and corresponding with NeuN positive cell in the RGCL and INL. Unfortunately available antibodies for the TRPC channels investigated are not good (Gilliam and Wensel 2011), therefore verification of localization of these channels was not possible by immunohistochemistry.

TRPM-2 has been shown to mediate hypoxia-induced neuronal cell death in the brain and inhibition of TRPM-2 activity had a neuroprotective role (Venkatachalam and Montell 2007; Gees, Colsoul et al. 2010). Whether the TRPM-2 could be involved in RGC death has not been investigated. Therefore, the HORC model was used to investigate TRPM-2 involvement under the oxygen and glucose deprivation conditions (simulated ischemia). The inhibitor ACA was used. ACA is an inhibitor of TRPM-2 which almost completely blocked current through TRPM-2 channel in

HEK293 cells (Kraft, Grimm et al. 2006). It is, however, not totally selective; several other human TRP channels are also sensitive to ACA (Harteneck, Frenzel et al. 2007) with the activities of TRPM-8, TRPC-6, TRPC-3/5 and TRPV-1/4 being found to be affected (Kraft, Grimm et al. 2006).

Measuring the LDH accumulation in the culture medium presents an overall assessment of retina damage. LDH releasing in HORCs was increased in simulated ischemia. Application of the TRPM-2 inhibitor, 20μ M ACA, did not suppresses the LDH, in fact there was a slightly increase in LDH in the presence of ACA, which may suggest some toxicity. Focussing specifically on RGC viability of ischemia, 20 μM ACA inhibited the loss of NeuN-positive cells, giving about 50% protection to RGCs. However, statistical significance was not reached. Decreased mRNA of the RGCs marker, THY-1, supported the data of RGC number changes. 3 hours OGD led to a significant loss of THY-1 mRNA, which was about 17% decrease. Application of 20 μM ACA to HORCs prevented the loss of THY-1 mRNA and in fact, the OGD/ACA treated HORCs had higher levels of THY-1 than control. However, the protection was not shown to be statistically different from OGD alone. This indicated that 20 μM ACA is possibly protective to RGCs, although again, this was not statistically significant. There are several factors which might impact the data significance. 3h OGD caused a small decrease (<25%) in both NeuN-positive and THY-1 measurements. Carrying out more repeats may have improved the significance, but when using human tissue this is difficult. Also, the personal variations of each donor may increase variability.

In the present experiments, TRPC-3 and also TRPM-2 were expressed in the inner retina and their pattern of distribution was consistent with expression exclusively in RGCs. The experiments presented here suggest that their activation might be involved in ischemia induced RGC death, however, more work needs to be done to confirm this. Meanwhile, the P2X$_7$ has been shown to contribute to RGC death in this model, (Niyadurupola, Sidaway et al. 2013) and it will be interesting to look at interaction between these channels in mediating Ca^{2+} overload and RGC death.

Chapter 7

General Discussion

The aim of this study was to investigate Ca^{2+} signaling pathways in relation to retinal ganglion cell (RGC) death in glaucoma using the human retina. This involved the use of human organotypic retinal cultures (HORCs), a system that has been validated under conditions of simulated ischemia (Niyadurupola, Sidaway et al. 2011). Moreover, a novel planar sectioning technique was successfully developed and used to analyze expression of genes which were predominately distributed in human RGC layer. Several Ca^{2+} related genes were identified.

The major achievement of this study was the development of the novel sectioning technique. This planar sectioning method was able to collect a high quantity of high quality mRNA from each single layer from retina. mRNA from the RGC layer was collected and compared with entire retinal macula. The mRNA distributions of different retinal cell markers, recoverin (*RCVRN*) for photoreceptors (Dizhoor, Ray et al. 1991), calbindin (*CALB*) for horizontal cells, choline acetyltransferase (*CHAT*) for amacrine cells (Haverkamp and Wassle 2000) and Thy-1 (Barnstable and Drager 1984), NeuN (Buckingham, Inman et al. 2008) and Brn3a (Nadal-Nicolas, Jimenez-Lopez et al. 2009) (*THY-1, RBFOX3 and POU4F1*) for RGCs, were measured in the human macula. They showed distinct distributions through the retinal layers which were consistent with the known distribution of the cells. At present, application of specific antibodies to retinal sections is the most common way to investigate distribution (Johansson, Eftekhari et al. 2010; Siegert, Cabuy et al. 2012). However, this is difficult to quantify and also depends on the antibody quality which can be very variable. PCR allows the use of very specific probes and together with the sectioning technique gives valuable information about the distribution of genes in the retina.

In order to be able to understand the advanced cellular and molecular events that might be involved in glaucoma pathophysiology, it is of great value to determine the gene expression profile of human RGCs. Therefore, this technique was further used to collect RGC layer mRNA from macular region of the retina. Global gene expression

of RGC layer was compared with entire retinal macula using Illumina gene arrays. There were a large number of genes that were predominantly or exclusively expressed in the RGC layer, and some of these had not been linked previously with RGCs. *AHNAK2* and *HSPA1B (HSP70-2)* were the two genes which were found to have highest expressed in the RGC layer. These results were verified by both QRT-PCR and immunolocalization. *AHNAK2* presented a distribution which was exclusive to the RGC layer and absent in other retinal layers. Therefore, the data presented in this thesis has identified a potential new specific markers for human retinal ganglion cells.

HSPA1B (the gene for heat shock 70kDa protein 1B) had a similar distribution in the inner retina to *THY-1* at mRNA level, but it also had some expression in the outer retina. This was consistent with its protein immunolocalization in the macula. HSP70 functions as a chaperone molecule to supervise protein denaturation, translocation, correct folding, activation and aggregation (Takayama, Reed et al. 2003). HSP70 has a potential neuroprotective function when over-expressed and has been shown to protect some neuronal cells from certain stressful insults (Yenari, Giffard et al. 1999). A recent report has indicated that HSP70 is specifically expressed in RGCs and is the earliest gene induced after optic nerve injury, and is crucial for RGCs survival in the zebra fish retina (Nagashima, Fujikawa et al. 2011). Heat shock 70kDa protein 8 (*HSPA8 or HSC70*), shares 85% sequence homology with HSP70 and has similar functions to the other members of HSP70 family (Liu, Daniels et al. 2012) and was also found to be enriched in human RGCs. *HSP70* and *HSC70* expression was also enhanced after cerebral ischemia (Muranyi, He et al. 2005). Furthermore, administration of HSP/HSC70 to the neonatal mouse with traumatic injury can reduce subsequent apoptotic loss of neurons (Tidwell, Houenou et al. 2004). The finding that HSP70 is highly expressed in human macula provides important evidence for the contribution of heat shock protein in neuroprotective function within retinal neurons in the human retina, particularly RGCs. It would be interesting to compare expression of this protein in retinas from different donors. Is HSP70 always present in human retina or is it expressed because it has been induced due to events that occurred to the retina during the donor's life? Looking at expression with age would be interesting in this respect.

Several animal models in rat and monkey, have been used to investigate global gene expression in RGCs. Purified RGCs using immunopanning was a popular approach for RGCs gene expression research. The method uses enzymes to digest the connections between RGCs and other cells and involves a period where the cells are in culture before being analysed. Potential drawbacks to the process include changes to the ganglion cell as a result of the culture period, in addition to the effect of the enzyme during the dissociation procedure. These factors could potentially change the gene expression pattern. It should be noted here that we have tried to isolate RGCs from human retina using this method, but it was not successful.

Recently, laser capture microdissection (LCM) was used as a powerful and precise way to capture the RGCs in the RGCL. Kim et al used this technique to investigate the gene expression profile of human adult RGCs (Kim, Kuehn et al. 2006). However, their methods had a number of drawbacks. Compared with our method, they used the para-macular region, which contained a much thinner RGCL and fewer RGCs. Importantly, the ratio of RGCs to other cell types is much higher in this region compared to the macula, therefore the sample used in those experiments was not highly enriched for RGCs. In addition, LCM does not yield much RNA, so they needed a separate amplification step, which could potentially introduce some errors if amplification weren't linear for all of the genes. Another point to consider was that the gene array list was compiled by comparing gene expression of RGCs with the rest of the retina and all of the retina beyond the IPL was taken. In the experiments described in this thesis, only the samples from the sections with highest expression of RGC markers were taken. Therefore, for several reasons, the sample we used was much more enriched for RGC mRNA and therefore the gene list is likely to be a much more accurate reflection of expression in human RGCs.

There were a large number of interesting genes were found out that expressed in the RGCL. Some calcium-related genes were found to be highly expressed in RGC layer by the gene array data. Calpain-1 was one of these genes. Calpain is a calcium-dependent cysteine protease (Johnson and Guttmann 1997; Sorimachi and Ono 2012). Calpain-1 (μ-calpain) and calpain-2 (m-calpain) are the two ubiquitously distributed and most extensively studied isoforms of calpain. QRT-PCR showed that *CAPN1* had a more advanced expression level and was dominant in the RGC layer which was

consistent with it distribution in the rabbit retina (Croall and Demartino 1991). It has been found that calpain activation involved in ischemia/hypoxia-induced retinal cell death in both in vivo (Sakamoto, Nakajima et al. 2000; Tamada, Nakajima et al. 2005) and in vitro of animal models (Tamada, Fukiagea et al. 2002; Tamada, Nakajima et al. 2005), and also in the experimental model of glaucoma (Huang, Fileta et al. 2010). In the HORCs model, both 3 hours and 12 hours OGD protocols increased LDH release which showed that the simulated ischemia led to retinal cell damage. In order to determine whether proteolysis was induced by calpain activation in this model, α-spectrin and SBDPs were assessed at different OGD exposures periods. Proteolytic activities were greater as the OGD time increased which the intact spectrin levels decreased and levels of spectrin breakdown products increased as the severity of the simulated ischemia increased.

Since it was found that both calpain-1 and 2 were expressed in the inner retina, and particular in the RGCL this was consistent with a possible role for these enzymes in the RGC cell death observed with simulated ischemia. MDL28170 is an inhibitor of both calpain-1 and 2 and was chosen to examine its protective effects in the OGD model in HORCs. It has been identified that MDL28170 is a highly cell-permeable molecule, which has been shown to inhibit ischemic damage in the brain (Lia, Howlett et al. 1998; Markgraf, Velayo et al. 1998; Brana, Benham et al. 1999; Rami, Agarwal et al. 2000; Kawamura, Nakajima et al. 2005). Specially, it reduced infarct volume in rat cerebral ischemia, and its protective activity extended after the induction of ischemia, still being effective if applied 6h after the brain initial ischemia (Markgraf, Velayo et al. 1998). The pharmacodynamic half-life was around 2 hours and peak reaction was obtained after 30 minutes (Markgraf, Velayo et al. 1998). Its neuroprotective role is achieved by inhibiting cell apoptosis and necrosis (Kawamura, Nakajima et al. 2005). In the HORCs, MDL28170 significantly inhibited appearance of both the 145 kDa and 150 kDa spectrin breakdown products, which indicated that calpain was indeed activated in the HORC simulated ischemia model. However, MDL28170 failed to prevent the retinal cell damage from the ischemic insult. RGC number was significantly reduced after 3 hours ischemia and followed by 21 hours reperfusion and *THY-1* mRNA level decreased. The inhibitor slightly prevented RGCs loss but this did not reach significance. *THY-1* mRNA did not enable detection of any protection of MDL28170. Therefore, it was concluded that calpain-induced

proteolysis was not part of the mechanism mediating RGC death in simulated ischemia. This, however, was unexpected and it would be important to carry out further work to confirm this. It is possible that other signaling pathway activated by Ca^{2+} are more significant in ischemia-induced cell death, including caspase-mediated pathways (Wang 2000). Also the retinal-specific calpain may play a role – the activity of MDL28170 at this enzyme is not known.

It is interesting to speculate about the correlation between heat shock proteins and calpain activation. It was shown in the research presented in this thesis that several members of the heat shock protein family were predominantly in the RGCs. Some previous reports have indicated that antibody titers to HSPs were elevated in serum, aqueous humor and the optic nerve head in the glaucoma patient (Tezel, Hernandez et al. 2000; Joachim, Bruns et al. 2007a; Joachim, Wuenschig et al. 2007b). In addition, it has been shown that the small heat shock proteins (aA- and aB-crystallin and HSP27) are elevated in glaucoma patients, and that this is greater in normal pressure glaucoma patients compare to those with primary open angle glaucoma (Tezel, Seigel et al. 1998; Wax, Tezel et al. 2000). It has also been demonstrated that in experimental glaucoma that there is increased expression of HSPs, particular HSP27, in both retinal ganglion cells and glial cells (Huang, Fileta et al. 2007) and that in cultured rat RGCs increased HSP72 expression is seen after hyperthermia (42 °C, 1 hour) and hypoxia (6 hours) treatment (Caprioli, Kitano et al. 1996). Furthermore, these pretreated cells were then found to have greater resistance to anoxia (6 hours) or glutamate treatment (6 hours) (Caprioli, Kitano et al. 1996). All these findings suggest that HSPs are assisting RGCs in maintenance of cell function and resisting the stressful insults of glaucoma. Calpain activation can lead to the breakdown of hundreds of protein substrates, such as cytoskeletal proteins, membrane-associated proteins, transcription factors, kinases and phosphatases (Goll, Thompson et al. 2003). There is some evidence that HSPs are substrates of calpain proteolysis, and an association between calpain activation, HSP70 cleavage and neuronal death in brain ischemia has been proposed (Yamashima and Oikawa 2009; Yamashima 2012). HSP70 is the highest expressed gene in the RGCL. Therefore if calpain broke down the HSP70 and HSP70 was protecting the cells, this would be detrimental to the RGCs.

The experiments presented in chapter 5, show that calpain activity was induced by simulated ischemia, which in turn indicates that calcium influx was elevated by OGD. It was therefore interesting to look at channels which mediate Ca^{2+} influx. The $P2X_7$ receptor has previously been studied in the lab and the techniques developed in this thesis were successfully used to investigate distribution of the $P2X_7$ receptor (Niyadurupola, Sidaway et al. 2013). This data was not included in this thesis, but the paper is attached in Appendix 1. The only plasma membrane Ca^{2+} conducting channel that appeared in the list of most highly expressed genes in human RGCs was the NMDA receptor. This, however, has been intensively studied in the retina previously, so it was decided to look at channels that did not have extensive literature in the retina. TRPC-1, TRPRC-3 and TRPM-2 are highly expressed in the brain (Venkatachalam and Montell 2007), however, their distributions in the retina are not clear. For the initial experiments the mRNA of the three TRP channels was investigated, and the data indicated that TRPC-3 and TRPM-2 were highly expressed in the RGCL. TRPC-1 was more expressed in the outer retina, which is similar to that observed in the mouse retina (Gilliam and Wensel 2011). Unfortunately, the available antibodies for the TRPC channels are not reliable (Gilliam and Wensel 2011). However, the TRPM-2 antibody worked well in the human retina and immunoreactivity was exclusively located in the RGCL and corresponded with NeuN-positive cells. TRPM-2 mediates neuronal cell death in brain when it was induced by hypoxic conditions and inhibition of TRPM-2 activity indicated a neuroprotective role (Venkatachalam and Montell 2007; Gees, Colsoul et al. 2010). However, its contribution to human retinal ischemia was unknown. The present experiments using the inhibitor ACA were inconclusive. This inhibitor is reported as a TRPM-2 inhibitor, but it also inhibits a number of other TRP channels, including TRPC-3 (Kraft, Grimm et al. 2006). Any inhibition observed could therefore not be attributed to inhibition of one particular TRP channel. Furthermore, the experiments themselves were inconclusive. LDH leakage of HORCs cultured with ACA did not protect against retinal cell death. When RGC viability was looked at directly by assessing the number of NeuN-positive cells and levels of *THY-1* mRNA, in each case there appeared to be a protection, but statistical significance was not achieved. Despite advantages of the HORC system, including that fact that it uses human retina, a drawback is that it is likely to be more variable and also the supply means that it is not possible to carry out large numbers of repeats. The current

experiment data did imply that TRP channel activation may contribute to ischemia induced RGC death, but more research would need to be carried out to confirm this.

This research has therefore developed novel techniques for studying the human retina, enabling identification of novel RGC markers and also genes that might be involved in glaucoma pathophysiology. In the future, this may help to identify targets for development of novel neuroprotective strategies for treatment of glaucoma.

Reference:

Abramov, A. Y., A. Scorziello, et al. (2007). "Three distinct mechanisms generate oxygen free radicals in neurons and contribute to cell death during anoxia and reoxygenation." The Journal of neuroscience **27**(5): 1129-1138.

Agarwal, R., S. K. Gupta, et al. (2009). "Current concepts in the pathophysiology of glaucoma." Indian journal of ophthalmology **57**(4): 257-266.

Ahmed, F., K. M. Brown, et al. (2004). "Microarray analysis of changes in mRNA levels in the rat retina after experimental elevation of intraocular pressure." Investigative ophthalmology & visual science **45**(4): 1247-1258.

Almasieh, M., A. M. Wilson, et al. (2012). "The molecular basis of retinal ganglion cell death in glaucoma." Progress in retinal and eye research **31**(2): 152-181.

Amerasinghe, N., J. A. Zhang, et al. (2011). "The Heritability and Sibling Risk of Angle Closure in Asians." Ophthalmology **118**(3): 480-485.

Ames, A. (2000). "CNS energy metabolism as related to function." Brain Research Reviews **34**(1-2): 42-68.

Anderson, D. R. and A. Hendrickson (1974). "Effect of Intraocular Pressure on Rapid Axoplasmic Transport in Monkey Optic Nerve." Investigative ophthalmology & visual science **13**(10): 13.

Araie, M. and C. Mayama (2011). "Use of calcium channel blockers for glaucoma." Progress in retinal and eye research **30**(1): 54-71.

Artal-Sanz, M. and N. Tavernarakis (2005). "Proteolytic mechanisms in necrotic cell death and neurodegeneration." FEBS letters **579**(15): 3287-3296.

Arthur, J. S. C., J. S. Elce, et al. (2000). "Disruption of the Murine Calpain Small Subunit Gene, Capn4- Calpain Is Essential for Embryonic Development but Not for Cell Growth and Division." Molecular and cellular biology **20**(12): 8.

Azuma, M., C. Fukiage, et al. (2000). "Identification and characterization of a retina-specific calpain (Rt88) from rat." Current eye research **21**(3): 710-720.

Azuma, M. and T. R. Shearer (2008). "The role of calcium-activated protease calpain in experimental retinal pathology." Survey of ophthalmology **53**(2): 150-163.

Baltan, S., D. M. Inman, et al. (2010). "Metabolic vulnerability disposes retinal ganglion cell axons to dysfunction in a model of glaucomatous degeneration." The Journal of neuroscience : the official journal of the Society for Neuroscience **30**(16): 5644-5652.

Barnett, N. L., D. V. Pow, et al. (2001). "Differential perturbation of neuronal and glial glutamate transport systems in retinal ischaemia." Neurochemistry international **39**(4): 291-299.

Barnstable, C. J. and U. C. Drager (1984). "Thy-1 Antigen - a Ganglion-Cell Specific Marker in Rodent Retina." Neuroscience **11**(4): 847-&.

Barres, B. A., B. E. Silverstein, et al. (1988). "Immunological, Morphological, and Electrophysiological Variation among Retinal Ganglion Cells Purified by Panning." Neuron **1**: 13.

Bates, C. A., N. Trinh, et al. (1993). "Distribution of Microtubule-Associated Proteins (Maps) in Adult and Embryonic Mouse Retinal Explants - Presence of the Embryonic Map, Map5/1b, in Regenerating Adult Retinal Axons." Developmental Biology **155**(2): 533-544.

Beere, H. M. (2005). "Death versus survival: functional interaction between the apoptotic and stress-inducible heat shock protein pathways." The journal of clinical investigation **115**(10): 2633-2639.

Berridge, M. J. (2004). "Calcium signal transduction and cellular control mechanisms." Biochimica Et Biophysica Acta-Molecular Cell Research **1742**(1-3): 3-7.

Berridge, M. J. (2009). "Inositol trisphosphate and calcium signalling mechanisms." Biochimica et biophysica acta **1793**(6): 933-940.

Berridge, M. J., M. D. Bootman, et al. (1998). "Calcium--a life and death signal." Nature **395**(6703): 645-648.

Berridge, M. J., M. D. Bootman, et al. (2003). "Calcium signalling: dynamics, homeostasis and remodelling." Nature reviews. Molecular cell biology **4**(7): 517-529.

Berridge, M. J., P. Lipp, et al. (2000). "The versatility and universality of calcium signalling." Nature Reviews Molecular Cell Biology **1**(1): 11-21.

Bi, S. H., Z. X. Jin, et al. (2012). "Calpain inhibitor MDL 28170 protects against the Ca2+ paradox in rat hearts." Clinical and experimental pharmacology & physiology **39**(4): 385-392.

Biermann, J., C. V. Oterendorp, et al. (2012). "Evaluation of intraocular pressure elevation in a modified laser-induced glaucoma rat model." Experimental eye research **104**: 7-14.

Biermann, J., C. van Oterendorp, et al. (2012). "Evaluation of intraocular pressure elevation in a modified laser-induced glaucoma rat model." Experimental eye research **104**: 7-14.

Biswas, S., F. Harris, et al. (2004). "Calpains: targets of cataract prevention?" Trends in Molecular Medicine **10**(2): 78-84.

Bonomi, L., G. Marchini, et al. (1998). "Prevalence of glaucoma and intraocular pressure distribution in a defined population - The Egna-Neumarkt study." Ophthalmology **105**(2): 209-215.

Brana, C., C. D. Benham, et al. (1999). "Calpain activation and inhibition in organotypic rat hippocampal slice cultures deprived of oxygen and glucose." European Journal of Neuroscience **11**(7): 2375-2384.

Brasnjevic, I., P. R. Hof, et al. (2008). "Accumulation of nuclear DNA damage or neuron loss: molecular basis for a new approach to understanding selective neuronal vulnerability in neurodegenerative diseases." DNA repair **7**(7): 1087-1097.

Bringmann, A., T. Pannicke, et al. (2009). "Role of retinal glial cells in neurotransmitter uptake and metabolism." Neurochemistry international **54**(3-4): 143-160.

Bringmann, A., O. Uckermann, et al. (2005). "Neuronal versus glial cell swelling in the ischaemic retina." Acta Ophthalmologica Scandinavica **83**(5): 528-538.

Brorson, J. R., C. J. Marcuccilli, et al. (1995). "Delayed Antagonism of Calpain Reduces Excitotoxicity in Cultured Neurons." Miller Stroke **26**(7): 9.

Buckingham, B. P., D. M. Inman, et al. (2008). "Progressive ganglion cell degeneration precedes neuronal loss in a mouse model of glaucoma." Journal of Neuroscience **28**(11): 2735-2744.

Cao, L. H. and X. L. Yang (2008). "Natriuretic peptides and their receptors in the central nervous system." Progress in neurobiology **84**(3): 234-248.

Caprioli, J., S. Kitano, et al. (1996). "Hyperthermia and hypoxia increase tolerance of retinal ganglion cells to anoxia and excitotoxicity." Investigative ophthalmology & visual science **37**(12): 6.

Caprioli, J., S. Kitano, et al. (1996). "Hyperthermia and hypoxia increase tolerance of retinal glanglion cells to anoxia and excitotoxicity." Investigative ophthalmology & visual science **37**(12): 6.

Carriedo, S. G., S. L. Sensi, et al. (2000). "AMPA Exposures Induce Mitochondrial Ca2+ Overload and ROS Generation in Spinal Motor Neurons In Vitro " The journal of neuroscience **20**(1): 11.

Casson, R. J. (2006). "Possible role of excitotoxicity in the pathogenesis of glaucoma." Clinical and Experimental Ophthalmology **34**(1): 54-63.

Cervetto, L., L. Lagnado, et al. (1989). "Extrusion of Calcium from Rod Outer Segments Is Driven by Both Sodium and Potassium Gradients." Nature **337**(6209): 740-743.

Chan, D. C. (2006). "Mitochondria: dynamic organelles in disease, aging, and development." Cell **125**(7): 1241-1252.

Chen, J., K. M. Connor, et al. (2007). "Overstaying their welcome- defective CX3CR1 microglia eyed in macular degeneration." The journal of clinical investigation **117**(10): 5.

Chen, S. and J. S. Diamond (2002). "Synaptically released glutamate activates extrasynaptic NMDA receptors on cells in the ganglion cell layer of rat retina." The journal of neuroscience **22**(6): 9.

Cheung, Z. H., H. K. Yip, et al. (2003). "Axotomy induces cytochrome c release in retinal ganglion cells." Neuroreport **14**(2): 279-282.

Chiu, K., T. T. Lam, et al. (2005). "Calpain and N-methyl-d-aspartate (NMDA)-induced excitotoxicity in rat retinas." Brain research **1046**(1-2): 207-215.

Choi, D. W. and S. M. Rothman (1990). "The role of glutamate neurotoxicity in hypoxic-ischemic neuronal death." Annual review of neuroscience **13**: 171-182.

CLAPHAM, D. E. (2005). "International Union of Pharmacology. XLIX. Nomenclature and Structure-Function Relationships of Transient Receptor Potential Channels " Pharmacological reviews **57**(4): 427-450.

Clapham, D. E. (2007). "SnapShot: mammalian TRP channels." Cell **129**(1): 220.

Claude, F., J. Burgoyne, et al. (2005). "The optic nerve head as a biomechanical structure: a new paradigm for understanding the role of IOP-related stress and strain in the pathophysiology of glaucomatous optic nerve head damage." Progress in retinal and eye research **24**(1): 35.

Coleman, A. L. (2003). Glaucoma: science and practice. Glaucoma: science and practice. I. P. P. John C. Morrison.

Crish, S. D. and D. J. Calkins (2011). "Neurodegeneration in glaucoma: progression and calcium-dependent intracellular mechanisms." Neuroscience **176**: 1-11.

Croall, D. E. and G. N. Demartino (1991). "Calcium-Activated Neutral Protease (Calpain) System: Structure, Function, and Regulation." Physiological Review **71**(3): 35.

Crousillac, S., M. Lerouge, et al. (2003). "Immunolocalization of TRPC channel subunits 1 and 4 in the chicken retina." Visual Neuroscience **20**(4): 453-463.

Curcio, C. A. and K. A. Allen (1990). "Topography of ganglion cells in human retina." The Journal of comparative neurology **300**(1): 21.

Dadon, D. and B. Minke (2010). "Cellular functions of transient receptor potential channels." The international journal of biochemistry & cell biology **42**(9): 1430-1445.

Dadon, D. and B. Minke (2010). "Cellular functions of Transient Receptor Potential channels." International Journal of Biochemistry & Cell Biology **42**(9): 1430-1445.

Davis, J. A. and R. R. Reed (1996). "Role of Olf-1 and Pax-6 transcription factors in neurodevelopment." Journal of Neuroscience **16**(16): 5082-5094.

Day, A. C., G. Baio, et al. (2012). "The prevalence of primary angle closure glaucoma in European derived populations: a systematic review." British Journal of Ophthalmology **96**(9): 1162-1167.

Dimasi, D. P., A. W. Hewitt, et al. (2007). "Prevalence of CYP1B1 mutations in Australian patients with primary congenital glaucoma." Clinical Genetics **72**(3): 255-260.

Dizhoor, A. M., S. Ray, et al. (1991). "Recoverin: a calcium sensitive activator of retinal rod guanylate cyclase." Science **251**(4996): 915-918.

Downs, J. C., M. D. Roberts, et al. (2011). "Glaucomatous cupping of the lamina cribrosa: A review of the evidence for active progressive remodeling as a mechanism." Experimental eye research **93**(2): 133-140.

Duncan, R. S., D. L. Goad, et al. (2010). "Control of Intracellular Calcium Signaling as a Neuroprotective Strategy." Molecules **15**(3): 1168-1195.

Farkas, R. H., J. Qian, et al. (2004). "Gene expression profiling of purified rat retinal ganglion cells." Investigative ophthalmology & visual science **45**(8): 2503-2513.

Feissner, R. F., J. Skalska, et al. (2009). "Crosstalk signaling between mitochondrial Ca2+ and ROS." Front Biosci **14**: 33.

Flammer, J., S. Orgul, et al. (2002). "The impact of ocular blood flow in glaucoma." Progress in retinal and eye research **21**(4): 359-393.

Forrester, J. V., A. D. Dick, et al. (2002). "The eye: Basic sciences in practice."

Foster, P. J., R. Buhrmann, et al. (2002). "The definition and classification of glaucoma in prevalence surveys." British Journal of Ophthalmology **86**(2): 238-242.

Foster, P. J. and G. J. Johnson (2001). "Glaucoma in China: how big is the problem?" British Journal of Ophthalmology **85**: 7.

Garway-Heath, D. F., S. T. Ruben, et al. (1998). "Vertical cup:disc ratio in relation to optic disc size- its value in the assessment of the glaucoma suspect." British Journal of Ophthalmology **82**(10): 118-124.

Gees, M., B. Colsoul, et al. (2010). "The role of transient receptor potential cation channels in Ca2+ signaling." Cold Spring Harbor perspectives in biology **2**(10): a003962.

Geijer, C. and A. Bill (1978). "Effects of raised intraocular pressure on retinal, prelaminar, laminar, and retrolaminar optic nerve blood flow in monkeys." Investigative ophthalmology & visual science **18**(10): 13.

Genderen, M. M., M. M. Bijveld, et al. (2009). "Mutations in TRPM1 are a common cause of complete congenital stationary night blindness." American Journal of Human Genetics **85**(5): 730-736.

Giangiacomo, A. and A. L. Coleman (2009). "The Epidemiology of Glaucoma " Glaucoma.

Gilliam, J. C. and T. G. Wensel (2011). "TRP channel gene expression in the mouse retina." Vision Research **51**(23-24): 2440-2452.

Gilliam, J. C. and T. G. Wensel (2011). "TRP channel gene expression in the mouse retina." Vision Research **51**(23-24): 2440-2452.

Goll, D. E., V. F. Thompson, et al. (2003). "The calpain system." Physiol Rev **83**: 71.

Grieshaber, M. C. and J. Flammer (2005). "Blood flow in glaucoma." Current Opinion in Ophthalmology **16**(2): 5.

Guerini, D. (1998). "The significance of the isoforms of plasma membrane calcium ATPase." Cell and Tissue Research **292**(2): 191-197.

Guerini, D., L. Coletto, et al. (2005). "Exporting calcium from cells." Cell calcium **38**(3-4): 281-289.

Guo, L., S. E. Moss, et al. (2005). "Retinal ganglion cell apoptosis in glaucoma is related to intraocular pressure and IOP-induced effects on extracellular matrix." Investigative ophthalmology & visual science **46**(1): 175-182.

Guo, Y., W. O. Cepurna, et al. (2010). "Retinal cell responses to elevated intraocular pressure: a gene array comparison between the whole retina and retinal ganglion cell layer." Investigative ophthalmology & visual science **51**(6): 3003-3018.

Harteneck, C., H. Frenzel, et al. (2007). "N-(p-Amylcinnamoyl)anthranilic Acid (ACA): A Phospholipase A2 Inhibitor and TRP Channel Blocker." Cardiovascular drug reviews **25**(1): 61-75.

Hartwick, A. T., C. M. Hamilton, et al. (2008). "Glutamatergic calcium dynamics and deregulation of rat retinal ganglion cells." The Journal of physiology **586**(14): 3425-3446.

Haverkamp, S. and H. Wassle (2000). "Immunocytochemical analysis of the mouse retina." The Journal of comparative neurology **424**(1): 1-23.

Hayreh, S. S. (2008). "Pathophysiology of Glaucomatous Optic Neuropathy: Role of Optic Nerve Head Vascular Insufficiency." Journal of Current Glaucoam Practice **2**(1): 12.

Heijl, A., M. C. Leske, et al. (2002). "Reduction of intraocular pressure and glaucoma progression - Results from the early manifest glaucoma trial." Archives of Ophthalmology **120**(10): 1268-1279.

Hernandez-Fonseca, K. and L. Massieu (2005). "Disruption of endoplasmic reticulum calcium stores is involved in neuronal death induced by glycolysis inhibition in cultured hippocampal neurons." Journal of Neuroscience Research **82**(2): 196-205.

Herson, P. S. and M. L. Ashford (1997). "Activation of a novel non-selective cation channel by alloxan and H2O2 in the rat insulin-secreting cell line CRI-G1." The Journal of physiology **501**(Pt 1): 59-66.

Hitchings, R. A. (2004). "A practical approach to the management of narmal tension glaucoma." 10.

Hong, S., Y. Iizuka, et al. (2012). "Isolation of primary mouse retinal ganglion cells using immunopanning-magnetic separation." Molecular Vision **18**: 9.

Hoyng, P. F. J. and Y. Kitazawa (2002). "Medical Treatment of Normal Tension Glaucoma." SURVEY OF OPHTHALMOLOGY **47**(Supplement 1): S116-S124.

Huang, W., J. Fileta, et al. (2010). "Calpain activation in experimental glaucoma." Investigative ophthalmology & visual science **51**(6): 3049-3054.

Huang, W., J. B. Fileta, et al. (2007). "Hsp27 phosphorylation in experimental glaucoma." Investigative ophthalmology & visual science **48**(9): 4129-4135.

Huang, Y. H. and K. K. W. Wang (2001). "The calpain family and human disease." Trends in molecular medicine **7**(8): 8.

Ikeda, H., E. Dawes, et al. (1992). "Spontaneous firing level distinguishes the effects of NMDA and non-NMDA receptor antagonists on the ganglion cells in the cat retina." European journal of pharmacology **210**(1): 9.

Inatani, M., K. Iwao, et al. (2008). "Long-term relationship between intraocular pressure and visual field loss in primary open-angle glaucoma." Journal of Glaucoma **17**(4): 275-279.

Inokuchi, Y., M. Shimazawa, et al. (2009). "A Na+/Ca2+ exchanger isoform, NCX1, is involved in retinal cell death after N-methyl-D-aspartate injection and ischemia-reperfusion." Journal of Neuroscience Research **87**(4): 906-917.

Ivanov, D., G. Dvoriantchikova, et al. (2005). "Microarray analysis of gene expression in adult retinal ganglion cells." FEBS letters **580**(1): 331-335.

Ivanov, D., G. Dvoriantchikova, et al. (2006). "Microarray analysis of gene expression in adult retinal ganglion cells." Febs Letters **580**(1): 331-335.

Jin, K. and M. Xiang (2011). "Ebf1 deficiency causes increase of Muller cells in the retina and abnormal topographic projection at the optic chiasm." Biochemical and biophysical research communications **414**(3): 539-544.

Joachim, S. C., K. Bruns, et al. (2007a). "Antibodies to alpha B-crystallin, vimentin, and heat shock protein 70 in aqueous humor of patients with normal tension glaucoma and IgG antibody patterns against retinal antigen in aqueous humor." Curr Eye Research **32**(6): 9.

Joachim, S. C., D. P. Wuenschig, N , et al. (2007b). "IgG antibody patterns in aqueous humor of patients with primary open angle glaucoma and pseudoexfoliation glaucoma." Molecular Vision **13**: 9.

Johansson, U. E., S. Eftekhari, et al. (2010). "A battery of cell- and structure-specific markers for the adult porcine retina." The journal of histochemistry and cytochemistry : official journal of the Histochemistry Society **58**(4): 377-389.

Johnson, E. C., L. M. H. Deppmeier, et al. (2000). "Chronology of optic nerve head and retinal responses to elevated intraocular pressure." Investigative ophthalmology & visual science **41**(2): 431-442.

Johnson, G. V. W. and R. P. Guttmann (1997). "Calpains: intact and active." BioEssays **19**(11): 8.

Jung, C. G., H. J. Kim, et al. (2005). "Homeotic factor ATBF1 induces the cell cycle arrest associated with neuronal differentiation." Development **132**(23): 5137-5145.

Kalmar, B. and L. Greensmith (2009). "Induction of heat shock proteins for protection against oxidative stress." Advanced drug delivery reviews **61**(4): 310-318.

Kampinga, H. H., J. Hageman, et al. (2009). "Guidelines for the nomenclature of the human heat shock proteins." Cell Stress & Chaperones **14**(1): 105-111.

Kaur, C., W. S. Foulds, et al. (2008). "Hypoxia-ischemia and retinal ganglion cell damage." Clinical Ophthalmology **2**(4): 12.

Kawamura, M., W. Nakajima, et al. (2005). "Calpain inhibitor MDL 28170 protects hypoxic-ischemic brain injury in neonatal rats by inhibition of both apoptosis and necrosis." Brain research **1037**(1-2): 59-69.

Kendell, K. R., H. R. Quigley, et al. (1995). "Primary Open-Angle Glaucoma Is Not Associated With Photoreceptor Loss." Investigative ophthalmology & visual science **36**(1): 6.

Kerrigan, L. A., D. J. Zack, et al. (1997). "TUNEL-positive ganglion cells in human primary open-angle glaucoma." Archives of ophthalmology **115**(8): 5.

Kielczewski, J. L., M. E. Pease, et al. (2005). "The effect of experimental glaucoma and optic nerve transection on amacrine cells in the rat retina." Investigative ophthalmology & visual science **46**(9): 3188-3196.

Kim, C., M. Kuehn, et al. (2006). "Gene expression profile of the adult human retinal ganglion cell layer." Molecular Vision **12**(187-90): 1640-1648.

Kim, C. Y., M. H. Kuehn, et al. (2006). "Gene expression profile of the adult human retinal ganglion cell layer." Molecular Vision.

Kim, T. S., M. Kawaguchi, et al. (2010). "The ZFHX3 (ATBF1) transcription factor induces PDGFRB, which activates ATM in the cytoplasm to protect cerebellar neurons from oxidative stress." Disease Models & Mechanisms **3**(11-12): 752-762.

Kirichok, Y., G. Krapivinsky, et al. (2004). "The mitochondrial calcium uniporter is a highly selective ion channel." Nature **427**(6972): 360-364.

Klinger, S. C., S. Glerup, et al. (2011). "SorLA regulates the activity of lipoprotein lipase by intracellular trafficking." Journal of cell science **124**(Pt 7): 1095-1105.

Klooster, J., J. Blokker, et al. (2011). "Ultrastructural localization and expression of TRPM1 in the human retina." Investigative ophthalmology & visual science **52**(11): 8356-8362.

Kong, G. Y. X., N. J. Van Bergen, et al. (2009). "Mitochondrial Dysfunction and Glaucoma." Journal of Glaucoma **18**(2): 93-100.

Kong, X. M., Y. H. Chen, et al. (2011). "Influence of Family History as a Risk Factor on Primary Angle Closure and Primary Open Angle Glaucoma in a Chinese population." Ophthalmic Epidemiology **18**(5): 226-232.

Koulen, P., E. L. Fletcher, et al. (1998). "Immunocytochemical localization of the postsynaptic density protein PSD-95 in the mammalian retina." Journal of Neuroscience **18**(23): 10136-10149.

Kraft, R., C. Grimm, et al. (2006). "Inhibition of TRPM2 cation channels by N-(p-amylcinnamoyl)anthranilic acid." British journal of pharmacology **148**(3): 264-273.

Krizaj, D. (2005). "Serca isoform expression in the mammalian retina." Experimental eye research **81**(6): 690-699.

Krizaj, D., S. J. Demarco, et al. (2002). "Cell-specific expression of plasma membrane calcium ATPase isoforms in retinal neurons." Journal of Comparative Neurology **451**(1): 1-21.

Kunz, S., E. Niederberger, et al. (2004). "The calpain inhibitor MDL 28170 prevents inflammation-induced neurofilament light chain breakdown in the spinal cord and reduces thermal hyperalgesia." Pain **110**(1-2): 409-418.

Lam, T. T., E. Siew, et al. (1997). "Ameliorative effect of mk-801 on retinal ischemia." Journal of ocular pharmacology and terapeutics **13**(2): 9.

Lao, A., V. Schmidt, et al. (2012). "Multi-compartmental modeling of SORLA's influence on amyloidogenic processing in Alzheimer's disease." BMC systems biology **6**: 74.

Lee, S. L., A. S. L. Yu, et al. (1994). "Tissue-specific Expressionof Na+-Ca2+ exchangIesroforms." The journal of biological chemistry **269**(21): 4.

Li, M. H., K. Inoue, et al. (2011). "Calcium-permeable ion channels involved in glutamate receptor-independent ischemic brain injury." Acta Pharmacologica Sinica **32**(6): 734-740.

Lia, P. A., W. Howlett, et al. (1998). "Postischemic treatment with calpain inhibitor MDL 28170 ameliorates brain damage in a gerbil model of global ischemia." Neuroscience Letters **247**(1): 4.

Liu, T., C. K. Daniels, et al. (2012). "Comprehensive review on the HSC70 functions, interactions with related molecules and involvement in clinical diseases and therapeutic potential." Pharmacology & therapeutics **136**(3): 354-374.

Louzadajunior, P., J. J. Dias, et al. (1992). "Glutamate Release in Experimental-Ischemia of the Retina - an Approach Using Microdialysis." Journal of Neurochemistry **59**(1): 358-363.

Ma, C. H. and J. S. Taylor (2010). "Trophic responsiveness of purified postnatal and adult rat retinal ganglion cells." Cell and tissue research **339**(2): 297-310.

Magnusson, A., L. S. Haug, et al. (1993). "Calcium-induced degradation of the Inositol (1,4,5)-trisphosphate receptor:Ca2'-channel." Federation of European Biochemical Societies **323**(3): 4.

Majsterek, I., K. Malinowska, et al. (2011). "Evaluation of oxidative stress markers in pathogenesis of primary open-angle glaucoma." Experimental and molecular pathology **90**(2): 231-237.

Markgraf, C. G., N. L. Velayo, et al. (1998). "Six-Hour Window of Opportunity for Calpain Inhibition in Focal Cerebral Ischemia in Rats." Stroke **29**(1): 152-158.

Martin, K. R. G., H. Levkovitch-Verbin, et al. (2002). "Retinal Glutamate Transporter Changes in Experimental Glaucoma and after Optic Nerve Transection in The Rat." Investigative ophthalmology & visual science **43**(7): 8.

Martin, K. R. G., H. A. Quigley, et al. (2003). "Gene therapy with brain-derived neurotrophic factor as a protection: Retinal ganglion cells in a rat glaucoma model." Investigative ophthalmology & visual science **44**(10): 4357-4365.

Mattson, M. P. (2007). "Calcium and neurodegeneration." <u>Aging Cell</u> **6**(3): 337-350.

McClintick, J. N. and H. J. Edenberg (2006). "Effects of filtering by Present call on analysis of microarray experiments." <u>BMC bioinformatics</u> **7**: 49.

McElnea, E. M., B. Quill, et al. (2011). "Oxidative stress, mitochondrial dysfunction and calcium overload in human lamina cribrosa cells from glaucoma donors." <u>Molecular Vision</u> **17**(133): 1182-1191.

McFadzean, I. and A. Gibson (2002). "The developing relationship between receptor-operated and store-operated calcium channels in smooth muscle." <u>British journal of pharmacology</u> **135**(1): 1-13.

Meyer-Franke, A., M. R. Kaplan, et al. (1995). "Characterization of the signaling interactions that promote the survival and growth of developing retinal ganglion cells in the cuture." <u>Neuron</u> **15**: 15.

Miao, Y., L. D. Dong, et al. (2012). "Involvement of calpain/p35-p25/Cdk5/NMDAR signaling pathway in glutamate-induced neurotoxicity in cultured rat retinal neurons." <u>PloS one</u> **7**(8): e42318.

Miller, B. A. (2006). "The role of TRP channels in oxidative stress-induced cell death." <u>The Journal of membrane biology</u> **209**(1): 31-41.

Minckler, D. S., A. H. Bunt, et al. (1977). "orthograde and retrograde axoplasmic transport during acute ocular hypertension in the monkey." <u>Investigative ophthalmology & visual science</u> **16**(5): 16.

Mitchell, P., F. Hourihan, et al. (1999). "The relationship between glaucoma and myopia." <u>Ophthalmology</u> **106**(10): 2010-2015.

Mitchell, P., W. Smith, et al. (1996). "Prevalence of open-angle glaucoma in Australia - The Blue Mountains eye study." <u>Ophthalmology</u> **103**(10): 1661-1669.

Momeni, H. R. (2011). "Role of Calpain in Apoptosis." Cell Journal **13**(2): 65-72.

Morton, J. D., H. Y. Lee, et al. (2013). "A macrocyclic calpain inhibitor slows the development of inherited cortical cataracts in a sheep model." Investigative ophthalmology & visual science **54**(1): 389-395.

Mullen, R. J., C. R. Buck, et al. (1992). "NeuN, a neuronal specific nuclear protein in vertebrates." Development **116**: 12.

Muranyi, M., Q. P. He, et al. (2005). "Induction of heat shock proteins by hyperglycemic cerebral ischemia." Brain research. Molecular brain research **139**(1): 80-87.

Nadal-Nicolas, F. M., M. Jimenez-Lopez, et al. (2009). "Brn3a as a marker of retinal ganglion cells: qualitative and quantitative time course studies in naive and optic nerve-injured retinas." Investigative ophthalmology & visual science **50**(8): 3860-3868.

Nagashima, M., C. Fujikawa, et al. (2011). "HSP70, the earliest-induced gene in the zebrafish retina during optic nerve regeneration: its role in cell survival." Neurochemistry international **58**(8): 888-895.

Nakajima, E., L. L. David, et al. (2006). "Calpain-specific proteolysis in primate retina: Contribution of calpains in cell death." Investigative ophthalmology & visual science **47**(12): 5469-5475.

Nakhai, H., S. Sel, et al. (2007). "Ptf1a is essential for the differentiation of GABAergic and glycinergic amacrine cells and horizontal cells in the mouse retina." Development **134**(6): 1151-1160.

Napper, G. A., M. J. Pianta, et al. (1999). "Reduced glutamate uptake by retinal glial cells under ischemic/hypoxic conditions." Visual Neuroscience **16**(1): 149-158.

Nath, R. (1996). "Non-erythroid a-spectrin break-down by calpain and interleukin 1b-converting-enzyme-like pro- tease(s) in apoptotic cells: contributory roles of both protease families in neuronal apoptosis." Biochemical Journal **319**: 7.

Neal, M. J., J. R. Cunningham, et al. (1994). "Effects of Ischaemia on Neurotransmitter Release from the Isolated Retina." Journal of Neurochemistry **62**(3): 9.

Nedergaard, M., J. J. Rodriguez, et al. (2010). "Glial calcium and diseases of the nervous system." Cell calcium **47**(2): 140-149.

Nemesure, B., R. Honkanen, et al. (2007). "Incident open-angle glaucoma and intraocular pressure." Ophthalmology **114**(10): 1810-1815.

Nemova, N. N., L. A. Lysenko, et al. (2010). "Proteases of the calpain family: Structure and functions." Russian Journal of Developmental Biology **41**(5): 318-325.

Nilius, B., G. Owsianik, et al. (2007). "Transient receptor potential cation channels in disease." Physiological Reviews **87**(1): 165-217.

Nilius, B., G. Owsianik, et al. (2007). "Transient Receptor Potential Cation Channels in Disease." The American Physiological Society **87**(1): 54.

Niyadurupola, N., P. Sidaway, et al. (2013). "P2X7 Receptor Activation Mediates Retinal Ganglion Cell Death in a Human Retina Model of Ischemic Neurodegeneration.." Investigative ophthalmology & visual science **54**(3): 2163-2170.

Niyadurupola, N., P. Sidaway, et al. (2011). "The development of human organotypic retinal cultures (HORCs) to study retinal neurodegeneration." The British journal of ophthalmology **95**(5): 720-726.

Nucci, C., R. Tartaglione, et al. (2005). "Neurochemical evidence to implicate elevated glutamate in the mechanisms of high intraocular pressure (IOP)-induced retinal ganglion cell death in rat." Neurotoxicology **26**(5): 935-941.

Okuno, T., T. Sugiyama, et al. (2004). "Diurnal variation in microcirculation of ocular fundus and visual field change in normal-tension glaucoma." Eye **18**(7): 697-702.

Ono, Y. and H. Sorimachi (2012). "Calpains: an elaborate proteolytic system." Biochimica et biophysica acta **1824**(1): 224-236.

Orrenius, S., B. Zhivotovsky, et al. (2003). "Regulation of cell death: The calcium-apoptosis link." Nature Reviews Molecular Cell Biology **4**(7): 552-565.

Osborne, N. N. (2010). "Mitochondria: Their role in ganglion cell death and survival in primary open angle glaucoma." Experimental eye research **90**(6): 750-757.

Osborne, N. N., R. J. Casson, et al. (2004). "Retinal ischemia: mechanisms of damage and potential therapeutic strategies." Progress in retinal and eye research **23**(1): 91-147.

Osborne, N. N., J. Melena, et al. (2001). "A hypothesis to explain ganglion cell death caused by vascular insults at the optice nerve head: possible implication for the treantment of glaucoma." British journal of ophthalmology **85**: 1252-1259.

Osborne, N. N., M. M. Ugarte, et al. (1999). "Neuroprotection in relation to retinal ischemia and relevance to glaucoma." Survey of ophthalmology **43**: S102-S128.

Osborne, N. N., J. P. M. Wood, et al. (2004). "Effectiveness of levobetaxolol and timolol at blunting retinal ischaemia is related to their calcium and sodium blocking activities: relevance to glaucoma." Brain Research Bulletin **62**(6): 525-528.

Pan, Z., J. E. Capó-Aponte, et al. (2012). "Transient Receptor Potential (TRP) Channels in the Eye." Advances in Ophthalmology: 13.

Paquet-Durand, F., L. Johnson, et al. (2007). "Calpain activity in retinal degeneration." Journal of Neuroscience Research **85**(4): 693-702.

Perrin, B. J. and A. Huttenlocher (2002). "Calpain." The International Journal of Biochemistry & Cell Biology **34**: 4.

Prinsen, C. F., R. T. Szerencsei, et al. (2000). "Molecular cloning and functional expression of the potassium-dependent sodium-calcium exchanger from human and chicken retinal cone photoreceptors." The Journal of neuroscience : the official journal of the Society for Neuroscience **20**(4): 1424-1434.

Qu, J., D. Wang, et al. (2010). "Mechanisms of retinal ganglion cell injury and defense in glaucoma." Experimental eye research **91**(1): 48-53.

Quigley, H. A. (2011). "Glaucoma." Lancet **377**(9774): 1367-1377.

Quigley, H. A. and D. R. Anderson (1976). "The dynamics and location of axonal transport blockade by acute intraocular pressure elevation in primate optic nerve." Investigative ophthalmology & visual science **15**(8): 11.

Quigley, H. A., S. J. McKinnon, et al. (2000). "Retrograde axonal transport of BDNF in retinal ganglion cells is blocked by acute IOP elevation in rats." Investigative ophthalmology & visual science **41**(11): 3460-3466.

Quigley, H. A., W. H. Nickells, et al. (1995). "Retinal Ganglion Cell Death in Experimental Glaucoma and After Axotomy Occurs by Apoptosis." Investigative ophthalmology & visual science **36**(5): 13.

Racette, L., M. R. Wilson, et al. (2003). "Primary Open-Angle Glaucoma in Blacks: A Review." Survey of ophthalmology **48**(3): 295-313.

Raffaello, A., D. De Stefani, et al. (2012). "The mitochondrial Ca(2+) uniporter." <u>Cell calcium</u> **52**(1): 16-21.

Raffaello, A., D. D. Stefani, et al. (2012). "The mitochondrial Ca(2+) uniporter." <u>Cell calcium</u> **52**(1): 16-21.

Rami, A. (2003). "Ischemic neuronal death in the rat hippocampus: the calpain– calpastatin–caspase hypothesis." <u>Neurobiology of Disease</u> **13**(2): 75-88.

Rami, A., R. Agarwal, et al. (2000). "m-Calpain activation, DNA fragmentation, and synergistic effects of caspase and calpain inhibitors in protecting hippocampal neurons from ischemic damage." <u>Brain research</u> **866**(1-2): 14.

Rardon, D. P., D. C. Cefali, et al. (1990). "Digestion of cardiac and skeletal muscle junctional sarcoplasmic reticulum vesicles with calpain II. Effects on the Ca2+ release channel." <u>Circulation Research</u> **67**(1): 84-96.

Richard, I., C. Roudaut, et al. (2000). "Loss of Calpain 3 Proteolytic Activity Leads to Muscular Dystrophy and to Apoptosis-associated IkBα/Nuclear Factor kB Pathway Perturbation in Mice." <u>The Journal of Cell Biology</u> **51**(7): 8.

Rollín, R., A. Mediero, et al. (2004). "Natriuretic peptide system in the human retina." <u>Molecular vision</u> **10**: 8.

Rudnicka, A. R. and C. G. Owen (2007). Chapter 1 - Epidemiology of primary open angle glaucoma. <u>Glaucoma Identification & Co-management</u>. D. F. Edgar.

Rudnicka, A. R. and C. G. Owen (2007). Epidemiology of primary open angle glaucoma. <u>Glaucoma Identification & Co-management</u>. F. E. David, Bsc, McOptomet al. Edinburgh, Butterworth-Heinemann**:** 1-16.

Ruiz-Ederra, J., M. Garcia, et al. (2005). "The pig eye as a novel model of glaucoma." <u>Experimental eye research</u> **81**(5): 561-569.

Ryskamp, D. A., P. Witkovsky, et al. (2011). "The polymodal ion channel transient receptor potential vanilloid 4 modulates calcium flux, spiking rate, and apoptosis of mouse retinal ganglion cells." The Journal of neuroscience : the official journal of the Society for Neuroscience **31**(19): 7089-7101.

Ryskamp, D. A., P. Witkovsky, et al. (2011). "The Polymodal Ion Channel Transient Receptor Potential Vanilloid 4 Modulates Calcium Flux, Spiking Rate, and Apoptosis of Mouse Retinal Ganglion Cells." Journal of Neuroscience **31**(19): 7089-7101.

Ryu, M., M. Yasuda, et al. (2012). "Critical role of calpain in axonal damage-induced retinal ganglion cell death." Journal of neuroscience research **90**(4): 802-815.

Sakamoto, Y., T. Nakajima, et al. (2000). "Involvement of calpain isoforms in ischemia-reperfusion injury in rat retina." Current eye research **21**(1): 571-580.

Sappington, R. M., T. Sidorova, et al. (2009). "TRPV1: contribution to retinal ganglion cell apoptosis and increased intracellular Ca2+ with exposure to hydrostatic pressure." Investigative ophthalmology & visual science **50**(2): 717-728.

Sasaoka, M., K. Nakamura, et al. (2008). "Changes in visual fields and lateral geniculate nucleus in monkey laser-induced high intraocular pressure model." Experimental eye research **86**(5): 770-782.

Scieglinska, D., W. Piglowski, et al. (2011). "Differential expression of HSPA1 and HSPA2 proteins in human tissues; tissue microarray-based immunohistochemical study." Histochemistry and cell biology **135**(4): 337-350.

Selles-Navarro, I., M. P. Villegas-Perez, et al. (1996). "Retinal ganglion cell death after different transient periods of pressure-induced ischemia and survival

intervals - A quantitative in vivo study." <u>Investigative ophthalmology & visual science</u> **37**(10): 2002-2014.

Selvaraj, S., Y. Y. Sun, et al. (2010). "TRPC Channels and their Implications for Neurological Diseases." <u>Cns & Neurological Disorders-Drug Targets</u> **9**(1): 94-104.

Shapovalov, G., Y. Lehen'kyi, et al. (2011). "TRP channels in cell survival and cell death in normal and transformed cells." <u>Cell calcium</u> **50**: 8.

Shen, Y., X. L. Liu, et al. (2006). "N-Methyl-D-Aspartate Receptors in the Retina." <u>Molecular neurobioloby</u> **34**(3): 17.

Shoshan-Barmatz, V., M. Zakar, et al. (2007). "Retina expresses a novel variant of the ryanodine receptor." <u>The European journal of neuroscience</u> **26**(11): 3113-3125.

Siegert, S., E. Cabuy, et al. (2012). "Transcriptional code and disease map for adult retinal cell types." <u>Nature Neuroscience</u> **15**(3): 487-495.

Siegert, S., E. Cabuy, et al. (2012). "Transcriptional code and disease map for adult retinal cell types." <u>Nature neuroscience</u> **15**(3): 487-495, S481-482.

Simard, J. M., K. V. Tarasov, et al. (2007). "Non-selective cation channels, transient receptor potential channels and ischemic stroke." <u>Biochimica Et Biophysica Acta-Molecular Basis of Disease</u> **1772**(8): 947-957.

Smith, M. A., P. S. Herson, et al. (2003). "Hydrogen-peroxide-induced toxicity of rat striatal neurones involves activation of a non-selective cation channel." <u>The Journal of physiology</u> **547**(Pt 2): 417-425.

Snell, S. R. and A. M. Lemp (1998). <u>Clinical anatomy of the eye</u>, Blackwell Science.

Sohan, S. H. and A. W. Thomas (1980). "Experimental occlusion of the central artery of the retina. IV: Retinal tolerance time to acute ischaemia." British journal of ophthalmology **64**: 9.

Solomon, A. S., M. Kimron, et al. (2003). "Up-regulation of semaphorin expression in retina of glaucomatous rabbits." Graefes Archive for Clinical and Experimental Ophthalmology **241**(8): 673-681.

Sorimachi, H. and Y. Ono (2012). "Regulation and physiological roles of the calpain system in muscular disorders." Cardiovascular Research **96**(1): 11-22.

Soto, I., E. Oglesby, et al. (2008). "Retinal ganglion cells downregulate gene expression and lose their axons within the optic nerve head in a mouse glaucoma model." The Journal of neuroscience : the official journal of the Society for Neuroscience **28**(2): 548-561.

Strouthidis, N. G. and M. J. Girard (2013). "Altering the way the optic nerve head responds to intraocular pressure-a potential approach to glaucoma therapy." Current Opinion in Pharmacology **13**(1): 83-89.

Sung, K. R., S. Lee, et al. (2009). "Twenty-four hour ocular perfusion pressure fluctuation and risk of normal-tension glaucoma progression." Investigative ophthalmology & visual science **50**(11): 5266-5274.

Szydlowska, K. and M. Tymianski (2010). "Calcium, ischemia and excitotoxicity." Cell calcium **47**(2): 122-129.

Takayama, S., J. C. Reed, et al. (2003). "Heat-shock proteins as regulators of apoptosis." Oncogene **22**(56): 9041-9047.

Tamada, Y., C. Fukiagea, et al. (2002). "Involvment of calpain in hypoxia induced damage in rat retina in vitro." Comparative biochemisstry and physiology part B: Biochemistry and Molecular biology **131**(2): 5.

Tamada, Y., E. Nakajima, et al. (2005). "Proteolysis of neuronal cytoskeletal proteins by calpain contributes to rat retinal cell death induced by hypoxia." Brain research **1050**(1-2): 148-155.

Tezel, G., M. R. Hernandez, et al. (2000). "Immunostaining of Heat Shock Proteins in the Retina and Optic Nerve Head of Normal and Glaucomatous Eyes." Laboratory Sciences **118**(4): 8.

Tezel, G., G. Seigel, et al. (1998). "Autoantibodies to small heat shock proteins in glaucoma." Investigative ophthalmology & visual science **39**(12): 11.

Thoreson, W. B. and P. Witkovsky (1999). "Glutamate receptors and circuits in the vertebrate retina." Progress in retinal and eye research **18**(6): 46.

Tidwell, J. L., L. J. Houenou, et al. (2004). "Administration of Hsp70 in vivo inhibits motor and sensory neuron degeneration." Cell Stress Chaperones **9**(1): 11.

Tielsch, J. M., J. Katz, et al. (1994). "Family History and Risk of Primary Open-Angle Glaucoma - the Baltimore Eye Survey." Archives of Ophthalmology **112**(1): 69-73.

Topaloğlu, H., P. Dinçer, et al. (1997). "Calpain-3 Deficiency Causes a Mild Muscular Dystrophy in Childhood." Neuropediatrics **28**(4): 5.

Trimarchi, J. M., M. B. Stadler, et al. (2007). "Molecular heterogeneity of developing retinal ganglion and amacrine cells revealed through single cell gene expression profiling." Journal of Comparative Neurology **502**(6): 1047-1065.

Tsuruga, H., H. Murata, et al. (2012). "A model for the easy assessment of pressure-dependent damage to retinal ganglion cells using cyan fluorescent protein-expressing transgenic mice." Molecular Vision **18**(258-59): 2468-2478.

Tymanskyj, S. R., T. M. E. Scales, et al. (2012). "MAP1B enhances microtubule assembly rates and axon extension rates in developing neurons." Molecular and Cellular Neuroscience **49**(2): 110-119.

Venkatachalam, K. and C. Montell (2007). "TRP Channels." Annual Review of Biochemistry **76**(1): 387-417.

Venkatachalam, K. and C. Montell (2007). "TRP channels." Annual review of biochemistry **76**: 387-417.

Verma, S., N. Quillinan, et al. (2012). "TRPM2 channel activation following in vitro ischemia contributes to male hippocampal cell death." Neuroscience Letters **530**(1): 41-46.

Vorwerk, C. K., S. A. Lipton, et al. (1996). "Chronic Low-Dose Glutamate Is Toxic to Retinal Ganglion Cells." Investigative ophthalmology & visual science **37**(8): 7.

Wang, J. T., N. J. Kunzevitzky, et al. (2007). "Disease gene candidates revealed by expression profiling of retinal ganglion cell development." Journal of Neuroscience **27**(32): 8593-8603.

Wang, K. K. W. (2000). "Calpain and caspase- can you tell the difference?" Trends in neurosciences **23**(1): 6.

Wang, Q. L., S. Chen, et al. (2004). "QRX, a novel homeobox gene, modulates photoreceptor gene expression." Human molecular genetics **13**(10): 1025-1040.

Wang, S. S., R. Y. L. Tsai, et al. (1997). "The characterization of the Olf-1/EBF-like HLH transcription factor family: Implications in olfactory gene regulation and neuronal development." Journal of Neuroscience **17**(11): 4149-4158.

Wang, S. S., R. Y. L. Tsai, et al. (1997). "The Characterization of the Olf-1/EBF-Like HLH Transcription Factor Family: Implications in Olfactory Gene Regulation and Neuronal Development." The journal of neuroscience **17**(11): 10.

Wang, X. L., L. L. Teng, et al. (2010). "TRPC6 Channel Protects Retinal Ganglion Cells in a Rat Model of Retinal Ischemia/Reperfusion-Induced Cell Death." Investigative ophthalmology & visual science **51**(11): 5751-5758.

Watanabe, M., Y. Miura, et al. (1996). "Developmental changes in expression of the ATBF1 transcription factor gene." Molecular Brain Research **42**(2): 344-349.

Wax, M. B. and G. Tezel (2009). "Immunoregulation of retinal ganglion cell fate in glaucoma." Experimental eye research **88**(4): 825-830.

Wax, M. B., G. Tezel, et al. (2000). "Serum autoantibodies to heat shock proteins in glaucoma patients from Japan and the United States." Ophthalmology **108**(2): 7.

Weinreb, R. N. and P. T. Khaw (2004). "Primary open-angle glaucoma." Lancet **363**(9422): 1711-1720.

Williams, S. E. I. (2007). "Glaucoma is a major global cause of irreversible blindness." CME **25**: 464-468.

Wolf, H. K., R. Buslei, et al. (1996). "NeuN: a useful neuronal marker for diagnostic histopathology." Journal of Histochemistry & Cytochemistry **44**(10): 1167-1171.

Xu, G. Z., J. Tian, et al. (2010). "Natriuretic peptide receptors are expressed in rat retinal ganglion cells." Brain research bulletin **82**(3-4): 188-192.

Yamashima, T. (2000). "Implication of cysteine proteases calpain, cathepsin and caspase in ischemic neuronal death of primates." Progress in Neurobiology **62**(3): 23.

Yamashima, T. (2012). "Hsp70.1 and related lysosomal factors for necrotic neuronal death." Journal of Neurochemistry **120**(4): 477-494.

Yamashima, T. and S. Oikawa (2009). "The role of lysosomal rupture in neuronal death." Progress in Neurobiology **89**(4): 343-358.

Yanagi, M., R. Kawasaki, et al. (2011). "Vascular risk factors in glaucoma: a review." Clinical and Experimental Ophthalmology **39**(3): 252-258.

Yasumasa, O., J. Y. Wei, et al. (1998). "Neurotoxic Effects of Low Doses of Glutamate on Purified Rat Retinal Ganglion Cells." Investigative ophthalmology & visual science **39**(6): 10.

Yenari, M. A., R. G. Giffard, et al. (1999). "The neuroprotective potential of heat shock protein 70." molecular medicine today **5**.

Yoshida, M., E. Okada, et al. (2001). "Age-specific prevalence of open-angle glaucoma and its relationship to refraction among more than 60,000 asymptomatic Japanese subjects." Journal of Clinical Epidemiology **54**(11): 1151-1158.

Zeevalk, G. D. and W. J. Nickias (1992). "Evidence that the loss of the voltage-dependent Mg2+ block at the N-methyl-D-aspartate receptor underlies receptor activation during inhibition of neuronal metabolism." J Neurochem **59**(4): 10.

Zhang, J. and J. S. Diamond (2006). "Distinct perisynaptic and synaptic localization of NMDA and AMPA receptors on ganglion cells in rat retina." The Journal of comparative neurology **498**(6): 810-820.

Zhang, X. M., D. T. L. Liu, et al. (2010). "Immunopanning Purification and long-term culture of human retinal ganglion cells " molecular vision **16**: 6.